Yukon University

Characterizing permafrost vulnerability to climate change induced thaw in the Traditional Territory of the Champagne and Aishihik First Nations

September 2025

CHAMPAGNE AND AISHIHIK FIRST NATIONS

This publication may be obtained from:

YukonU Research Centre, Yukon University

500 University Drive P.O. Box 2799

Whitehorse, Yukon Y1A 5K4

867 456 6986 or 1 800 661 0504

www.YukonU.ca/research

Recommended Citation:

Calmels, F., Laurent, C., Amyot, F., Roy, L.P., Buchanan, C.A., Koot, C., Sedore, P., 2025. Characterizing permafrost vulnerability to climate change induced thaw in the Traditional Territory of the Shadhäla and Ashihik First Nations. YukonU Research Centre, Yukon University, 160p.

Project Team

Authors

Fabrice Calmels	YukonU Research Centre
Cyrielle Laurent	YukonU Research Centre
Frances Amyot	YukonU Research Centre
Louis-Philippe Roy	YukonU Research Centre
Cathy Koot	YukonU Research Centre
Philip Sedore	YukonU Research Centre
Casey Buchanan	YukonU Research Centre

Acknowledgments

We appreciate the support of all participants and partners who have contributed to this project. This includes the members of Shadhäla and Äshèyi First Nations who have shared their knowledge with us in workshops, field visits and general assemblies. This work would not have been possible without their knowledge of their land and their help guiding us. We would especially like to thank Kenny Joe, Harry Smith, Charlie, Zabrina Leslie and the land guardians for their help in the field.

Thank you to Crown Indigenous Relations and Northern Affairs Canada (CIRNAC) and the Climate Change Preparedness in the North (CCPN) for funding this project, and Ray Gunness who acted as manager and liaison between CAFN and YukonU during this project, taking over from Megan Grabowski. Additional funding was provided by ArcticNet.

We would also like to thank the field and research assistants who made this work possible, including Pamela Godin, Moya Painter, Sheilany Bouchard, and Tristan Sparks.

1. Contents

2. List of Figures

3. List of Tables

4. Introduction

This project is a collaboration between the Shadhäla yè Äshèyi Kwädǎn (Champagne and Aishihik First Nations, CAFN) and the YukonU Research Centre that studies how permafrost impacts environmental conditions and community wellbeing in the CAFN traditional territory. The goal of this project is to map and characterize permafrost occurrences at important sites within CAFN territory, address permafrost thaw vulnerability, and collect data that is valuable to CAFN in developing future adaptation and climate change strategies.

CAFN's draft of the Climate Change Adaptation Plan - Community Infrastructure (2016) and Community-Based Fish and Wildlife Management Plan (2017) show the high level of community concern about permafrost thaw and its impacts on erosion processes, slope stability, vegetation, hydrology, infrastructure, and the contamination of country food by heavy metals.

The few studies previously conducted in the area suggest that the permafrost present on CAFN land is warm and vulnerable to degradation. In CAFN's traditional territory, permafrost thaw is likely to induce thermokarst processes, meaning that land will collapse and degrade as the ice within it melts. This can lead to general ground subsidence, the formation of thermokarst landforms, the erosion of land around water bodies and removal of peat cover (Calmels et al., 2008). With the ground temperature close to 0°C, it is possible that the thaw process will be completed in just a few decades. Under certain climate warming scenarios (RCP 4.5), discontinuous permafrost could cease to exist by 2100 (Slater and Lawrence, 2013). When permafrost thaws, the hydrology of the landscape changes as substantial amounts of water are released into the environment through surface and subsurface flows, impacting the surrounding lakes and rivers (Walvoord and Kurylyk, 2016).

The concerns voiced by the CAFN community are also echoed by Western scientific knowledge. Thawing permafrost changes the topography of the land and increases active layer thickness, which has important impacts on the hydrology of an ecosystem. In many cases permafrost degradation leads to increased surface and subsurface runoff and erosion, transporting liquid and solid matter into lakes and streams. As a result, water chemistry, the discharge of rivers and lakes, and the timing of this discharge change. Permafrost peat bogs, which historically act as storage sinks for contaminants such as mercury, may become contaminant sources as the climate changes and permafrost begins to thaw. As a result, it is important to know the condition of permafrost and how it's thaw may impact hydrology, and the potential for contaminant mobilization into the watershed and CAFN food sources (Martinez Cortizas et al., 2007; Rydberg et al., 2010; Smieja-Król et al., 2010).

Water quality, lake health, traditional harvest of fish, and connections to permafrost thaw have been stated as priorities by CAFN, along with concerns about how human-related land development may exacerbate climate impacts. To better understand the complex implications of a changing permafrost landscape, we aim to study the connection of permafrost vulnerability and hydrology along selected roads and lakes shores areas across CAFN territory.

In the short term, the project objectives are to:

- Characterize permafrost and map its distribution around K'ùa Mān, Äshèyi Mān and other basins of community interest within the traditional territory of CAFN;
- Use remote sensing, GIS, and Indigenous Knowledge to extrapolate permafrost distribution;
- Install permafrost temperature sensors to assess potential climate change impacts;
- Assess the vulnerability of permafrost to climate change related thawing (includes both temperature data analysis and assessment of thaw mechanisms and influences);
- Engage with key citizens to develop research protocols, interpret, and communicate the results.

In the long term, the project objectives are to:

- Establish the knowledge base for a community-led program to study permafrost;
- Collect continuous data to assess the rate of permafrost thaw with climatic change;
- Develop adaptive strategies for the community based on CAFN priorities;
- Create a template for study of other permafrost affected regions in the North.

5. Climate History

5.1 Introduction

To get a better understanding of how climate change is affecting Shadhäla yè Äshèyi Kwädn̄ (Champagne and Aishihik First Nations) territory, we have done a climate analysis using data from Environment Canada, including temperature and precipitation. All the climate data is accessible online from the Environment Canada website, and the formatted spreadsheets will be available in Appendix 1.

5.2 Methodology

The climate analysis was done using a script written in the Python programming language to integrate and analyzed as they become available. The most time-consuming part of the analysis is the data cleaning and processing. This is important with climate data, because missing data, which is common, can skew the dataset and create false trends. For example, if most of January and February are missing, the average annual temperature will be slightly warmer because two of the coldest months are missing. The same goes for missing summer months, which can make a year seem colder than it actually was. Because of this, data quality is very important, and the data needs to be cleaned to either remove years with too much missing data or interpolate (predict) the missing values.

The climate records for Dakwäkäda (Haines Junction) are quite complete from 1945 to today, though there are multiple missing years: notably a large gap between 1982–1993, as well as 1971, 2001–2002, 2013 and 2020, that were all missing too much data to use. Regardless, this is the best climate dataset available for this region and is suitable for an in-depth analysis of regional climate change over the last nearly 80 years.

To make use of years with missing data for cumulative indicators (such as thaw–degree-days or monthly averages, see below for a detailed explanation), as long as less than 7 days in any month were missing, the missing data were estimated using a linear interpolation method. If more than 7 days in any month were missing, the year was not included in the analysis. This is slightly above the recommended five missing day cutoff by the World Meteorological Organization (WMO, 2017) but was adapted to allow for more years to be included without compromising data quality. Data processing and analysis were also conducted in Python using the Pandas and SciPy packages.

To make meaningful interpretations of the data sets, a variety of climate indicator graphs have been created, including:

-*Mean annual air temperature (MAAT)*, which represents the average temperature for a whole year. This provides a picture of the whole year, and can show warming, cooling, or no change year over year. This is useful for comparing between regions but does not show when the changes (warming or cooling) are occurring;

-*Mean daily air temperature*, which represents the average daily temperature. It is shown as the comparison of the mean daily temperature from the current period (1990-2019) to a reference period (1960-1989). It is standard in climate analysis to use 30-year periods to remove inter-annual variability and highlight long-lasting trends;

-*Thaw degree days (TDD)*, which is an indicator that helps to identify the intensity of summer. It does so by taking to the total sum of the positive temperatures. For example, one day that reaches 9°C and the next day 10°C, the TDD for those two days would be 19;

-*Growing degree-days (GDD)*, which is an indicator like TDD, but it only takes into account days with temperatures above 5°C. This temperature is chosen because it is generally considered the temperature at which plant growth is stimulated/optimized. GDD also helps to identify the intensity of summer;

-*Freezing degree-days (FDD)*, which are like TDD and GDD but represent that total sum of negative temperatures (below 0°C). This indicator helps identify the intensity of winter.

-*Total annual precipitation*, which shows the total precipitation (snow and rain) in a year. Because precipitation data is often missing from the dataset more often than temperature data, there were more years missing for total annual precipitation compared to the various temperature indicators.

5.3 Results

The first indicator that is helpful to detect changes in climate is the mean annual air temperature (MAAT), shown in Figure 1. This graph shows that since the end of the 1940s, mean annual temperature has, on average, been increasing through time. The box in the upper left corner of the graph shows the 'r-value' and the 'p-value', which are statistical terms. The r-value is the Pearson's correlation coefficient, which represents strength of a relationship between two variables (here, time and temperature). The closer the r-value is to 1, the stronger the relationship. The p-value allows us to interpret how certain we can be that the relationship actually exists (if the $p<0.05$, then the correlation is accepted as likely). For this dataset, these statistical values show that there is a statistically important increase in temperature from the end of the 1940s to 2020.

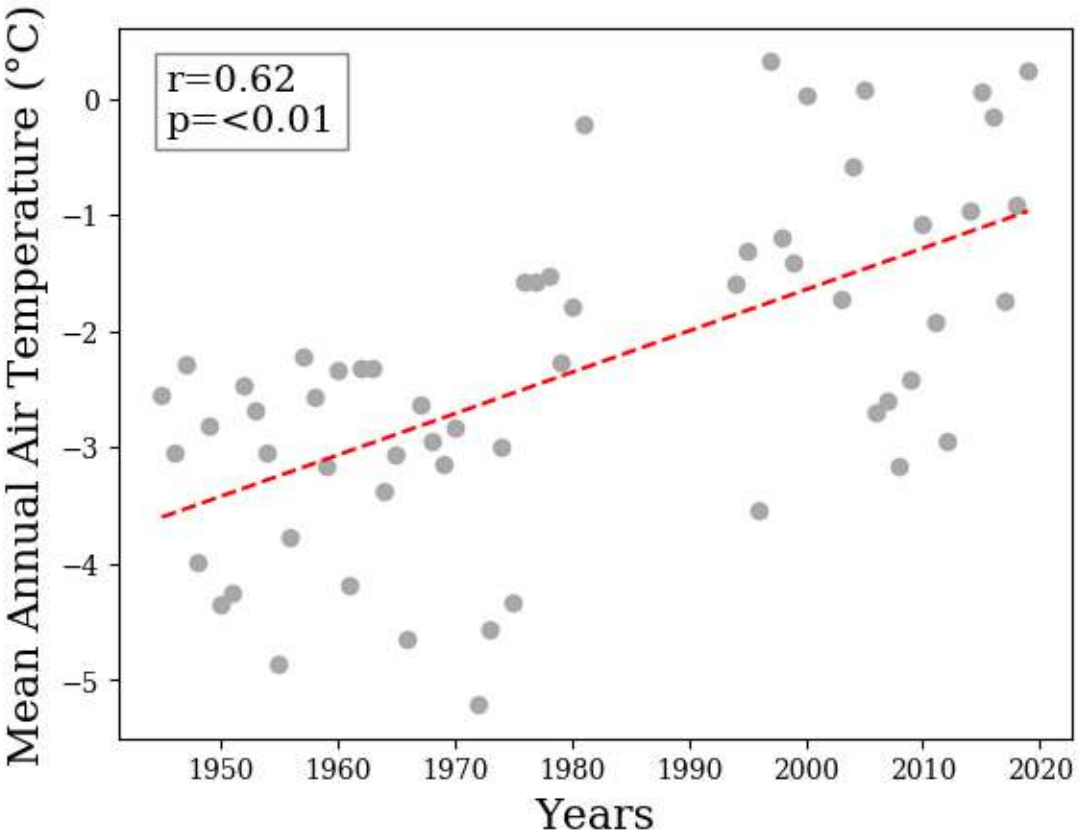

FIGURE 1 MEAN AIR TEMPERATURE (MAAT) FOR DAKWÄKÄDA.

To make sense of how exactly this increase is occurring, we can compare the mean daily temperature for the current 30-year period (1990-2019) to the reference period (1960-1989). This reference period is used as a comparison for present day temperatures because it is thought that this represents a time before the impacts of climate change were felt. Additionally, 30-year periods are used to smooth out annual variability in climate. In Dakwäkäda, the MAAT for the reference period was -2.85°C, and for the current period it is -1.42°C. This means that temperatures have increased by 1.43°C in this period. The average temperature from the 1945-1975 period (the first 30-year period available) was -3.3°C suggesting an increase of 1.9°C between this earlier period and the current period. This is similar to the average temperature increase across Canada of 1.8°C over the same period (Environment Canada, 2021).

This comparison between the current period and the reference period is shown in Figure 2. In this figure, the blue line represents the reference period, and the orange line represents the current period. This graph shows that the lines overlap in certain parts of the year but diverge in others. For example, in the winter months on either side of the graph, there is a larger gap, suggesting that temperatures have increased more in the winter months than in the summer months, and in the spring more than in the fall, when the temperatures seem to have changed little.

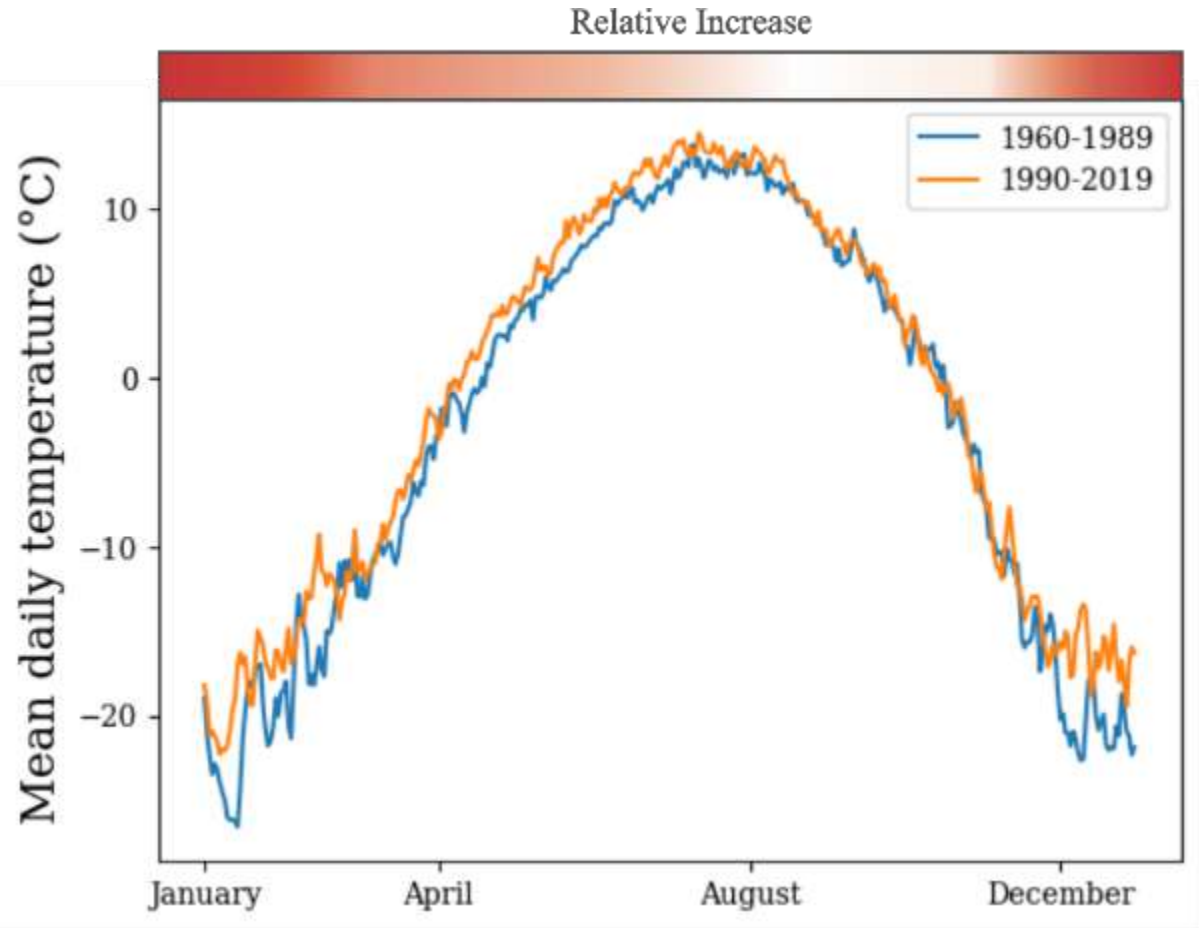

FIGURE 2 MEAN DAILY AIR TEMPERATURE GRAPH COMPARING THE 30-YEAR REFERENCE PERIOD TO THE CURRENT PERIOD FOR DAKWÄKÄDA

These trends can also be seen in the mean monthly temperature anomalies from the current period (1990-2019) to the reference period (1960-1989), as seen in Figure 3. This figure shows that the greatest increase in temperature occurs in December (>4°C), and January (~3°C) followed by February-June with increases between 1°C and 2°C and increases of less than 1°C between July and November, and a slight decrease in temperatures in October. This graph is helpful in showing the changes in temperature over time for specific months and make sense of the trends throughout the year.

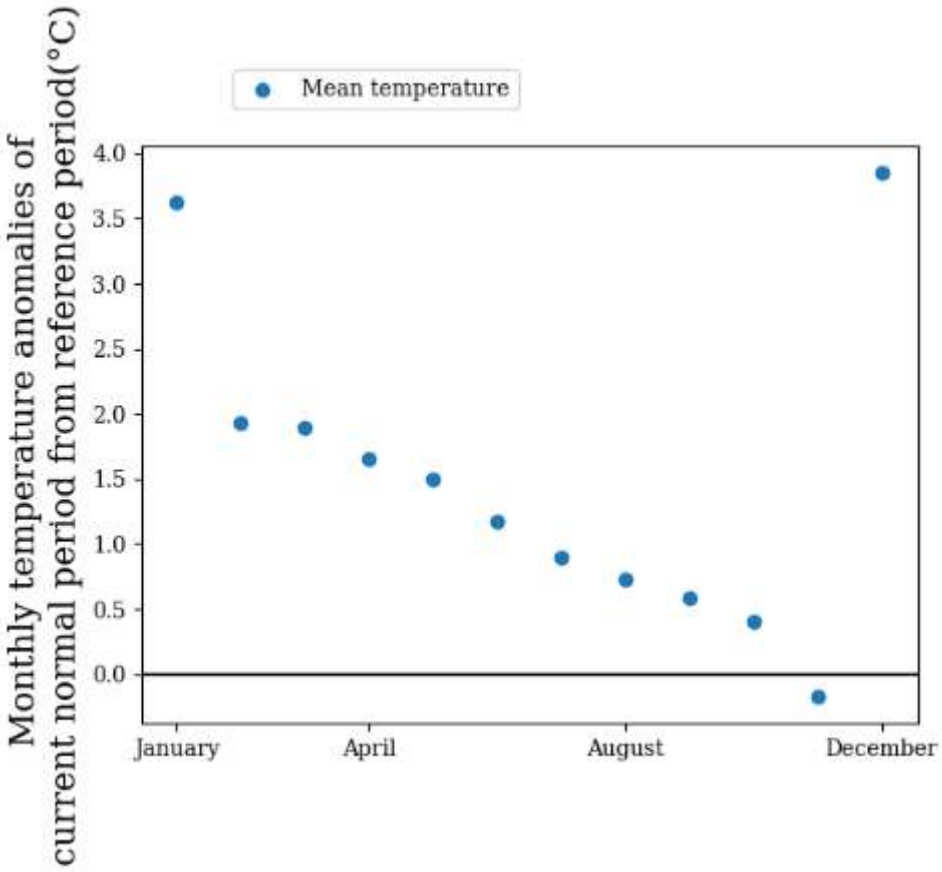

FIGURE 3 MONTHLY TEMPERATURE ANOMALIES OF THE CURRENT PERIOD COMPARED TO THE REFERENCE PERIOD

Figure 4 shows the number of thaw degree-days, which represents the sum of positive temperatures through the thawing season (summer). This helps to highlight the intensity of summer temperatures. In this case, there is a clear increase in the number of thaw degree-days over time. The r=0.63 and the p=0.000 reference the high correlation between the increase in thaw degree-days and time (r=0.63), and the high degree of certainty ($p < 0.000$).

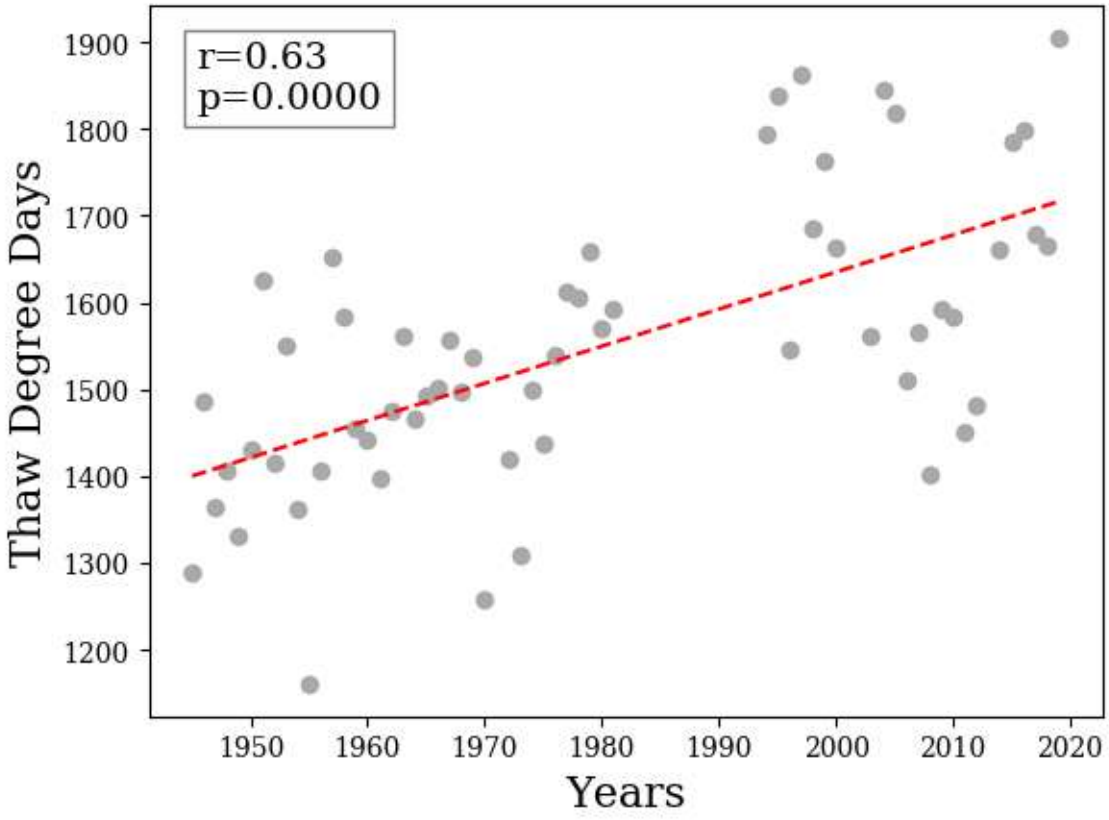

FIGURE 4 THAW DEGREE-DAYS FOR DAKWÄKÄDA

This trend in increasing TDD is also highlighted in the increase in growing degree-days (GDD), that is seen in Figure 5. This graph shows similar results to those in Figure 4, but highlight the increasing intensity of the heat, specifically in terms of conditions that are favorable to plant development.

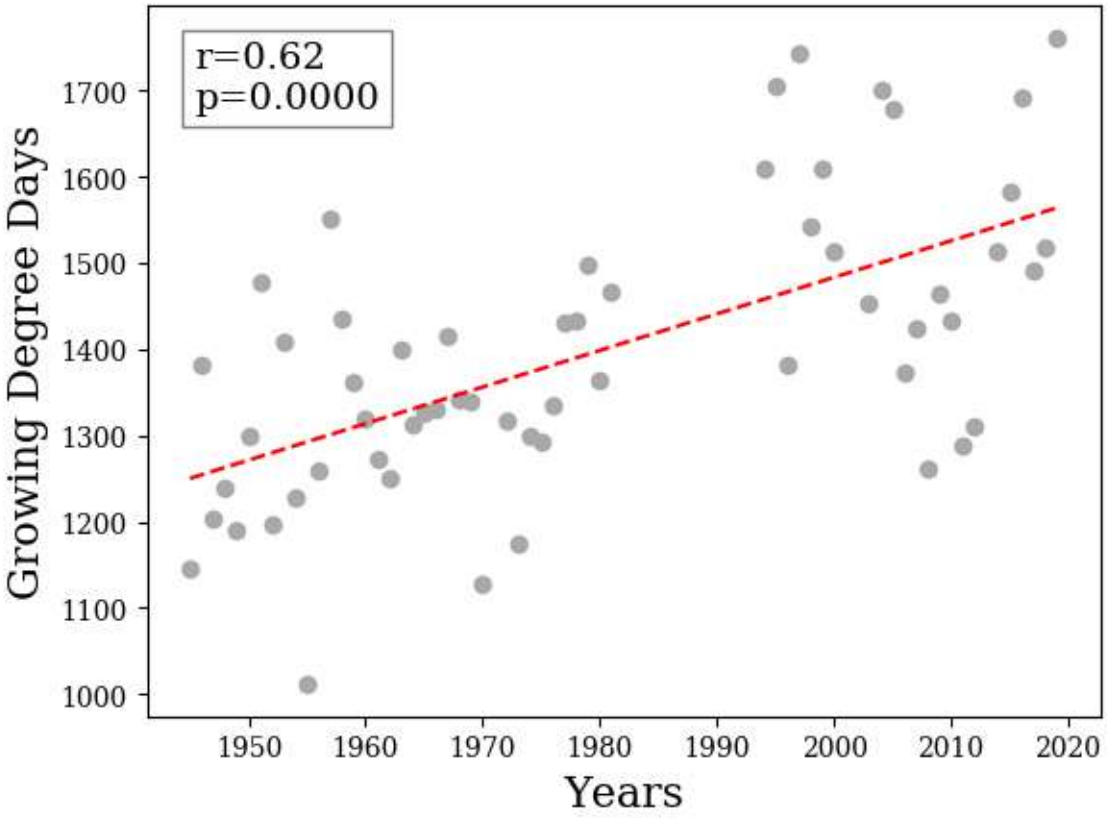

FIGURE 5 GROWING DEGREE-DAYS IN DAKWÄKÄDA

Freezing degree-days (FDD) are the inverse of TDD, and represent the number of days below 0°C. There is a decrease in the number of FDD since the end of the 1940s that indicates a decrease in either the total number of cold days, or the intensity of the cold days, or both, resulting in an overall decrease in cooling. Based on the other available data, it appears that the decrease in FDD is related to the high increase in temperature in December and January (Figure 6).

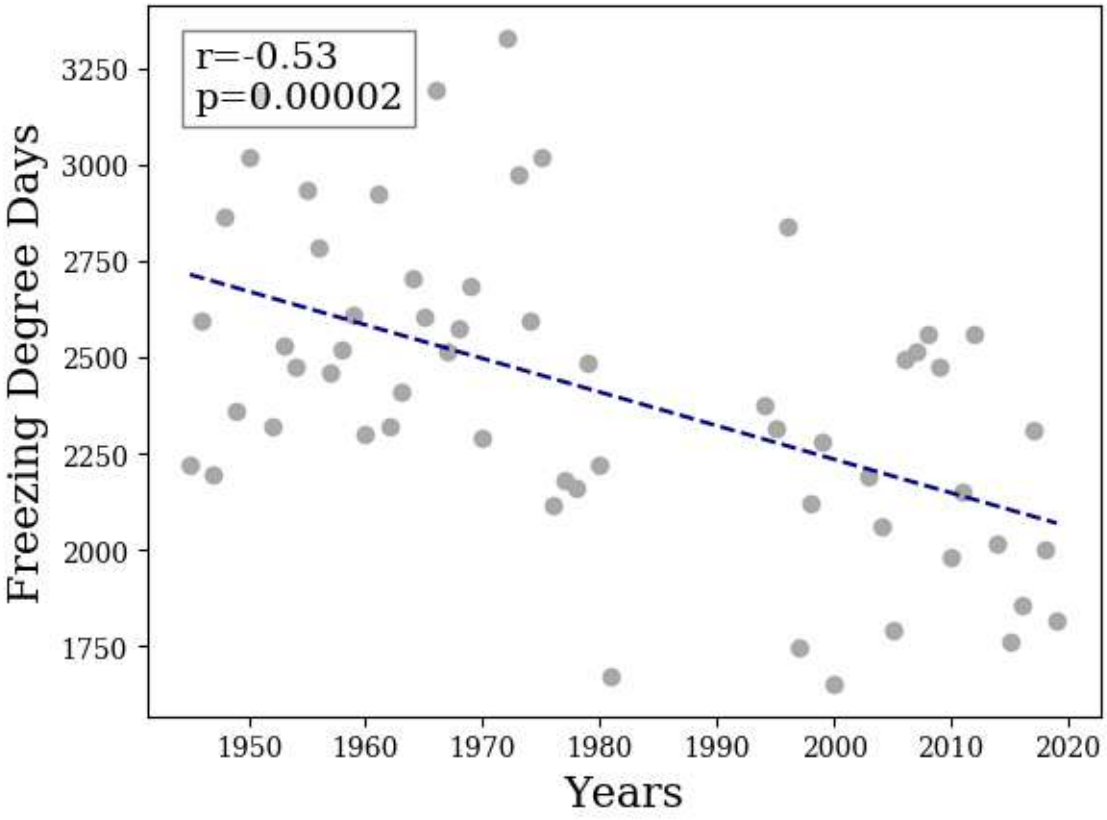

FIGURE 6 FREEZING DEGREE-DAYS IN DAKWÄKÄDA

Because precipitation data is cumulative, meaning that total precipitation is often the desired indicator, and the fact that, unlike temperature, one day's precipitation is unlikely to influence the next day's, it is difficult to fill in the many missing data gaps. Therefore, the record is more incomplete, and it is more difficult to paint an accurate picture through time using only data. For example, in Figure 7, because of missing data it is not possible to include the record-breaking precipitation from 2020-2021. And the picture is therefore incomplete.

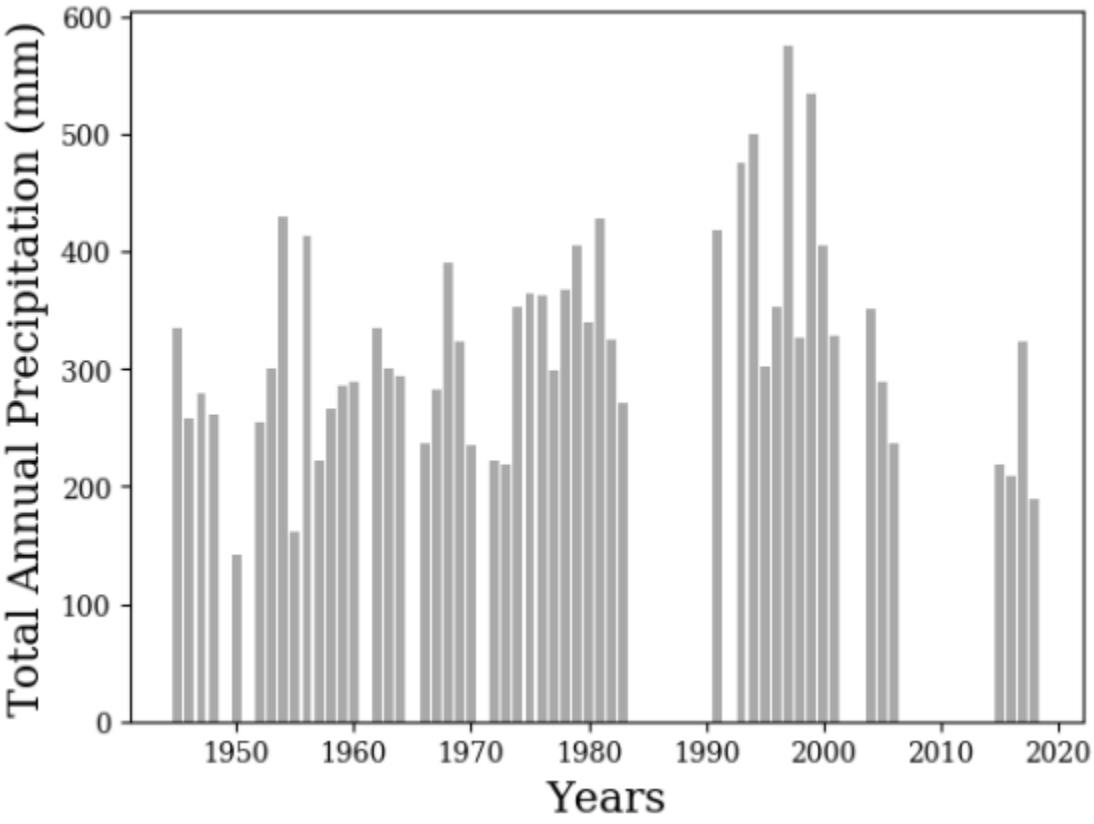

FIGURE 7 TOTAL ANNUAL PRECIPITATION FOR DAKWÄKÄDA

By looking at the two decades with the most complete precipitation records, 1972-1981 and 1992-2001, it is possible to see the beginnings of a trend in increased precipitation (Figure 8). Based on these decades, precipitation seems to have increased mostly in the spring and fall, more than in the winter and summer. Without more complete precipitation records for recent years, it is not possible to say whether these trends have continued, despite record-breaking snowpack in recent years.

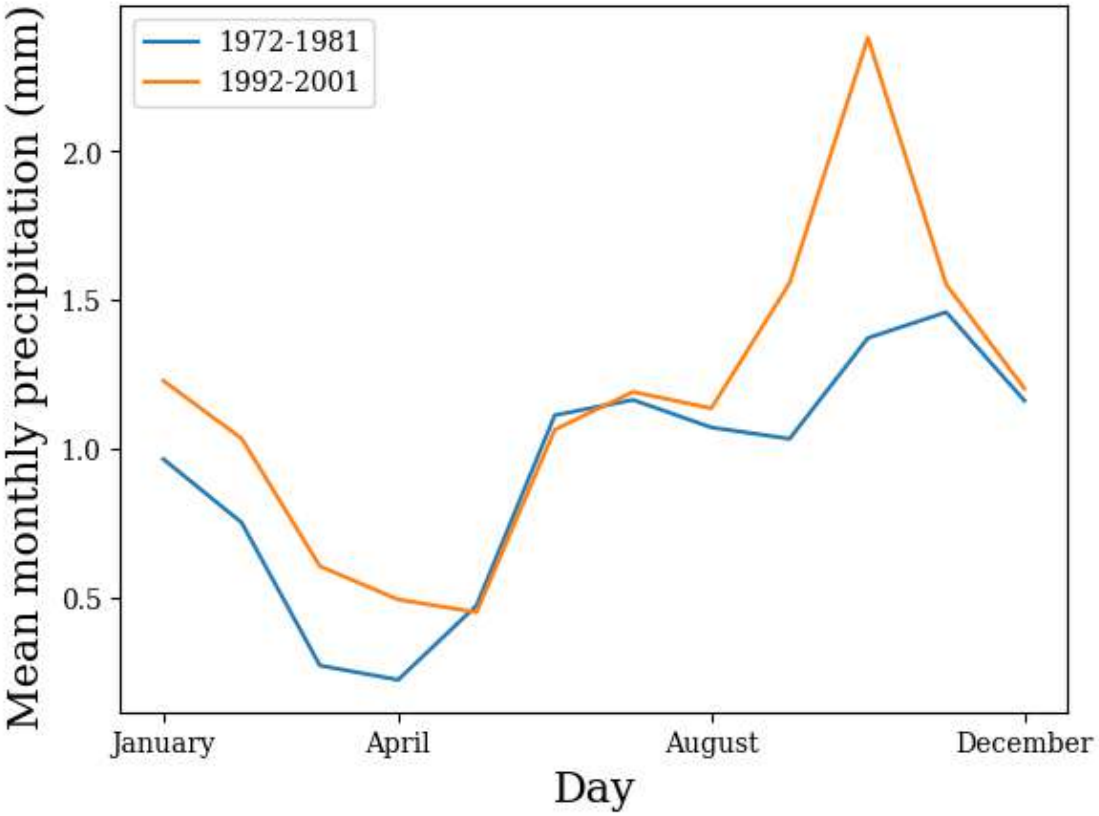

FIGURE 8 MEAN MONTHLY PRECIPITATION FOR THE DECADES WITH THE MOST COMPLETE RECORDS: 1972-1981 AND 1992 TO 2001.

Overall, these data show that in the Dakwàkàda region, there has been a 1.4°C increase in temperature since the 1960–1989 period, and an increase of 1.9°C since the 1945–1975 period. This increase is especially important in the winter (with an increase as high as >4°C in January), and to a lesser extent in the spring, summer, and less than 1°C in the fall. This is comparable to the rest of Canada, where the average increase in temperature since 1945 has been 1.8°C (Environment Canada, 2021), and the greatest increase has been seen in the winter. It is difficult to make sense of the changes in precipitation because of the amount of missing data, especially for 2021, which by all accounts was a record-breaking year for precipitation. As with all changes in climate, the data can be used to complement local knowledge.

Historical climate data are also available from Äshèyi for 1943–1966, where a weather station was also set up in 2019. There has not been enough data collected since 2019 to make a reliable comparison between historic and present-day temperature for this area. The historical climate data for Äshèyi has been included in Appendix 2.

5.4 Climate History Summary

In general, the temperatures are warming in the traditional territories of the Shadhäla yè Äshèyi Kwädän. Mean annual air temperature has increased by 1.43°C since the 1960–1989 period, and by 1.9°C since the 1945–1975 period. This is similar to the average increase in Canada of 1.8°C since the 1940s. Much like in other parts of the country, the greatest temperature increases occur in the winter. They are also increasing, but to a lesser extent in the spring and summer, and temperatures are relatively stable in the fall.

There is an increase in the number of thaw degree-days and growing degree-days, highlighting that the intensity of warming in the summer is increasing. Conversely, there is a decrease in freezing degree-days, suggesting a decrease in intensity of freezing in the winter.

Missing data makes it impossible to reliably track changes in precipitation based on the data, but data from other places in the Yukon suggests that precipitation is increasing.

Overall, the warming temperatures in the CAFN traditional territories will have important effects on the landscape, from permafrost thaw to changes in ecology.

6. Site Assessments

6.1 Site Assessment Methodology

To better understand permafrost conditions in the traditional territories of the Shadhäla yè Äshèyi Kwädän, site assessments were performed at study areas that were chosen based on community priorities and interests. The assessments included field observations, and various survey methods including Electrical Resistivity Tomography (ERT) surveys, unmanned aerial vehicle (UAV, or drone) surveys, shallow borehole drilling and permafrost coring, followed by laboratory analyses. The locations of these assessments are shown by the regional map in OBJ9.

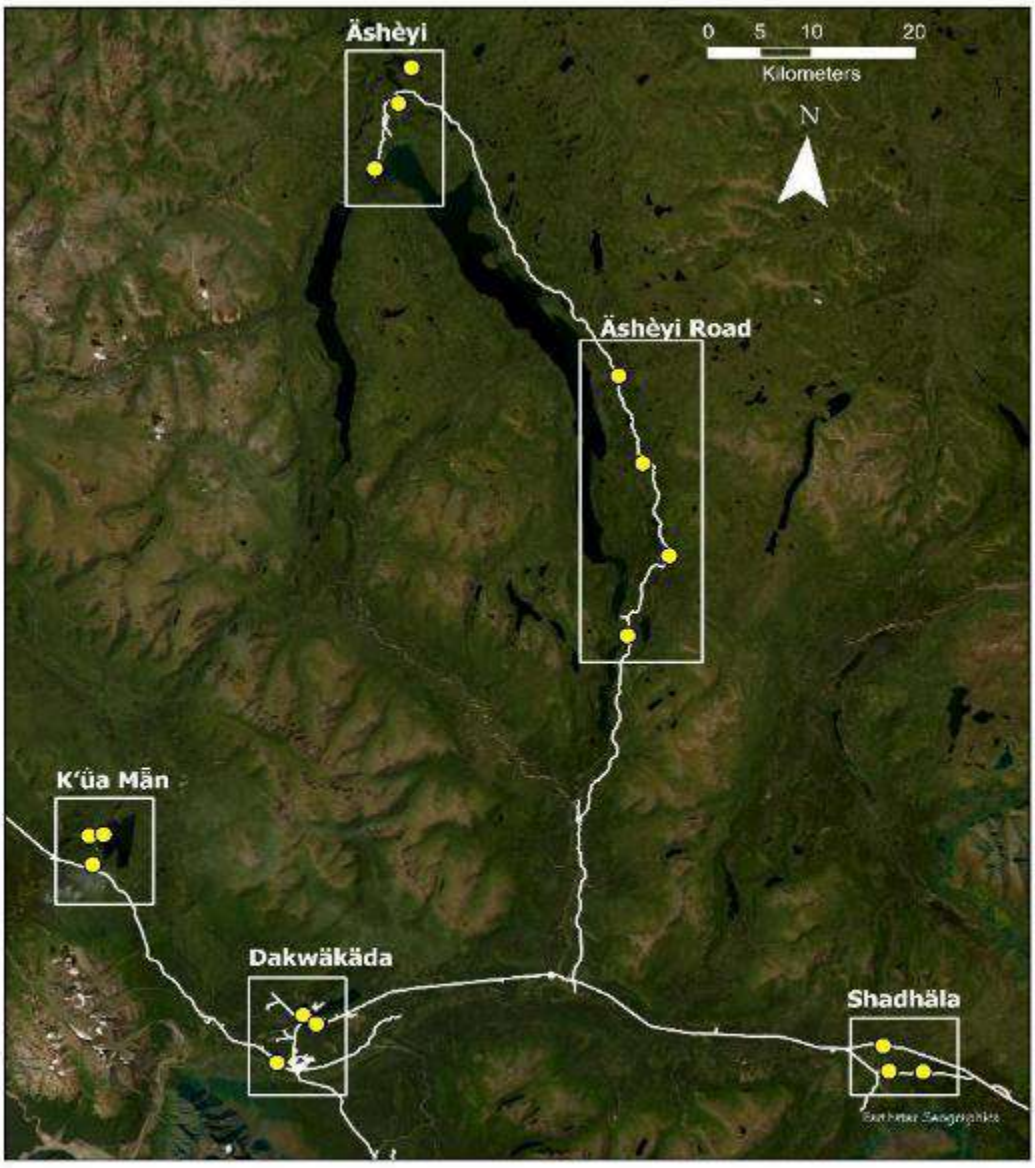

OBJ9POINTS). LOCAL STUDY AREA MAPS ARE PRESENTED IN THE FOLLOWING SECTIONS.OBJ

6.1.1 Electrical Resistivity Tomography

Electrical Resistivity Tomography (ERT) is a geophysical method that passes electrical current through stainless steel electrodes that are driven into the ground surface. A current meter (called "Terrameter") located at a central "station" measures the resistivity distribution of the subsurface between electrode pairs. Resistivity is the opposite of conductivity and indicates the difficulty of an electrical current to pass through a material. Mineral materials (except for specific substances such as metallic ores) are mostly non-conductive (resistive). Therefore, variation in the resistivity of a soil or rock profile is governed primarily by the amount and resistivity of pore water present in the profile, and the arrangement of the pores. This makes ERT very well suited to permafrost and hydrology applications. Ice is highly resistive relative to liquid water, and permafrost usually contains ground ice, often in high amounts, while containing little liquid water.), permafrost distribution can be inferred based on changes in resistivity between frozen and unfrozen ground.

Three different types of electrode configurations or "arrays" were used during the surveys: the Wenner, the dipole-dipole, and the Schlumberger arrays. These arrays differ in how they pair current and potential electrodes. A direct current (DC) electrical pulse is sent from the resistivity meter along the survey line in two current electrodes (C1 and C2), and the measurement is performed by two potential electrodes (P1 and P2). The resulting data consists of a cross-sectional (2D) plot of the ground's resistivity (ohm·m) versus depth (m) for the length of the survey. In general, the Wenner array is good at detecting vertical resistivity changes (i.e. horizontal structures), but relatively poor in detecting horizontal resistivity changes (i.e. narrow vertical structures). Inversely, the dipole-dipole array is very sensitive to horizontal changes in resistivity, but relatively insensitive to vertical changes in the resistivity, therefore these configurations complement each other very well.

6.1.2 Unmanned Aerial Vehicle

An unmanned aerial vehicle (UAV) was used to make high resolution imagery (orthomosaics), digital elevation models (DEMs), and 3D models. The model of drone used was the DJI Matrice 210 RTK, paired with a DJI Zenmuse X7 camera. The drone was flown in a grid pattern to take many photos with high overlap. These photos were then uploaded to a computer and the photogrammetry software Agisoft Photoscan was used to create orthomosaics and DEMs. Orthomosaics are high-resolution composite images of photographs that are geometrically corrected to remove distortions. Digital elevation models (DEMs) are computer-generated grids where each pixel represents the elevation at that location. The orthomosaics and DEMs allowed for a more in-depth analysis of ground conditions, and to view areas that are otherwise inaccessible.

6.1.3 Drilling and Permafrost Coring

The same sampling and drilling protocols were followed for each borehole drilled by the YukonU research team. The site was first described (e.g., hydrology, vegetation type and density, topography), photos were taken, and locations were recorded using a hand-held GPS.

A light and portable GÖLZ Earth-drill system was used to drill shallow boreholes. Boreholes were initiated by shoveling down to the thaw front. At the thaw front, the Earth-drill system was used. The drill uses a small Stihl engine with 600 rpm high-speed transmission. The drill is coupled with stainless steel rods (1 meter in length and 4.5 cm in diameter) and a core barrel (40 cm long and 10 cm in diameter) with diamonds set in carbide alloy teeth. The drill is used in unconsolidated, fine to medium-grain material (sand to clay). A core catcher tool was used to extract frozen cores from the borehole, allowing for the collection of continuous, undisturbed permafrost samples. This type of drilling is limited to a maximum drilling depth of approximately 5 to 6 m under optimal conditions. Drilling is usually terminated if a significant layer of gravel is encountered due to the tendency of the barrel to become stuck in this material.

Each core sample was described in situ (e.g., soil type, soil moisture, presence or absence of organic matter, any notable features). Each extracted sample was identified by borehole name and depth. Samples were put in polybags and sealed immediately after extraction. Samples were kept frozen and stored in a freezer that was taken back to the laboratory for further analysis. In the laboratory, each core was cleaned with cold water to remove drilling mud and then photographed.

Drilled boreholes were fitted with PVC tubing instrumented with HOBO loggers and temperature sensors at various depths depending on the total depths of the boreholes. The lined boreholes were filled with neutral, food-grade silicone oil to improve the accuracy of temperature measurements.

6.1.4 Laboratory Analyses

Laboratory analyses were carried out to measure the properties of the permafrost samples. Both soil grain characteristics and ice characteristics were evaluated. To evaluate soil grain characteristics, a grain-size analysis was performed on selected samples. To evaluate ice characteristics in permafrost samples, the cryostructures (the geometry of the ice in the permafrost) were described, while volumetric excess ice content and gravimetric ice content were calculated. A log for each permafrost borehole was then created by assembling laboratory photos of the cores. Borehole logs include maximal depths, grain size ratio and volumetric excess ice content. These methods are described below. For more information, please refer to Andersland and Ladanyi (2004).

6.1.4.1 Grain Size Analysis

Grain size analyses were performed using sieves and hydrometers following a specifically modified American Standard and Testing Method protocol (ASTM D422-63, 2000). The sieves used were 4.75, 2, 1, 0.5, 0.25, 0.125 and 0.063 mm. Samples collected in 2023 were measured using a combination of sieves and a Malvern Panalytical Mastersizer 3000E laser diffraction particle size analyzer. Samples were sieved at 4.75, 2, and 1 mm and the finer fractions (<1 mm) were run through the analyzer that measures grain size from 1–0.00001 mm.

6.1.4.2 Cryostructure

Cryostructure is the geometry of the ice in permafrost soils. Cryostructures depends on water availability, the soil's ice-segregation potential, and the time of freezing, all of which affect the development of ice structures in the soil matrix. Information such as soil origin, climate conditions at the time of freezing, permafrost development history, and ground vulnerability when permafrost degrades can be interpreted from cryostructures, cryofacies (groups of cryostructures and ice content), and general cryostratigraphy (groups of cryofacies).

Field descriptions are based only on a brief visual inspection of the core, so sample cryostructures were described a second time more thoroughly in the laboratory using standard terminology (Murton and French 1994) and photographed in high-resolution. Frozen core samples were warmed to near 0°C and any refrozen mud was scraped off before the sample was described and photographed.

6.1.4.3 Organic Matter Content

When applicable, organic matter content was calculated using the Loss-on-Ignition method with 2g of dry sediments under combustion at 575°C for 15 minutes. The organic matter content was calculated using the following equation:

$$OM = \frac{S_d - S_b}{S_d}$$

where OM is the organic matter content (gravimetric), measured as mass loss after a subsample of dry sediment (Sd) has burned (Sb). Results are expressed as percentages (dimensionless). The sediments were sieved to <2 mm while subsampling.

6.1.4.4 Gravimetric Ice Content

Ice content was calculated using:

$$Ice = \frac{M_i}{M_s}$$

where M_i is the ice mass, measured as mass loss after drying (g), and Ms is the dry soil mass in grams. Results are expressed as percentages.

6.1.4.5 Volumetric Excess Ice Content

Volumetric ice content was measured using a water displacement method. The frozen sample was placed into a vacuum-sealed bag, weighed, and lowered into a reservoir made of a four inch-diameter plexiglass cylinder and filled with 1.5 L of water such that the entire sample and bag was submerged. The displaced water was then extracted until the initial water level (1.5 L) was achieved. The amount of displaced water was measured using a 250 mL graduated cylinder with a precision of ±2 mL. The bagged sample material was then removed from the reservoir cylinder, placed in a clean tin tray, and dried completely in a drying oven at 60°C. The dry sample was then weighed, broken up using a mortar and pestle, vacuum sealed in a clear plastic bag, and labelled according to the borehole and sample increment. The volumes of the vacuum-sealed dry samples were measured using the same displacement method as before, and the volume of the vacuum bags was subtracted from the measurement to obtain a dry sample volume. Assuming the density of ice to be 1.09 cm^3/g, the volumetric ice content was calculated using:

$$IVC_{(\%)} = \left(\frac{Wc \times 1.09}{Vtot}\right) \times 100$$

where W_c is the water mass content and V_{tot} is the total (frozen) core volume. Results are expressed as percentages. For the consolidation test samples, the volume has been measured using Glycol displacement. This allowed the possibility to keep the samples under 0°C and avoid the use of vacuumed sealed bags. The volume of excess ice content was calculated using:

$$V_{ice} = V_{tot} - V_{sed}$$

where V_{tot} is the total frozen core volume and V_{sed} is the dry soil volume. The volumetric excess ice content (V_{ice}) is then divided by the total frozen core volume (V_{tot}) and expressed as a percentage. This method is valid for mineral soils only.

6.1.4.6 Borehole Logs

A log for each permafrost borehole was created by assembling laboratory photos of the cores. Borehole logs include maximal depths, grain size ratio and volumetric excess ice content. These logs were used as supporting data for mapping.

6.1.5 Ground Temperature Monitoring

Drilled boreholes were fitted with PVC piping and instrumented with HOBO loggers and temperature sensors at various depths depending on the total depth of each borehole. Temperature data were collected each year and were compiled in Excel. Graphs were created using Excel and RStudio. The temperature data were also imported into the gridding software Surfer to create temperature grids that are helpful to visualize temperature changes in time. The temperature data was downloaded on an ongoing basis to monitor permafrost conditions.

6.2 Äshèyi (Aishihik)

Five sites, shown in Figure 10 were surveyed in the Äshèyi study area. All the sites, except for the active kettle pond (section 7.2.5), were documented using a drone to produce high-resolution imagery (orthomosaics) of the sites, and digital elevation models. At the Äshèyi village, a geophysical assessment (ERT) was also performed, as described in section 6.2.1. A palsa (section 6.2.2) and a pingo (section 6.2.4) were investigated using shallow geotechnical drilling and temperature monitoring, in addition to ERT surveys.

FIGURE 10 LOCATIONS OF THE SITES INVESTIGATED IN THE ÄSHÈYI REGION.

In the summer of 2023, a permafrost core and an ERT profile were collected from the old Äshèyi settlement on the peninsula across from the current location of Äshèyi. These activities are described in section 7.2.3. Finally, site visits highlighted the presence of a kettle pond forming, as described in section 7.2.5.

6.2.1 Äshèyi Site

Permafrost was surveyed in Äshèyi using a drone survey (Figure 11), electrical resistivity tomography (ERT) (Figure 13 and Figure 14), shallow geotechnical borehole (Figure 16). Because the site of the village has been subject to decades of land use activities, the pre-existing natural ground surface conditions are not present anymore. The 200-m long ERT survey was conducted at this site in the summer of 2019 to assess the distribution of ground ice.

The type and origin of soil is a determining factor when it comes to the geotechnical properties of permafrost. The village is situated on fine-grained soil that is a mixture of silt and clay, that was deposited as lake sediment when lake levels were higher. Silty and clay-rich soils are considered frost susceptible, which means that when permafrost develops in this type of ground, a significant amount of ice can form within the fine sediment when it freezes. Therefore, if this type of ground thaws, the terrain tends to become unstable, especially on slopes. Some ground subsidence may occur due to the loss of volume of ground ice.

When looking at the drone imagery, both slope instability and subsidence are present at this site. Some landslides are present on the hill slope, marked with yellow "S" indicators in Figure 11. There, the vegetation has been stripped away, and soil is exposed (Figure 12). These slides appear to be superficial and restricted to the top layer of the soil and are therefore not endangering the community. There is water ponding in a fenced area, marked by a blue "W" indicator, in addition to some other wet spots observed in the area (Figure 11). It is possible that the human activity taking place within this enclosure may have eroded the soil, stripped the organic layer, and triggered water accumulation and subsidence.

To determine whether there is permafrost underneath the study site, a 200m ERT survey was conducted parallel to the lake shore, following the access road (see ERT line 1, Figure 11) using two ERT configurations: the dipole-dipole and the Wenner arrays). The results of these surveys are presented in Figure 13. Both the dipole-dipole and the Wenner survey profiles suggest that permafrost is present, where highly resistive areas (blue areas in Figure 13) represent cold, frozen ground and less resistive areas (red areas in Figure 13), represent unfrozen ground. The Wenner profile shows a single bulk frozen area. However, the dipole-dipole profile shows a more detailed characterization of ground resistivity, with a main resistive layer, likely representing permafrost (marked with "P" in Figure 13), inset by even more resistive areas. These high resistivity pockets likely represent ice-rich permafrost (marked by "ice" in the same figure). Although these profiles do not constitute a geometrically exact representation of ground properties, they suggest that permafrost is present 3 to 5 meters below the ground surface and could extend as far as 10-15 m deep.

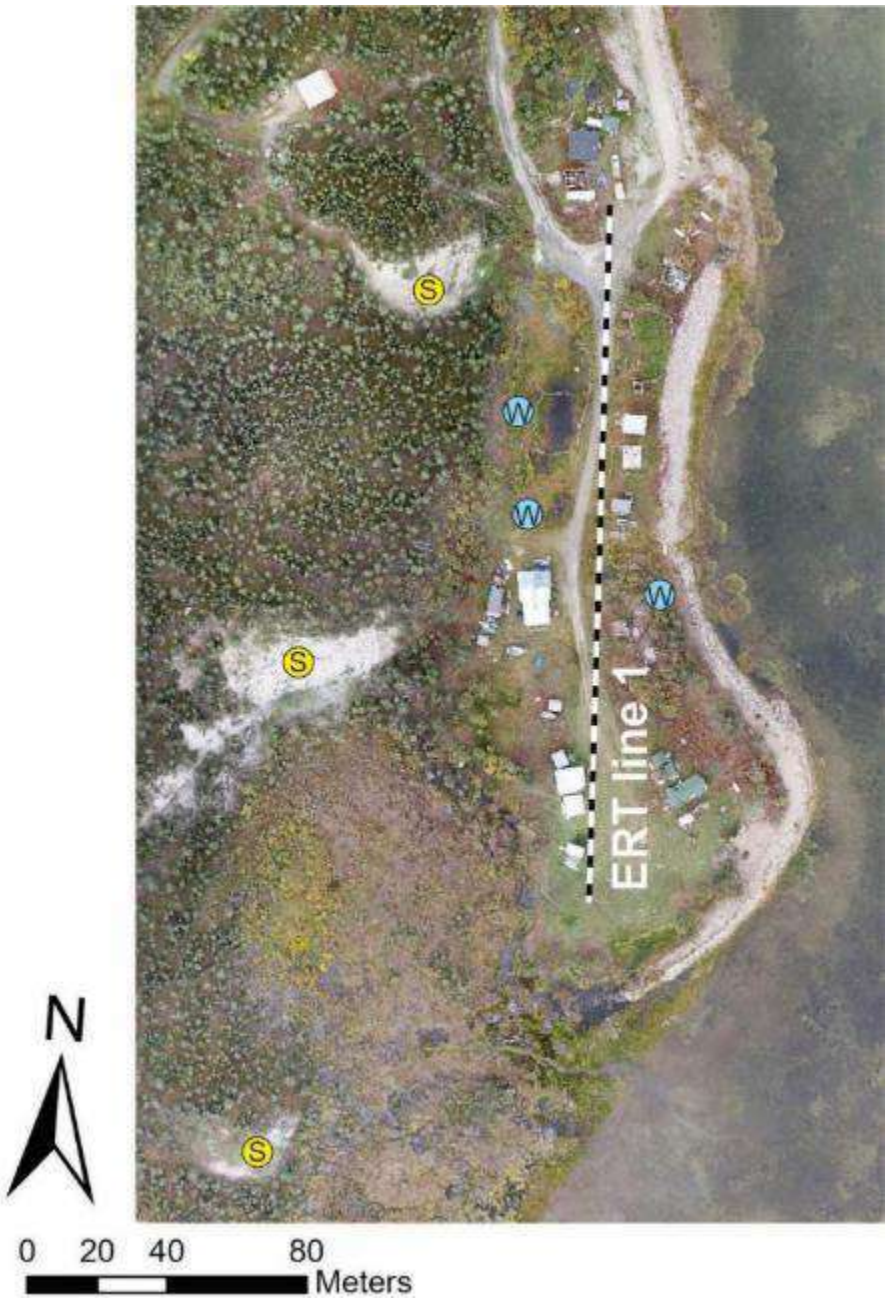

FIGURE 11 AERIAL IMAGE OF ÄSHÈYI ON THE LAKE SHORE, WHERE SLOPE INSTABILITY (YELLOW S SYMBOL) AND SUBSIDENCE (BLUE W SYMBOL) ARE SEEN.

Figure 14 shows a comparison between the dipole-dipole ERT profile and the aerial drone imagery. The comparison suggests that the highest resistivity areas may match wet areas observed in the field. Therefore, these depressed, wet spots may result from permafrost thaw. Geotechnical drilling could validate these hypotheses.

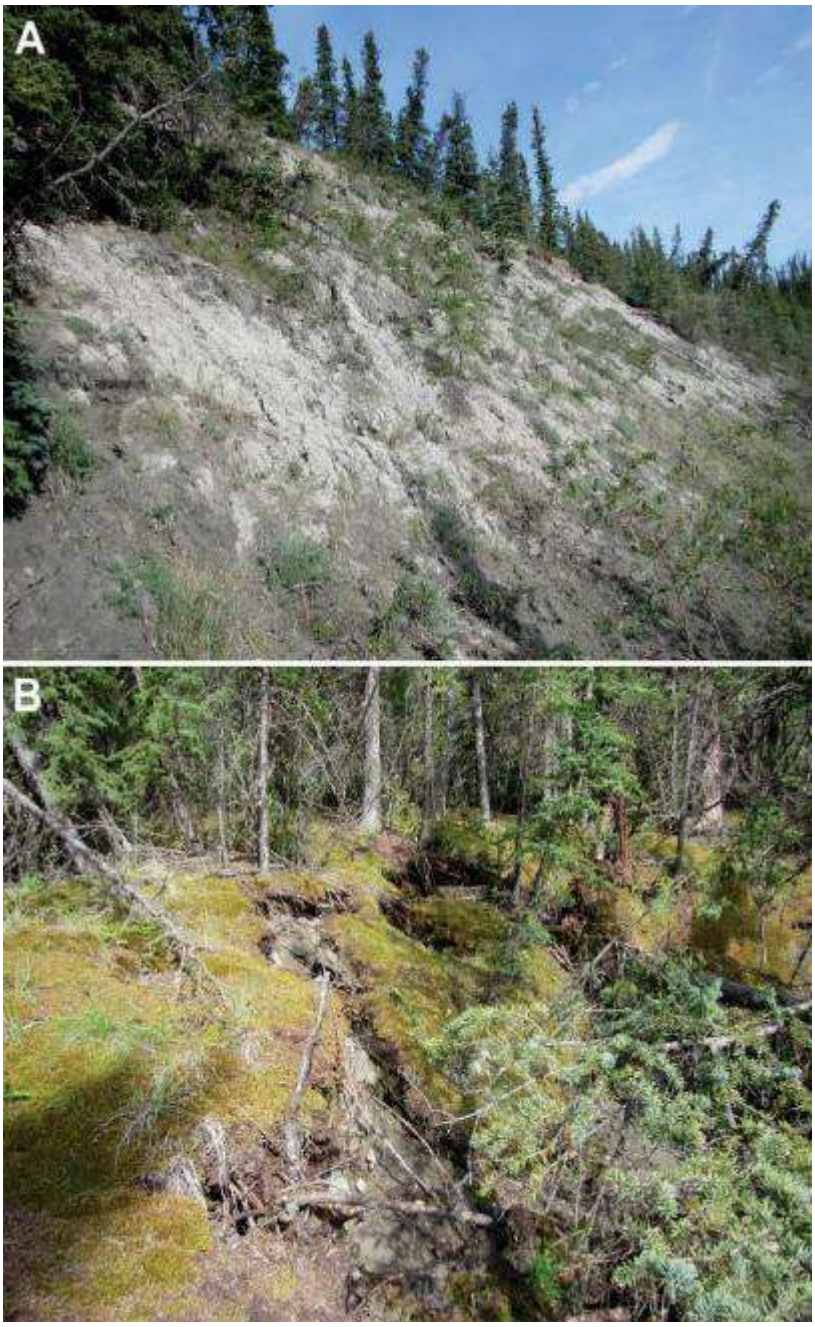

FIGURE 12 LANDSLIDE DEVELOPING ON THE WEST SIDE OF ÄSHÈYI. A- BARE BLUFF WHERE VEGETATION HAS BEEN STRIPPED; B- TOP OF THE SLIDE WITH RAFT OF VEGETATION TOPPLING.

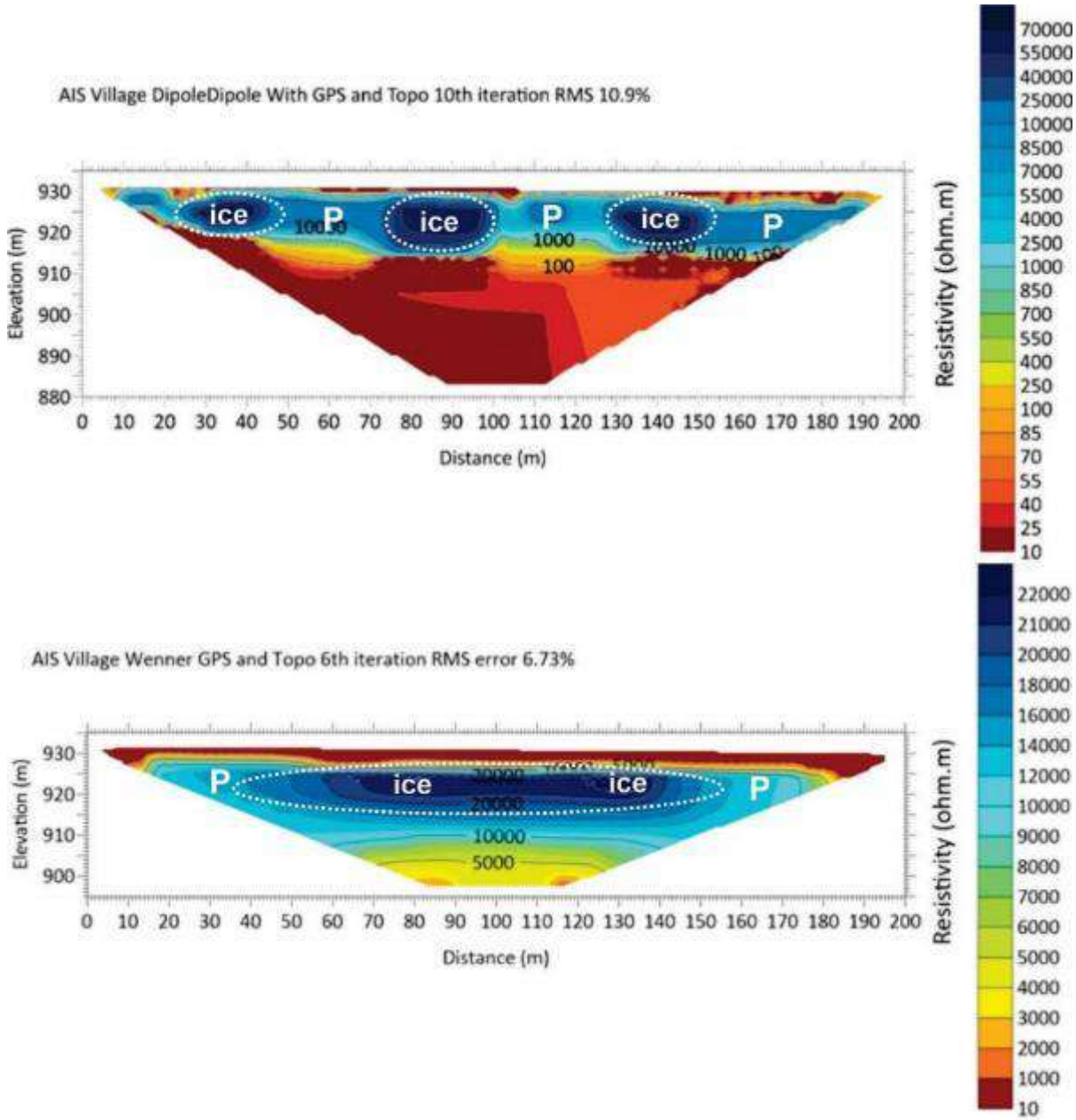

FIGURE 13 ELECTRICAL RESISTIVITY PROFILES AT ÄSHÈYI. "P" MARKS POTENTIAL PERMAFROST AREAS AND "ICE" INDICATES POTENTIAL ICE-RICH AREAS.

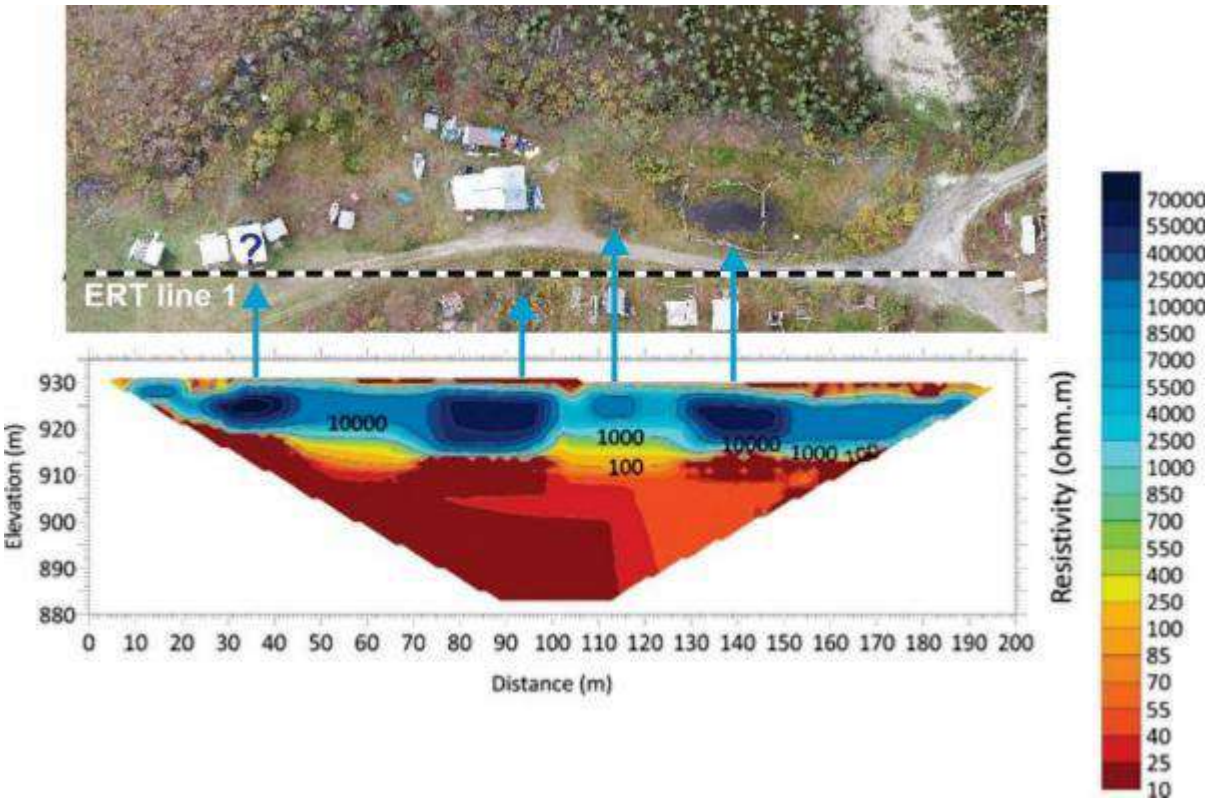

Figure 14 Comparison between ERT profile and drone imagery at Äshèyi.

6.2.2 Palsa Site

The *Palsa* site is a permafrost mound located between the foot of a hillslope and the shore of Äshèyi Mān about 150 m south of Äshèyi (Figure 15). A palsa is a permafrost mound with a frozen peat and sediment core. This site appears to be unaltered by human activities and likely represents permafrost conditions in the village before its settlement. In the summer of 2019, the location was drilled, permafrost cores were collected, and the resulting borehole was instrumented with ground temperature monitoring equipment (BH1 Palsa in Figure 15). An ERT survey also was conducted (ERT line 2 in Figure 15), and a drone survey was done in summer 2021.

FIGURE 15 AERIAL IMAGERY OF THE *PALSA* SITE WITH BOREHOLE AND ERT LINE LOCATIONS.

The borehole AIS_BH1 (at *Palsa* Site) was drilled in what appears to be a permafrost mound located between the foot of a hillslope and the shore of Äshèyi Mān (Figure 15). The cores were collected down to a depth of 6.72 m. The thaw front was at 87 cm depth at the time of drilling (July 27th, 2019). The log

shows an organic layer of 10 cm followed by organic silty sand down to 40 cm. Below 40 cm, gray sandy and silty sediment is alternated with more clayey layers (Figure 16). The borehole ends at 6.72 m in ice-rich sandy silt. Centimeter-scale ice lenses are visible all along the profile in the silty material, with volumetric excess ice contents ranging from 3 to 40%. Overall, the borehole has a mean volumetric excess ice content of 23%, which represents a potential subsidence of 1.6 m if permafrost were to thaw.

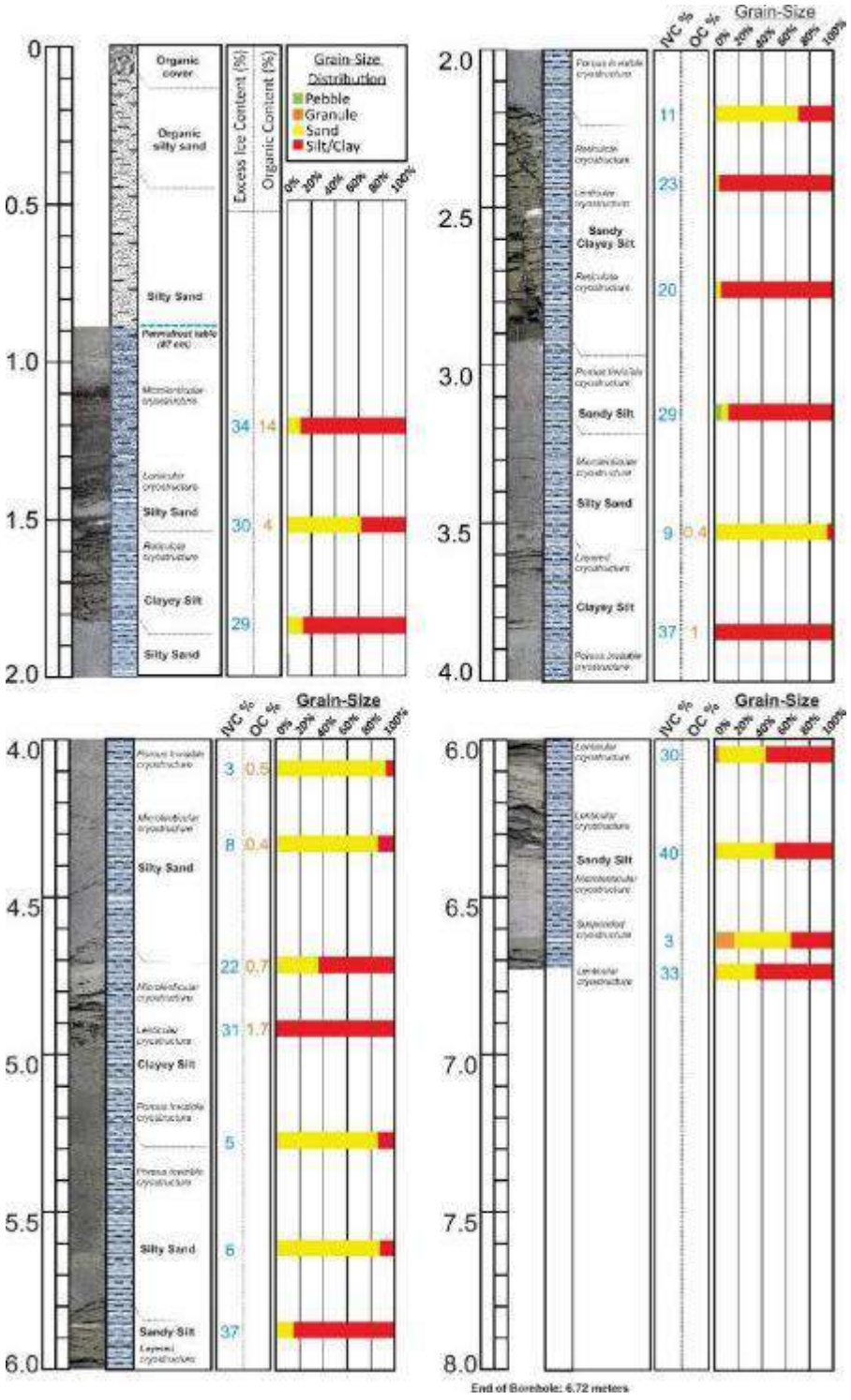

FIGURE 16 BOREHOLE LOG FOR AIS_BH01 (*PALSA* SITE) WITH SOIL TEXTURE, ORGANICS AND GROUND ICE CONTENT.

The borehole AIS_BH01 (*Palsa* Site) was lined with PVC piping and instrumented with two 4-channel Hobo loggers to record ground temperatures at depths of 0, 0.5, 1.0, 2.0, 3.5, 5.0, and 6.84 m. The recording started July 31st, 2019. Data was last downloaded on February 27th, 2024, providing over four full years of monitoring. A data gap exists between October 12th, 2022 and March 6th, 2023 because PGR could not recollect the data for this period. Ground temperature profiles for September 1st for years 2020 – 2023 are presented in Figure 17. This figure shows that active layer thicknesses on these dates are approximately 1.7m, 0.9m, 1.0m, and 1.2m, respectively. Figure 18 presents a time series of ground temperature for AIS_BH01 recorded from January 1st 2019 to January 1st, 2024. Variations in the maximum active layer thickness between years does not appear to exhibit any trend and is thus interpreted as stable. Ground temperatures between 1–2m depth in Figure 18 sometimes become warmer than 0°C during winter. This is probably the continued downward movement of heat from the summer into the ground. This is a common phenomenon in permafrost-affected ground and is further protracted by the release of latent heat by subsequent re-freezing in later winter months if the ground is moist or wet.

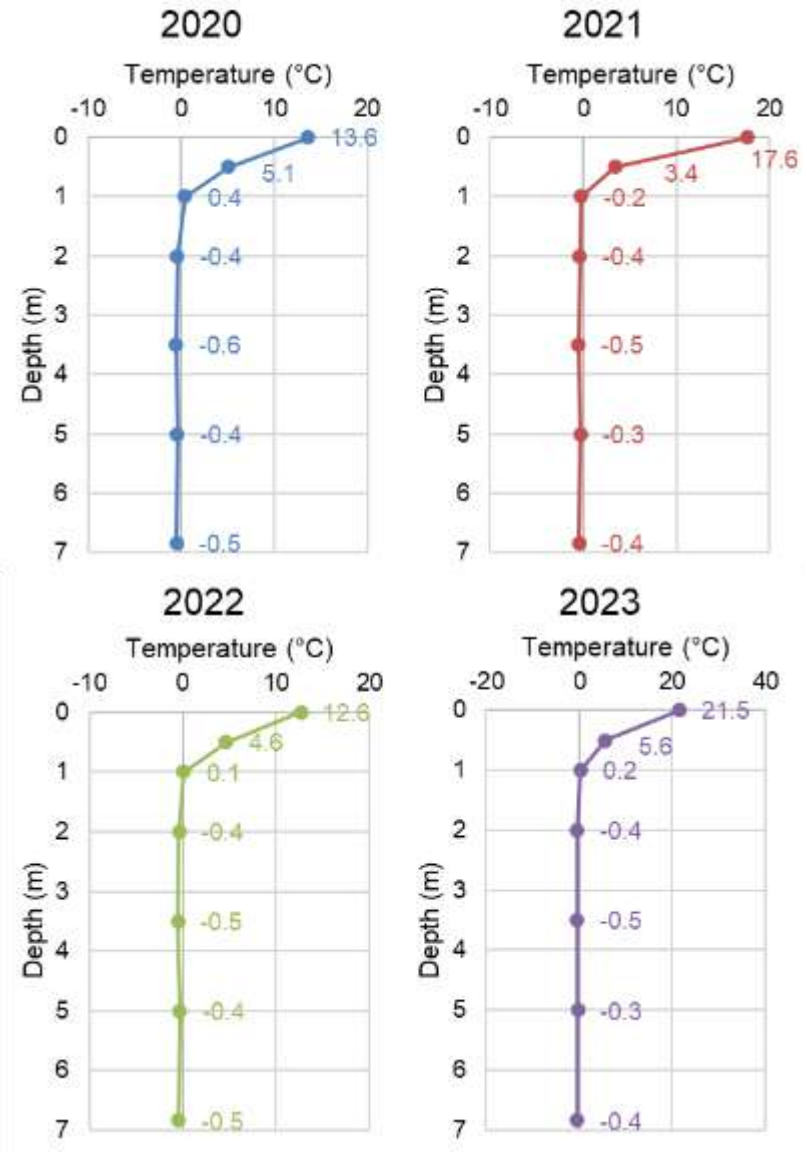

FIGURE 17 GROUND TEMPERATURE PROFILES ON SEPTEMBER 1ST FOR YEARS 2020 – 2023 FROM AIS_BH01 (*PALSA* SITE).

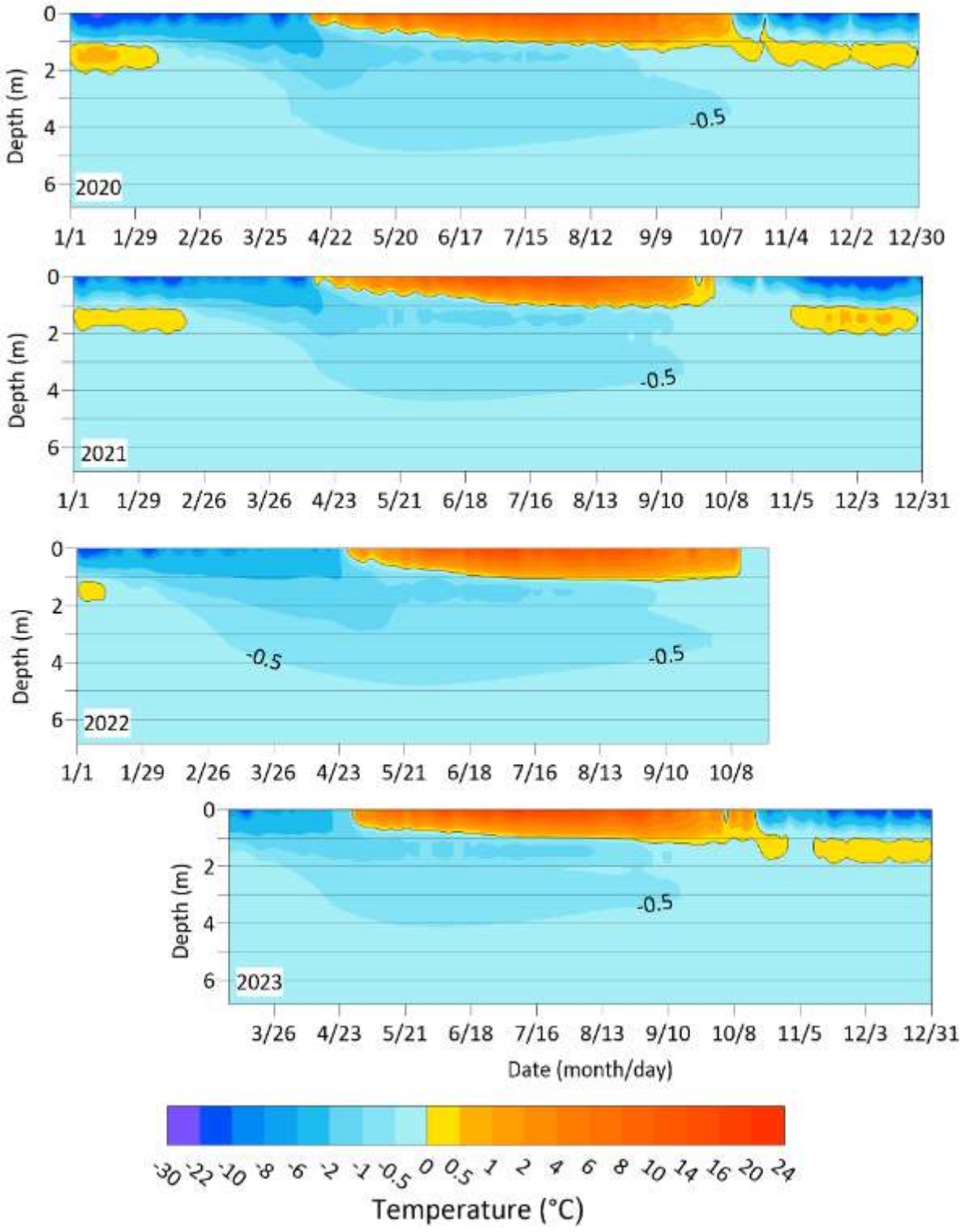

FIGURE 18 GROUND TEMPERATURE FOR AIS_BH01 (*PALSA* SITE) FROM JULY 2019 TO FEBRUARY 2024.

To assess permafrost distribution underneath the study site, an 80-m ERT survey was conducted from the lake shore to the hillside using the dipole-dipole and Wenner arrays. The ERT profiles for this survey are presented in Figure 19. Both the dipole-dipole and Wenner profiles suggest that permafrost is present, where highly resistive areas, (blue colors), represent frozen ground and less resistive areas, (red colors), represent unfrozen ground. While the Wenner profile shows a single uninterrupted frozen layer across the length of the profile (marked with "P" in Figure 19), with ice-rich ground located on the hillside (marked by "ice" in the same figure), the dipole-dipole profile shows a more detailed characterization of ground resistivity, with ice-rich ground also present near the lake shore. The lake shore ground ice is most likely derived from water that saturated the sediment when the lake level was higher. Also, the dipole-dipole survey has a greater depth of investigation and reveals a deep unfrozen section between 30 and 40 m along the transect (marked by "unfrozen" in Figure 19). The top 2 meters of both profiles appear either ice-poor or unfrozen, which is consistent with the ground temperature records from borehole BH1 (Figure 18).

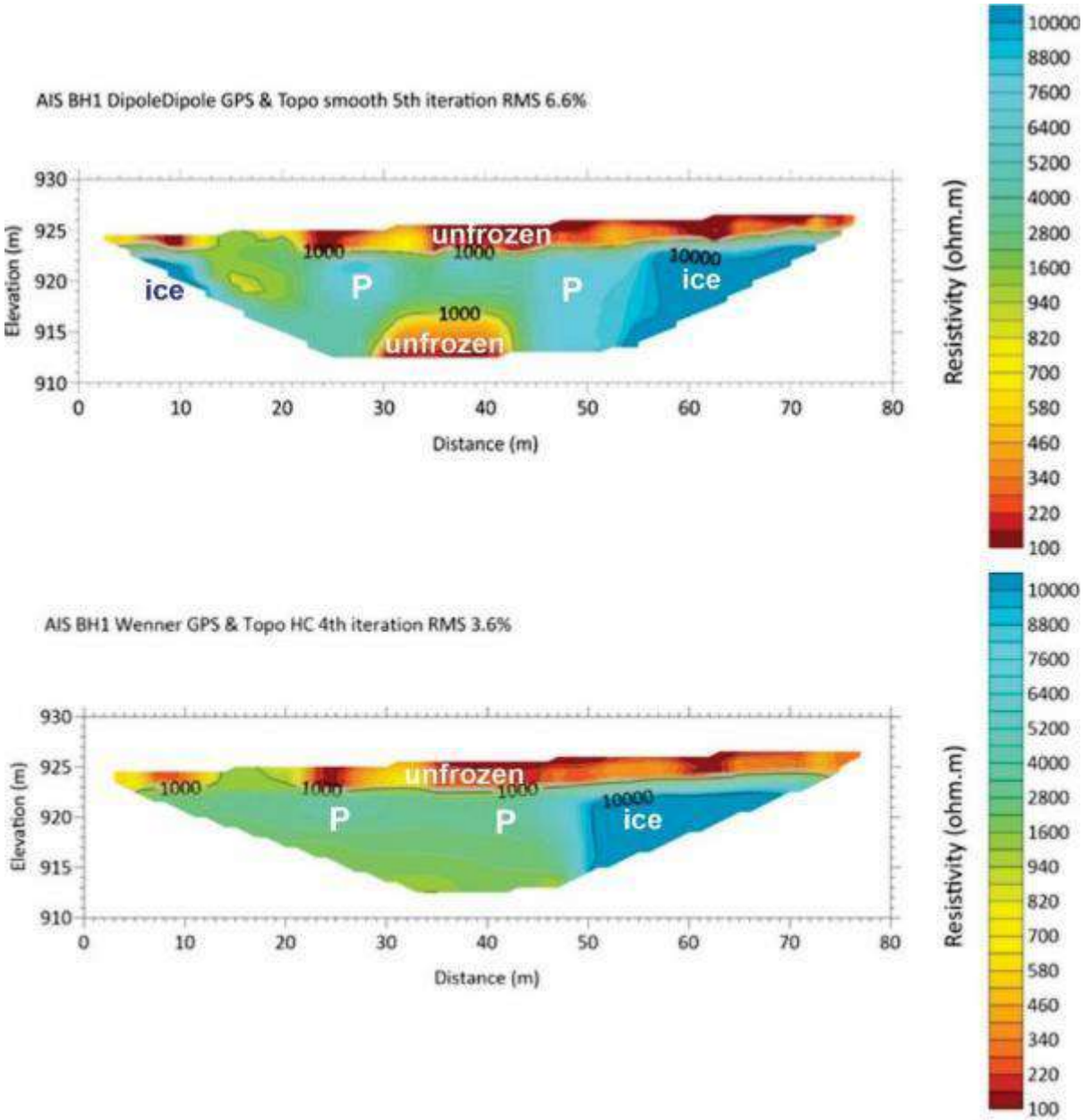

FIGURE 19 ELECTRICAL RESISTIVITY PROFILES AT THE *PALSA* SITE NEXT TO ÄSHÈYI. "P" REPRESENTS POTENTIAL PERMAFROST AREAS, "ICE" INDICATES POTENTIAL ICE-RICH AREAS, AND "UNFROZEN" SHOWS THE NON-PERMAFROST ZONES SUCH AS THE ACTIVE LAYER.

6.2.3 Äshèyi Old Settlement Site

The peninsula where the old Äshèyi settlement is located was surveyed by drone in August 7th, 2021. The orthomosaic produced by this survey is show in (Figure 20). A borehole was drilled (Figure 23) and

ground temperature station, with sensors at 0m, 0.5m, 1m, 1.5m, 2m, 2.5m, 3m and 4.45m depth, was installed in summer of 2023 to assess ground ice and ground temperature properties. The ground temperature data are displayed in Figure 25 and Figure 26. An ERT dipole-dipole survey was also conducted to assess the spatial extent of frozen ground (Figure 27).

The observations collected through the drone survey on August 7th, 2021 had two main objectives: first, to identify and locate heritage buildings on the peninsula; and second, to observe and locate signs of permafrost and/or degradation.

Three heritage sites were identified (No. 1, 3, and 4 in Figure 20 and Figure 21). Two sites were identified along the lake shore (1- northwest part of peninsula; 4- southeast part of peninsula), and a third one inland (3- north part of peninsula). While the southern shore site (4) does not seem to be impacted by a retreat of the shore; the northwestern site (1) appears to be threatened as one of the building's footprints is nearly in the water (lower arrow in panel 1, Figure 21). It is not clear if the retreat of the shore is attributable to wave erosion or permafrost-related subsidence of the ground surface. Dark, wetter areas suggest that subsidence may be occurring in this area (arrows in 2, Figure 21). Water saturation seems to be the main process driving subsidence. Similar darker ground surface areas also are visible surrounding heritage buildings at the inland (3) and southern (4) sites (see arrows in panels 3 and 4 of Figure 21).

Several markers of permafrost thaw appear to be visible on the aerial imagery. As for some of the heritage sites, darker, wetter spots are visible across the peninsula such as those visible in Figure 22, image 5. There, the dark colours suggest that vegetation has died, and organic soil is visible. This could be due to subsidence resulting from the thaw of ice-rich permafrost as is occurring at the *Palsa* site (section 6.2.2), on the other side of the lake. Another potential indicator of permafrost thaw is the presence of several nearby ponds that could be of thermokarst origin, i.e. resulting from subsidence as ice-rich permafrost thaw. Collapsing trees and vegetation along the edges of these ponds also suggest permafrost degradation (Figure 22, site 6 and 7). The trees, which are collapsing towards the ponds, suggest that the edges are receding, and the ponds are expanding. This process is consistent with permafrost degradation, though increasing water level cannot be excluded as the driver of these changes.

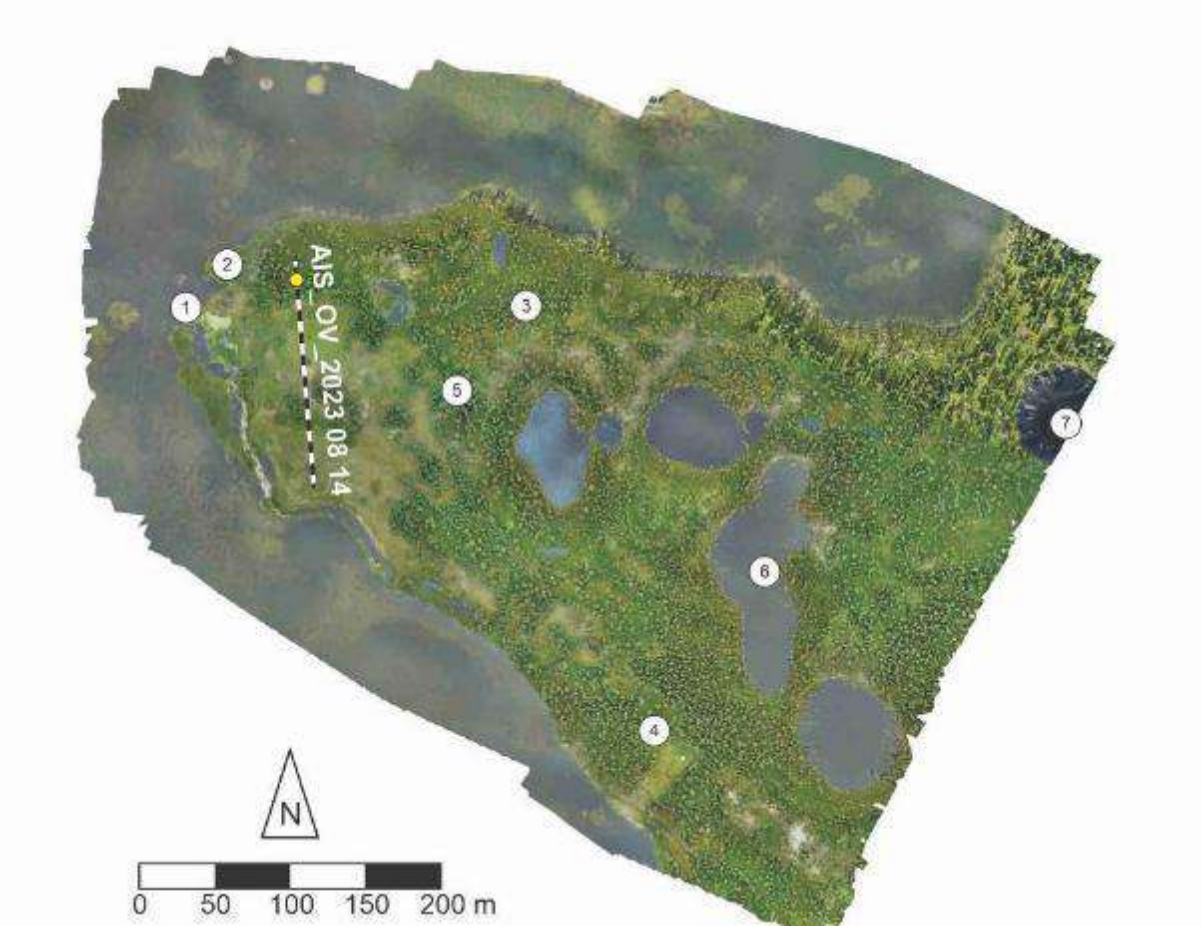

FIGURE 20 AERIAL IMAGERY OF THE OLD ÄSHÈYI SETTLEMENT. SYMBOLS MARK SITES OF INTEREST (DETAILED IN NEXT FIGURES): 1- HERITAGE BUILDINGS; 2- DEGRADATION IMPACTING HERITAGE BUILDINGS; 3- HERITAGE BUILDING; 4- HERITAGE BUILDINGS; 5- DEGRADING AREAS; 6- DEGRADING POND EDGE; AND 7- DEGRADING POND EDGE. DASHED LINE REPRESENTS THE ERT SURVEY. YELLOW DOT IS THE LOCATION OF THE BOREHOLE.

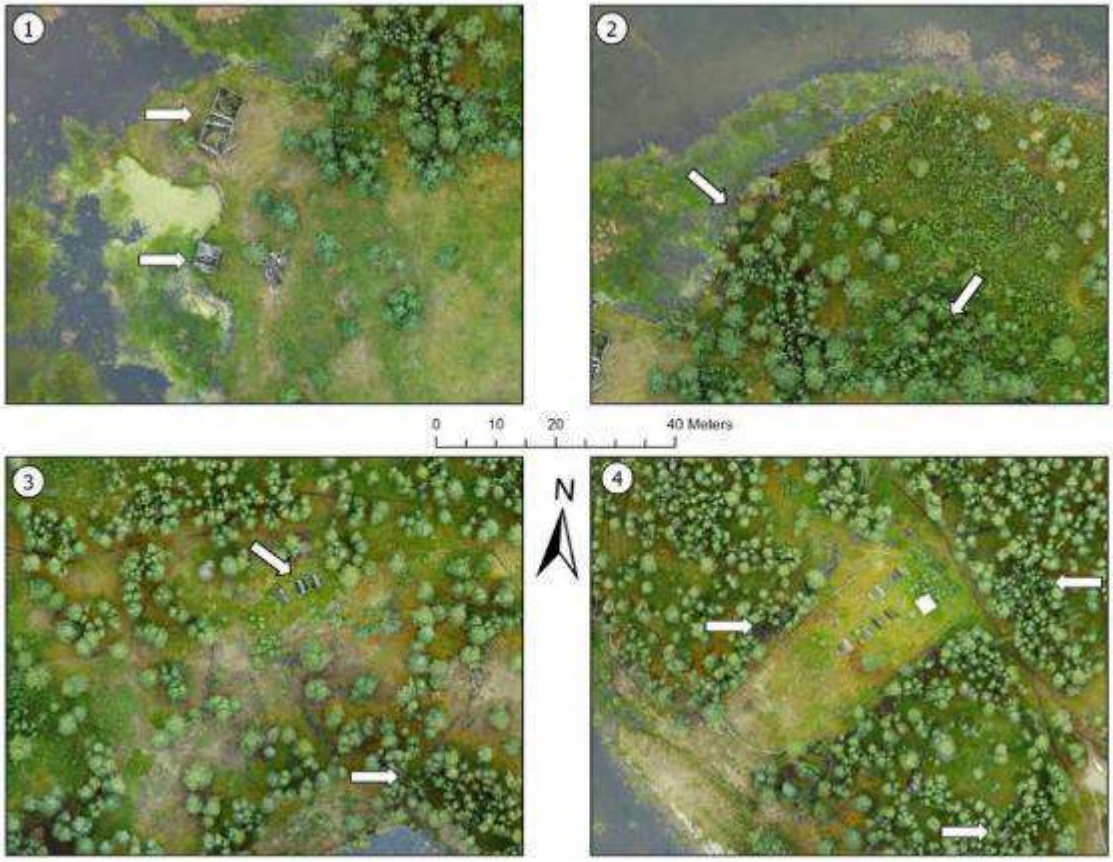

FIGURE 21 HERITAGE SITES OBSERVED USING DRONE IMAGERY AT 3 DISTINCT LOCATIONS IN THE OLD ÄSHÈYI SETTLEMENT. CABINS AT THE NORTHWEST END OF THE PENINSULA (1) THREATENED BY SHORE EROSION AND COLLAPSING TO THE NORTH (2); ISOLATED CABIN SURROUNDED BY WET AREAS (3); AND ENCLOSED PLOT AND BUILDINGS AT SOUTHERN SHORE (4).

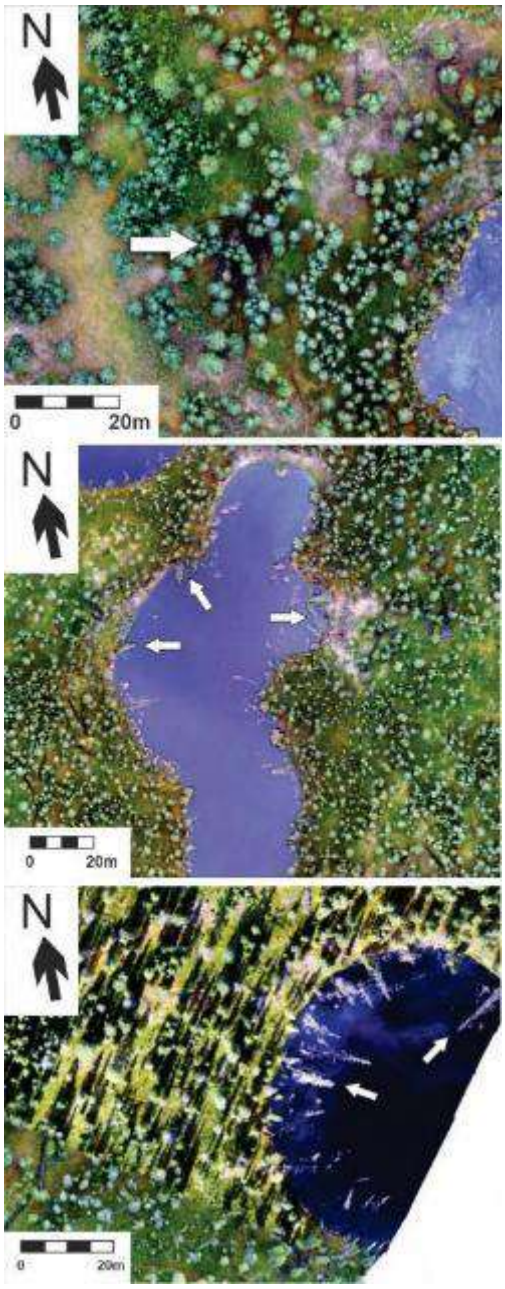

FIGURE 22 EXAMPLES OF INDICATORS OF POTENTIAL PERMAFROST DEGRADATION ON THE OLD ÄSHÈYI SETTLEMENT PENINSULA. DARK, WET AREAS ARE POTENTIAL INDICATORS OF GROUND SUBSIDENCE (5), POND EDGES WITH COLLAPSING TREES (6, 7).

In August 2023, a borehole was drilled (AIS_BH05) at *Äshèyi Old Settlement* to assess the sediment and ice properties of the soil, and an ERT survey was conducted to investigate the lateral extent of these properties. The grain size in the sediment profile coarsens upwards, reflecting a shift from an ancient lakebed to a higher-energy shoreline environment, probably because of dropping lake level. The ground beneath *Äshèyi Old Settlement* is exceedingly ice-rich (13 – 93%) and increases in excess ice

with increasing depth (Figure 23). This ground ice formed when past lake level receded, and the underlying sediments were exposed to a post-glacial climate with air temperatures colder than today. The sediment was saturated with water, which allowed thick lenses and layers of ground ice to form by ice segregation when the frost progressed downward into the ground. The core contains primarily layered and reticulate cryostructures. Both the cryostructures and high ice contents are similar to those found at the Palsa site. The pore ice in the sandy (upper) part of the core is the typical cryostructure found in sands, where the ice segregation process is less effective. By adding up the thicknesses of the excess ice structures in the core, a surface subsidence of approximately 2 m is to be expected if the section of ground represented by the core were to thaw. This is similar to the cumulative excess ice estimation, which predicts approximately 1.75m of subsidence (Figure 24).

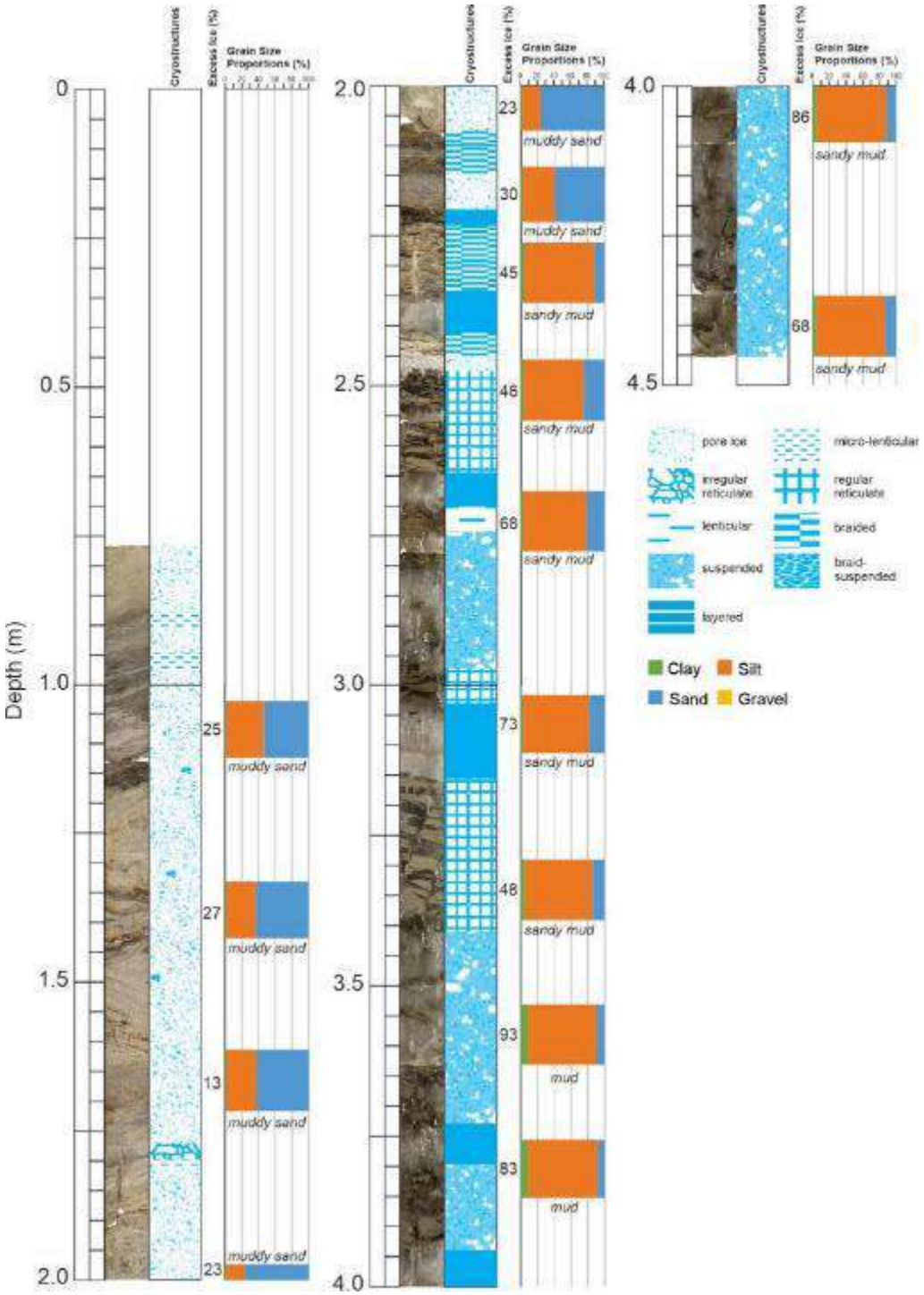

FIGURE 23 GEOTECHNICAL LOG OF THE BOREHOLE DRILLED AT *ÄSHÈYI OLD SETTLEMENT* (AIS_BH05) IN AUGUST 2023.

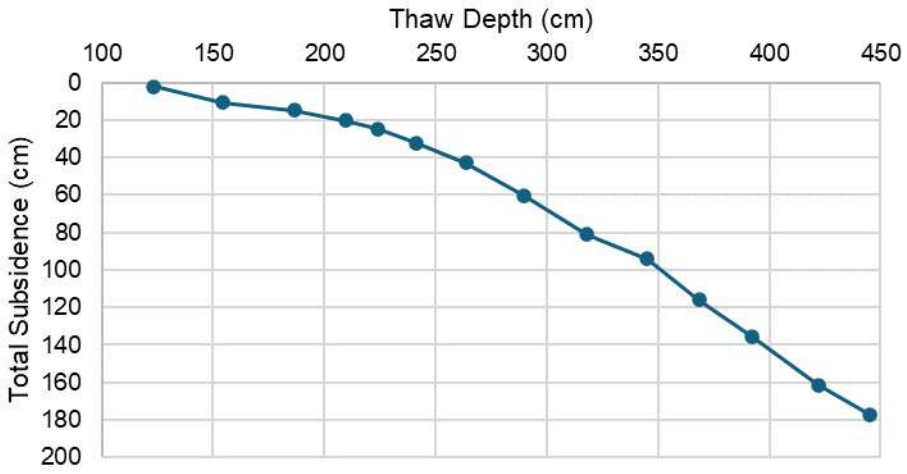

FIGURE 24 CUMULATIVE THAW SUBSIDENCE MODELLING FOR AIS_BH05 (*ÄSHÈYI OLD SETTLEMENT*) USING EXCESS ICE VALUES.

Ground temperature data recorded in borehole AIS_BH05 from late August 2023 to late February 2024, a little over six months, is presented in Figure 26. Although this does not constitute full-year recording, it shows that the maximum active layer thickness in 2023 was around 110cm depth. This agrees well with the temperature profile for September 1st, 2023 presented by Figure 25. The summer heat wave continued to propagate deeper than 110cm even after active layer freeze-back, raising permafrost temperatures, though not greater than 0°C. Small periods of above-0°C ground temperature were observed below approximately 110cm (small yellow regions Figure 26) between August 20th and January 1st. These could indicate temporary intrusion of ground water, but could also be an artifact resulting from both the interpolation process used to produce this graph and the precision of the loggers when ground temperatures are at 0°C. The cold winter temperature wave begins to follow the 2023 summer heat wave in late winter (circa January 30th of 2024), re-cooling the ground.

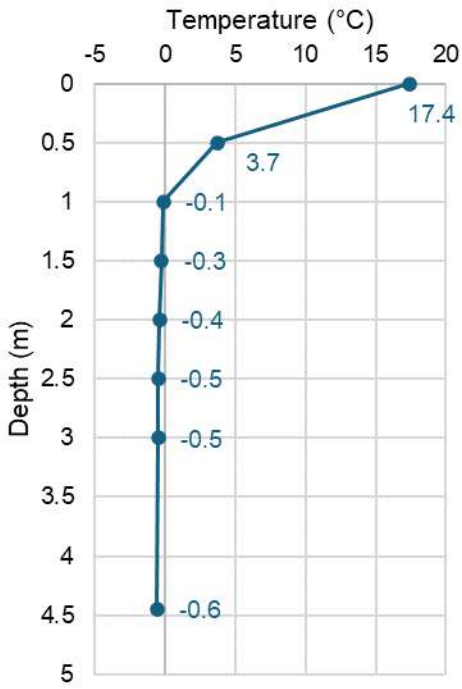

FIGURE 25 GROUND TEMPERATURE PROFILE OF AIS_BH05 (*ÄSHÈYI OLD SETTLEMENT*) BOREHOLE ON SEPTEMBER 1ST, 2023.

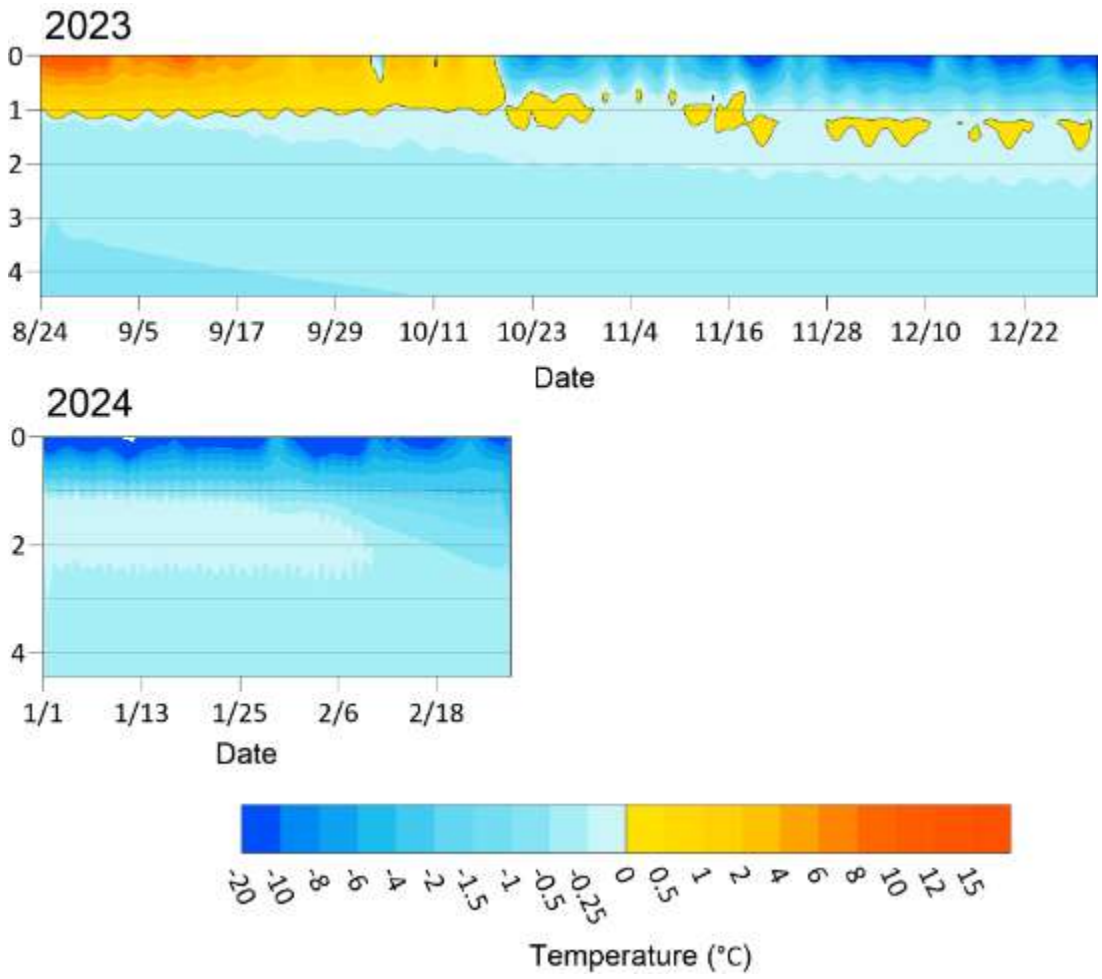

FIGURE 26 TIME SERIES OF GROUND TEMPERATURE IN THE AIS_BH05 (*ÄSHÈYI OLD SETTLEMENT*) BOREHOLE.

An ERT dipole-dipole survey was conducted on site to extend the observations from the AIS_BH05 borehole and to investigate the lateral extent of ground properties. The ERT profile intersects the borehole location at 25m distance (Figure 27). The root-mean-squared (RMS) error of the survey was greater than ideal, meaning there may be higher inaccuracies. However, the profile still provides a good enough picture to assess the general ground ice distribution. At the borehole AIS_BH05 location, the profile shows blue hues which can be interpreted as highly resistive, ice-rich ground areas, as observed in the borehole. Any highly resistive areas observed in the profile can be assumed to possess similar properties to the ice-rich core sampled from the borehole. Those high-resistivity areas (approximately 600,000 – 800,000 ohm-m) are visible from the start of the ERT profile to 65 m distance (dark blue region), then from 75 m to 90 m, and from 95 m to 125 m distance. The middle ice-rich area and the south (right end of the figure) area seem to extend deeper into the ground profile. These deeper regions are possibly buried relict bodies of glacial ice. If this is the case, at least some of the thermokarst lakes to the east of the site (Figure 20) may be kettle lakes. This matter is further discussed in section 4.2.5, including Figure 38 on the process of glacial ice burial and development of kettle lakes.

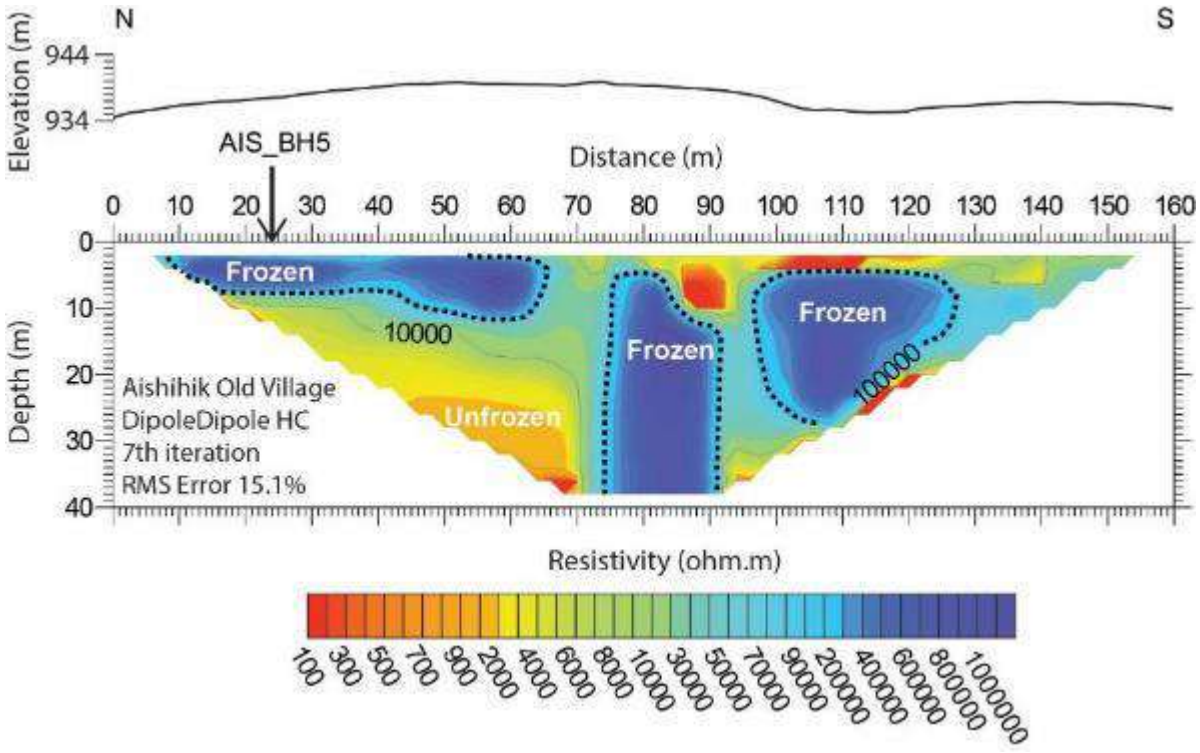

FIGURE 27 ERT DIPOLE-DIPOLE SURVEY OF GROUND ICE EXTENT ON THE WESTERN END OF THE OLD ÄSHÈYI SETTLEMENT PENINSULA.

6.2.4 Pingo Site

The pingo near Äshèyi is a landform located about 750 m northeast of the northern end of the Äshèyi airstrip (Figure 10).

FIGURE 28 AERIAL IMAGERY OF THE PINGO NEAR ÄSHÈYI AND ERT SURVEYS PRESENTED IN THIS WORK.

A pingo is a dome-shaped mound consisting of a layer of soil over a large core of ice, that form in permafrost landscapes. Pingos are classified as either open-system pingos (hydraulic pingos) or closed-system pingos (hydrostatic pingos). Open-system pingos are formed by the doming of frozen ground due to the freezing of injected water from groundwater moving downslope through taliks (unfrozen ground zones) to the site of the pingo, where it moves towards the surface (Figure 29, left). Closed-system pingos are formed by the doming of frozen ground due to the freezing of water injected by the expulsion of pore water during permafrost formation in the closed talik under a former water body (Figure 29, right).

The Äshèyi Pingo has previously been studied by Geurts and Dewez (1985) in 1984. Figure 30 shows the pingo in a photograph from the 1984 study, and one taken in 2021. There does not appear to be any noticeable differences between the two photographs, suggesting that the shape of the pingo has remained stable over the last 37 years.

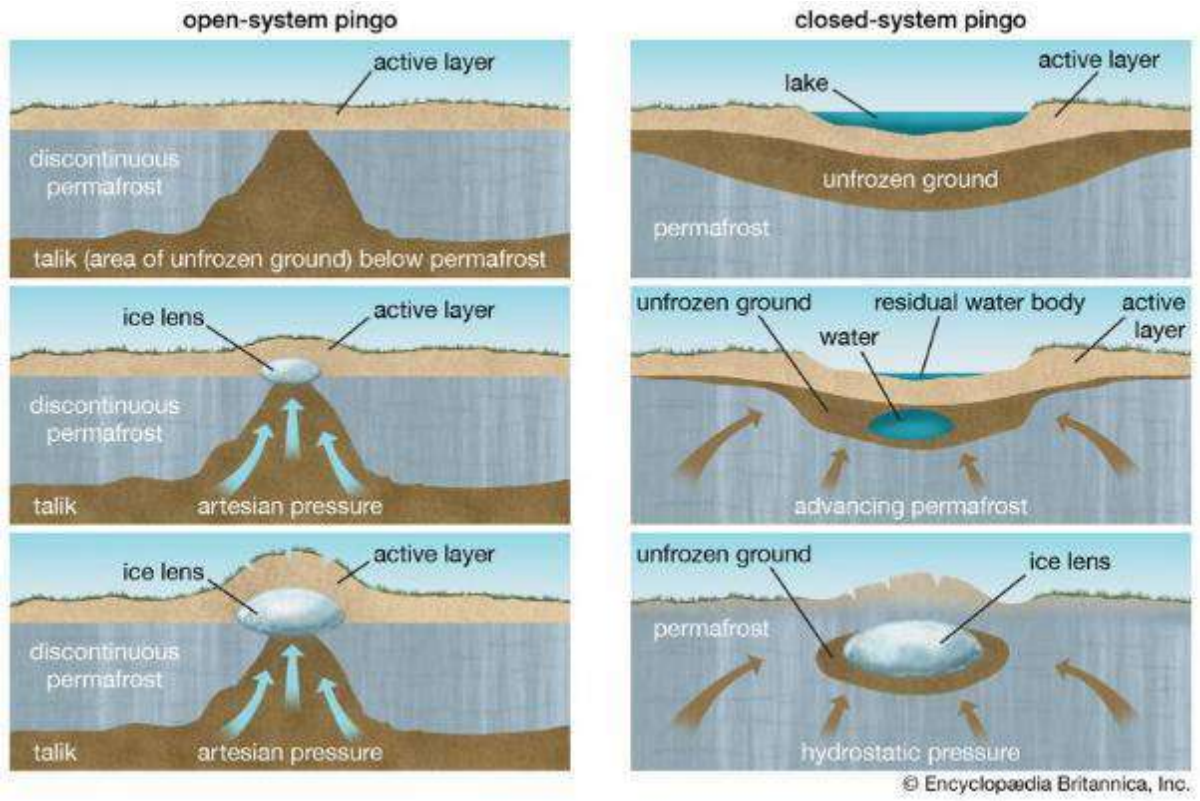

FIGURE 29 FORMATION OF PINGOS: LEFT) OPEN-SYSTEM PINGO; RIGHT) CLOSED-SYSTEM PINGO.

FIGURE 30 PICTURES OF THE ÄSHÈYI PINGO TAKEN IN 1984 BY GEURTS AND DEWEZ (TOP) AND IN 2021 BY THE YUKON UNIVERSITY TEAM.

During their study, Geurts and Dewez created a north-south topographical profile of the pingo that the YukonU team attempted to reproduce in the summer of 2019. The comparison between the 1984 and 2019 topography is presented in Figure 31. The survey suggests that the pingo may have grown by as much as 1 meter during the 35-year time-period.

Altogether, the field surveys suggest that the pingo has not undergone degradation since 1984 and instead may have continued to grow.

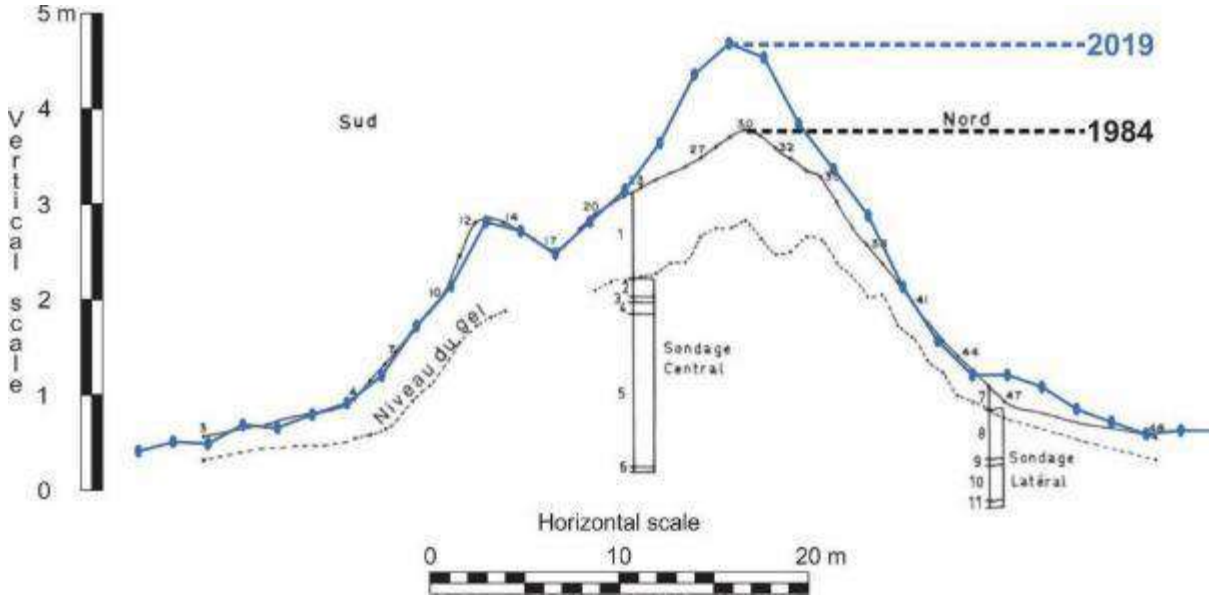

FIGURE 31 COMPARISON BETWEEN 1984 AND 2019 TOPOGRAPHICAL SURVEYS OF THE ÄSHÈYI PINGO.

The borehole AIS_BH02 (*Pingo*) was drilled at the highest elevation of the Äshèyi Pingo, in a central location (Figure 31). The cores were collected down to a depth of 6 m. The thaw front was at a depth of 190 cm at the time of drilling (July 28th, 2019). The log (Figure 32) shows an unfrozen organic silty sand layer down to between 20–40 cm depth, followed by unfrozen sandy silt with gravel collected with a hand-auger down to 190 cm. Below 1.90 m, an ice-rich gray sandy silt layer extends to 225 cm depth, where pure ice was encountered. The pure ice extended down to about 5.10 m, where gravely, silty and sandy sediment returned down to 6.0 m depth, which was the end of the borehole. Below the pure ice, centimeter-scale ice lenses are visible all along the profile in the silty and sandy material, with volumetric excess ice content ranging from 27 to 65%. Overall, the borehole has a mean volumetric excess ice content of 42%. The cumulated ice content represents a potential subsidence of 3.4 m if permafrost were to thaw.

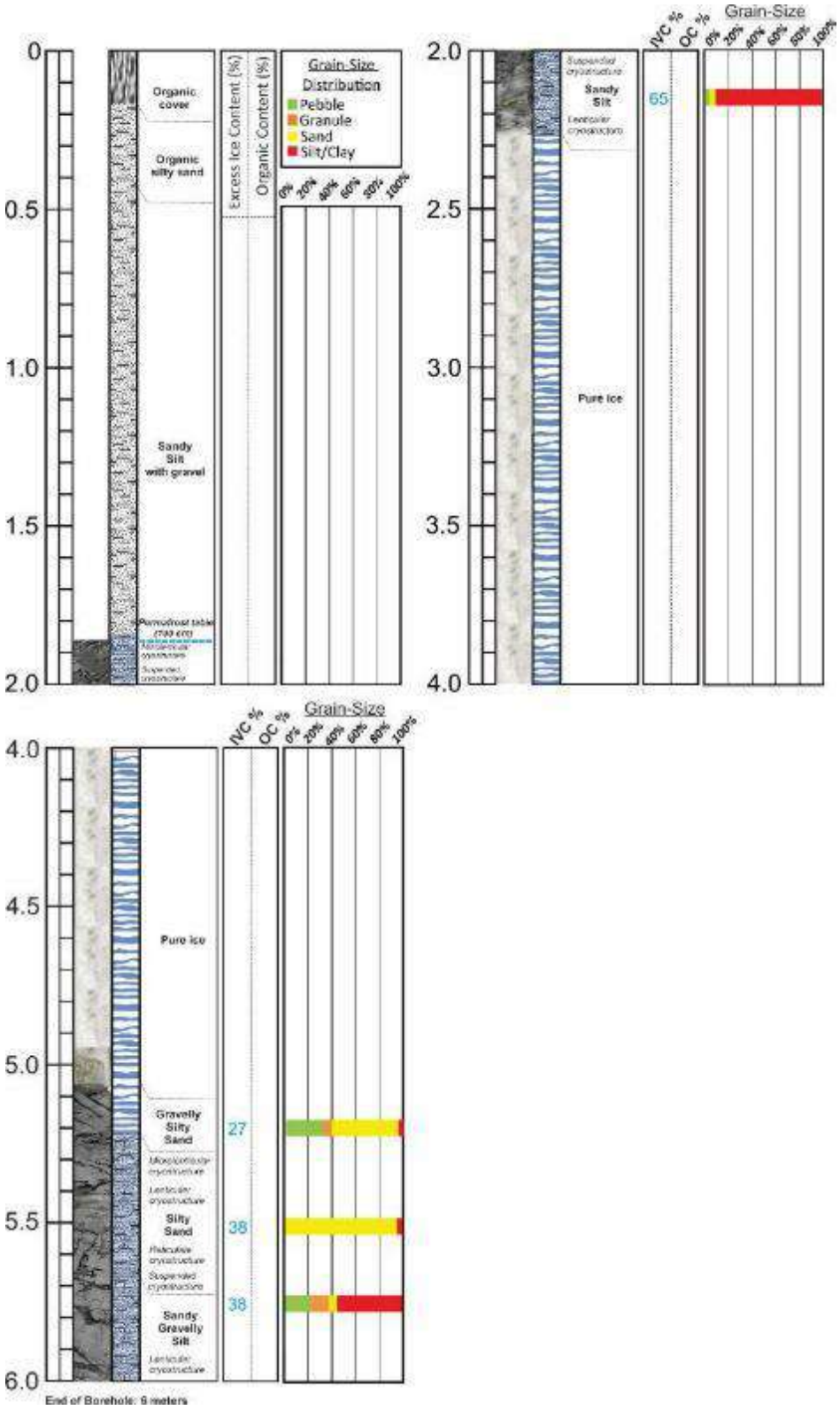

FIGURE 32 BOREHOLE LOG OF BH02 (*PINGO*) WITH SOIL TEXTURE, ORGANICS AND GROUND ICE CONTENT.

The borehole AIS_BH02 (*Pingo*) was lined with PVC piping and instrumented with two 4-channel Hobo loggers to record ground temperatures at 0, 0.5, 1.5, 2.0, 2.5, 4.0, and 6.0 m depths. The recording started August 1st, 2019. Data were last downloaded on February 26th, 2024, providing four full years of monitoring. Figure 33 shows ground temperature profiles on September 11th (the approximate date of maximum thaw depth) for the years 2020, 2021, 2022 and 2023. This figure indicates maximum thaw depth was 2m in all years except 2023, for which it was about 2.25m. A time series of ground temperature data for borehole AIS_BH02 (*Pingo*) is presented in Figure 34. This time series indicates maximum thaw depth is generally around 2.25m depth but can reach down as far as 2.4m depth. These depths are slightly deeper than those presented in Figure 33. This is likely due to the interpolation process used to create the time series plot. Nevertheless, the time series plot indicates that thaw depth is very consistent from year to year at depths that roughly correspond to the interface between the overlying soil and underlying massive ice that forms the pingo core. The blue region of the time series, representing temperatures between -2 to -6°C, pinches out sooner each year, indicating that ground temperature deeper in the borehole (below ~2.5m) began increasing in temperature earlier each year from 2020 to 2023. Although these deeper temperatures are still shallow enough to respond to annual surface temperatures swings, ground temperature tends to respond increasingly more to longer term temperature variations with increasing depth. This is due to the time required for

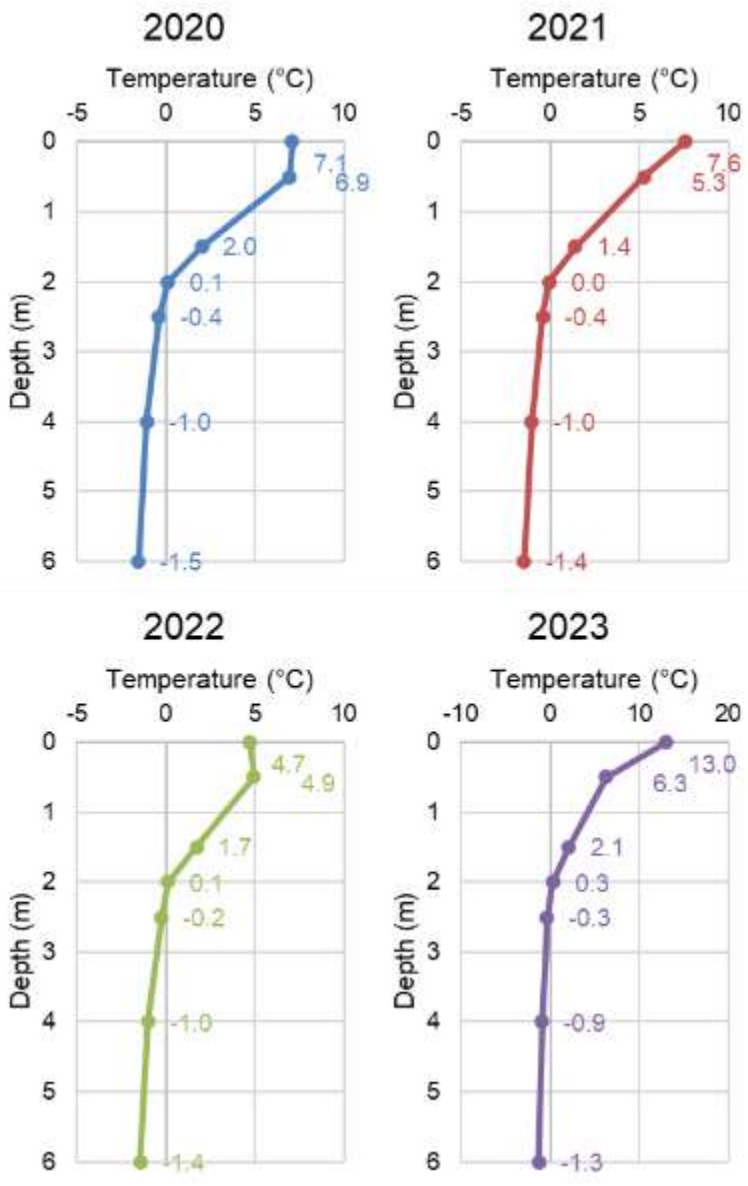

FIGURE 33 GROUND TEMPERATURE PROFILE IN BOREHOLE AIS_BH02 (*PINGO*) ON SEPTEMBER 11TH FOR 2020, 2021, 2022 AND 2023.

temperature changes to propagate deeper into the soil profile. Therefore, it is possible that this warming trend was partly driven by general climate trends spanning (in the order of) several years prior to 2020. However, it is difficult to say this with certainty because thermal swings travel faster through pure ice like the core of this pingo than through ice-soil mixtures, theoretically resulting in a more immediate temperature response at depth to surface temperature changes.

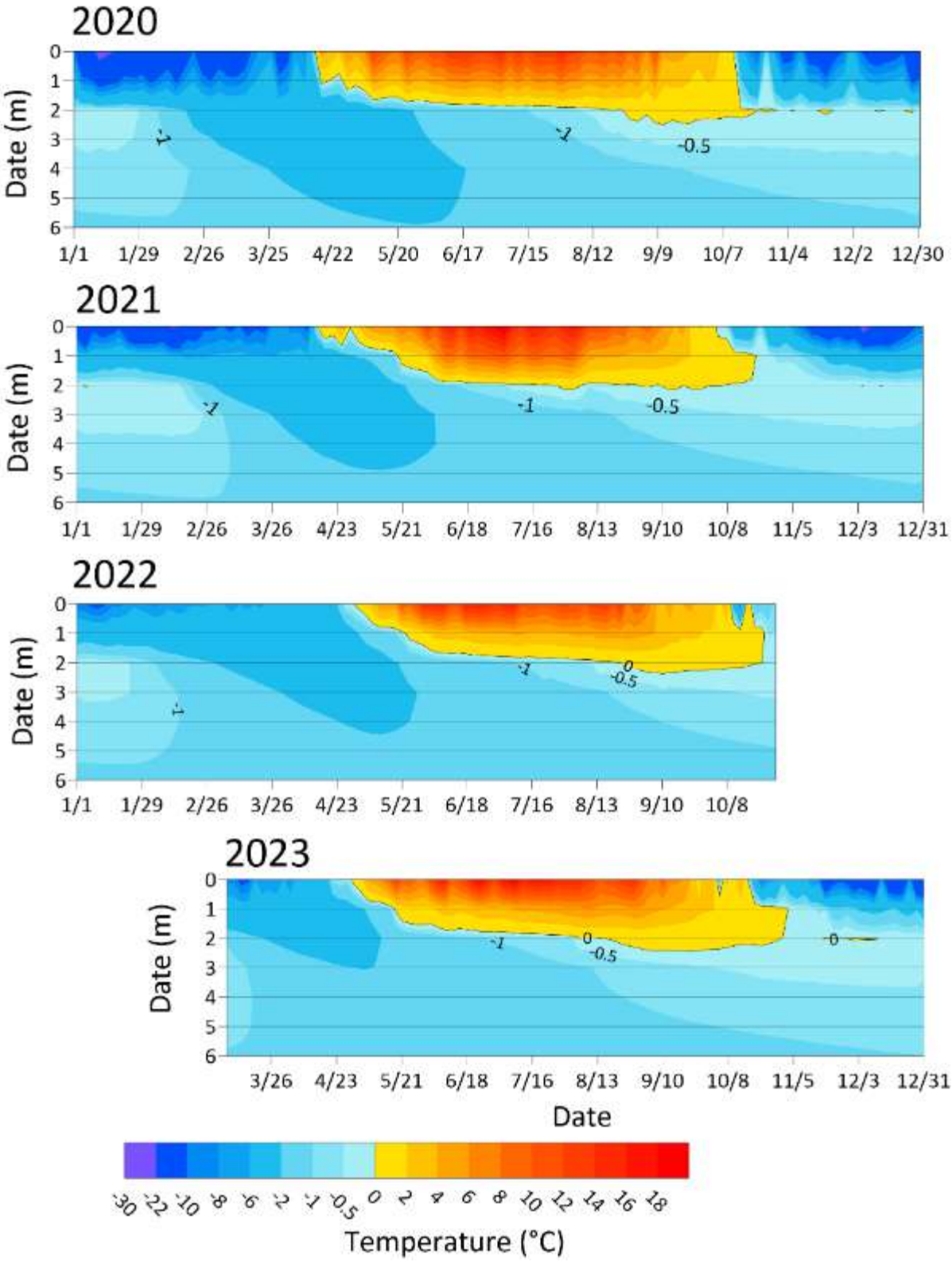

FIGURE 34 GROUND TEMPERATURE OF AIS_BH02 (*PINGO*) FROM JULY 2019 TO FEBRUARY 2024.

To assess permafrost distribution underneath the observation site, two ERT surveys, line A and line B, were conducted, intersecting orthogonally at their midpoint, located at the summit of the pingo (Figure 28). ERT line A is 200 m long and has a north-south orientation, while ERT line B is 160 m long and has an east-west orientation. Both lines were surveyed using dipole-dipole and Wenner arrays. The ERT profiles of these surveys are presented in Figure 35. Both the dipole-dipole and Wenner profiles along line A suggest that permafrost is present. Highly resistive areas (green and blue colors) represent frozen ground (marked "P") and less resistive areas (red colors) represent unfrozen ground. The low resistivity areas are located close to the surface, they are either related to the active layer (the layer of soil that thaws each summer and re-freezes in the fall) or to wet areas. The Wenner and dipole-dipole surveys appear to be very similar, with dipole-dipole showing higher resistivity overall. Ice-rich ground, marked by "ice" in Figure 35, is located just below the pingo, at the center of the profiles. This represents the pure-ice core of the pingo sampled in the borehole AIS_BH02. The presence of such high-resistivity material affects the ERT surveys and makes it appear as though the material extends deeper than it really does. This artifact is less prominent in the dipole-dipole surveys.

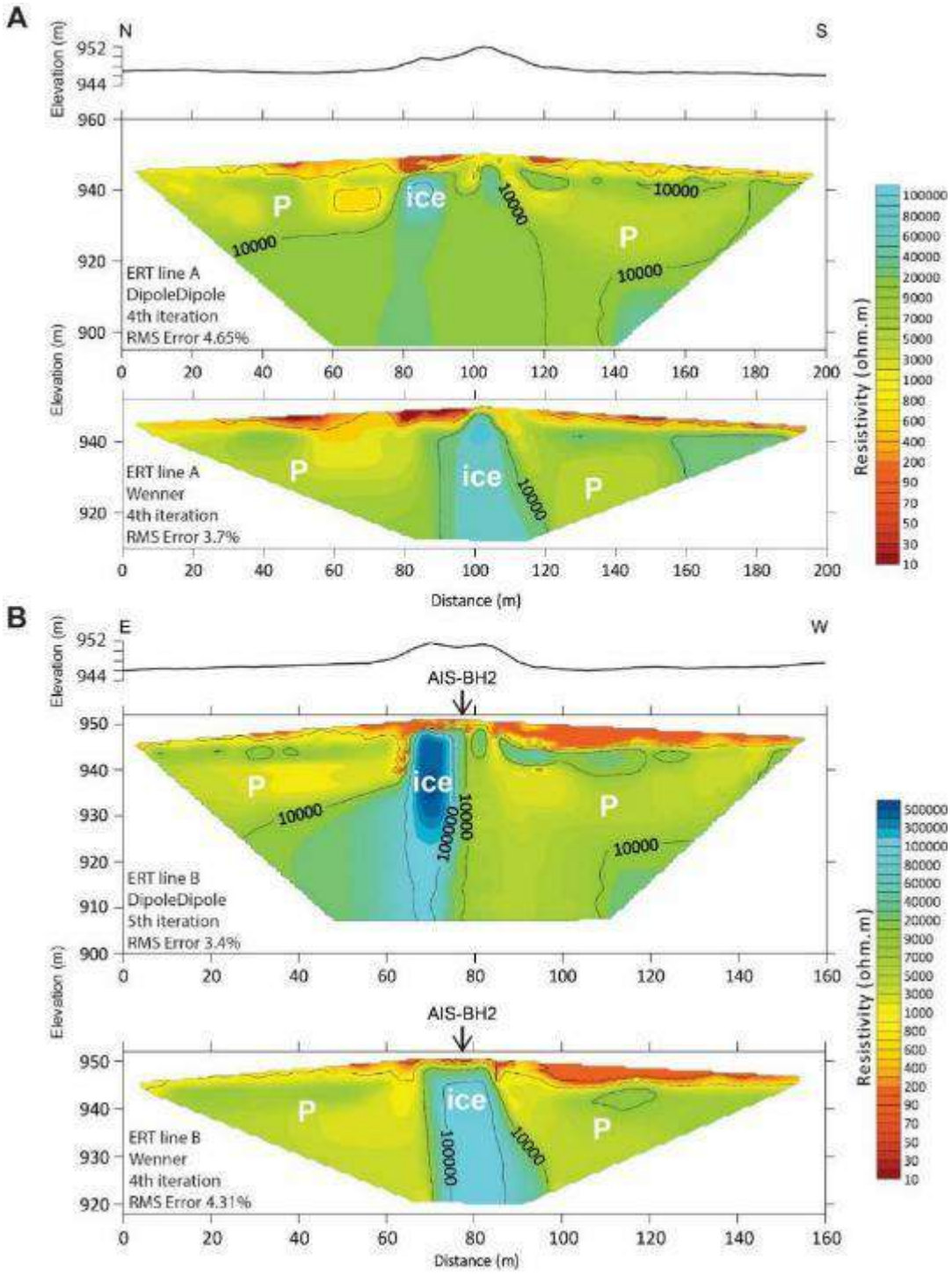

FIGURE 35 ELECTRICAL RESISTIVITY PROFILES A AND B AT *PINGO*. "P" MARKS POTENTIAL PERMAFROST AREAS, "ICE" INDICATES POTENTIAL ICE-RICH AREAS, AND "UNFROZEN" THE NON-PERMAFROST ZONES SUCH AS THE ACTIVE LAYER.

6.2.5 Kettle Pond Site

Among the various sites visited in the summer of 2021, a pond located about 500m southeast of Stevens Lake drew attention. The site was only accessible by quad and therefore was only visited and not surveyed. Because of its geomorphology, the site has been called *Kettle*. The pond is circular in shape and is located in a forested area (Figure 36 and Figure 37) in a deep depression surrounded by steep slopes. This suggests that a thermokarst process, where the ground surface is subsiding because ice is melting in thawing permafrost, is developing. This hypothesis is reinforced by the fact that the steep edge of the pond shows signs of collapsing with numerous longitudinal cracks forming around the pond. As the pond expands and the bank collapses, trees begin to lean and topple toward the pond (Figure 36 and Figure 37).

FIGURE 36 THE KETTLE POND SITE, WITH TILTED TREES AND SOIL CRACKING IN FOREGROUND.

FIGURE 37 THE KETTLE POND SITE, WITH TILTED TREES AND SOIL CRACKING IN BACKGROUND

The formation of the pond is likely due to thermokarst processes. This suggests that as permafrost is thawing a significant amount of ice is melting, which results in a depression that fills with water. The amount of ground-ice involved exceeds the amount present in permafrost mounds such as palsas or lithalsas, and no such mounds were observed in the vicinity of the site. The possibility of a degrading pingo does not seem likely because the site is located high in elevation compared to the surrounding area, which does not promote hydraulic formation processes, and a collapsing pingo usually results in an uplifted, rim-shaped boundary.

This analysis suggests that the pond may be a kettle, also called a kettle hole. Kettles are fluvioglacial landforms that occur as the result of blocks of ice calving from the front of a receding glacier that become partially to wholly buried by glacial outwash (Figure 38). When they are filled with water, they are called kettle lakes or ponds. Most kettles are circular in shape because melting blocks of ice tend to become rounded. Small kettles may be formed from ice blocks that were not left as the glacier retreated but rather were later floated into place by shallow meltwater streams. Kettles may occur by themselves or in groups. Several kettles were observed in the studied area; a fine example can be seen in front of the Shäkät Kų Hall in Äshèyi.

At the kettle site, the buried ice is still melting, and the lake is continuing to expand. This is a process that has been observed elsewhere in the Yukon, such as at kilometer 1840 of the Alaska Highway at the

Dry Creek rest area. At this site, similar thermokarst processes are driven by the melting of buried ice and has led Yukon Highways and Public Works to implement stabilizing and protective measures to ensure the safety of the road.

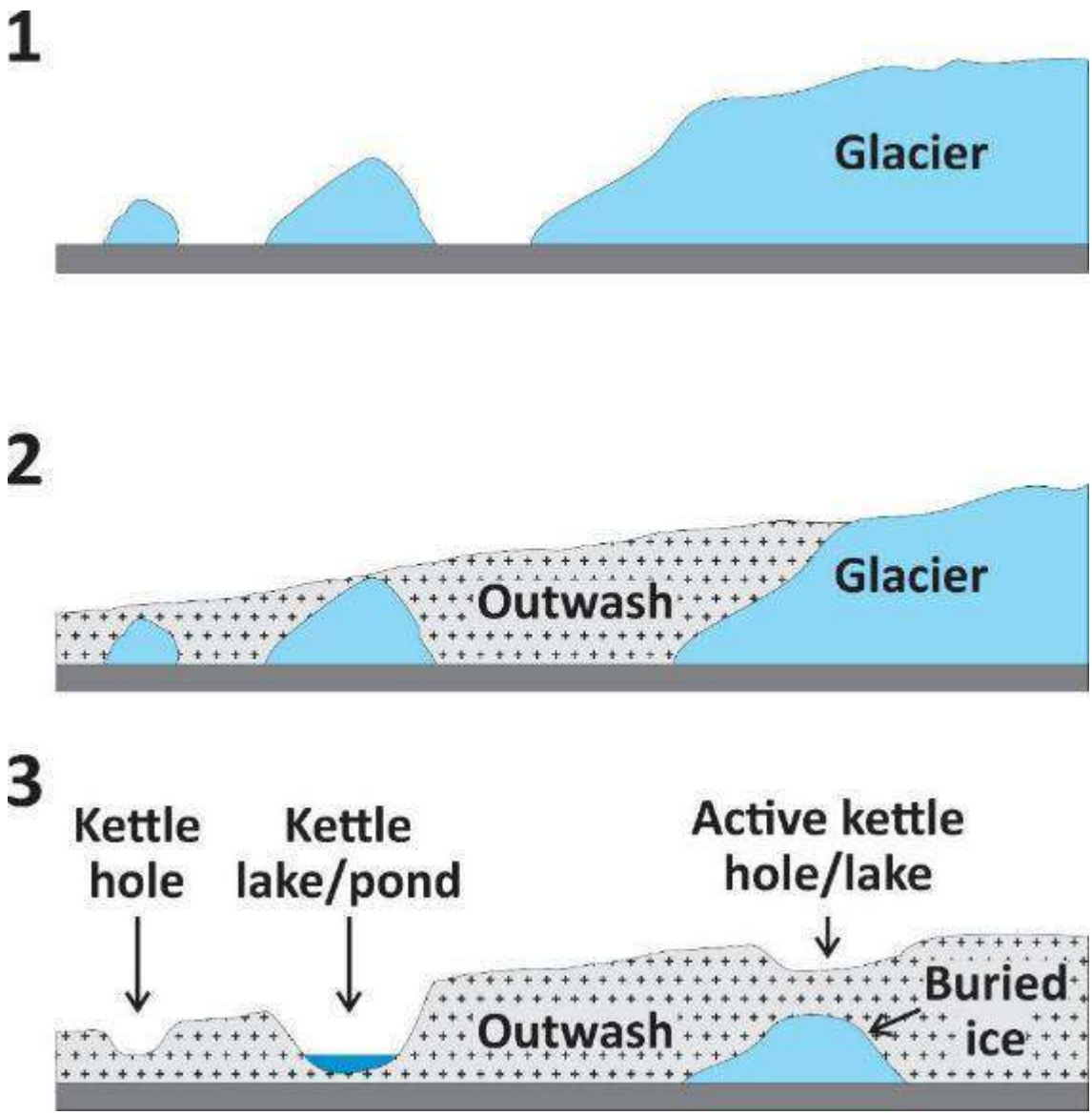

FIGURE 38 FORMATION OF KETTLES OR KETTLE HOLES. OUTWASH IS SEDIMENT THAT HAS BEEN LITERALLY WASHED OUT OF OR FROM UNDER THE ADJACENT GLACIER BY GLACIALLY SOURCED STREAMS AND RIVERS.

6.2.6 Summary of Sites in the Äshèyi Village Area

Permafrost is widespread in the Äshèyi community area, and its characteristics are influenced by the type of deposits that are present. Permafrost at the sites in this area was encountered in sediment that was deposited by water, either lacustrine (lakes) or fluvial (rivers). The permafrost encountered in lacustrine sediment contains more ground ice than in fluvial sediment, likely because of its finer grain size (texture). Fine-grained sediment like silts and clays are frost susceptible, which means that segregated ice (visible ice structures) is likely to form, and the soil will eventually become ice-rich. In these conditions, frost-heave will occur, forming mounds such as palsas, lithalsas, or permafrost plateaus.

The *Palsa* site, discussed in section 6.2.2, is a prime example of this type of landform that is encountered along lake shores or in other wet areas. When permafrost thaws and these landforms degrade, subsidence occurs and ponds form. Thaw degradation is also impacting the cabins in the old Äshèyi settlement, discussed in section 7.2.3.

On the lake shore, permafrost is present where land use has altered ground surface conditions. Permafrost was observed in the field and confirmed using geophysical surveys, as discussed in section 6.2.1., where water ponding has been observed and seems to match ice-rich markers in ERT profiles. On the hillslopes surrounding the community shore, a few active layer detachments are also occurring, but do not threaten any of the infrastructure.

As distance from the lake increases, the sediment becomes either glacial or fluvial. In these sediment types, permafrost may be less thaw-sensitive because it contains less ground ice, owing to the more sandy or gravelly textures of the sediment. Nevertheless, specific sites with these materials may also contain important amounts of ground ice.

The Äshèyi Pingo, discussed in section 6.2.4, formed in fluvial deposits under specific hydrological conditions that induced the formation of massive ice through the injection of water. Between 2020 and 2023, the annual spring and summer ground temperature warming below about 2.5 m depth started sooner each year, indicating some ground warming occurred at depth. However, there is not enough data to definitively suggest that this trend reflects longer-term permafrost warming at the site. This would require a few more years of data collection. Furthermore, the pingo has not displayed signs of physical instability or degradation over the observation period.

Cont...

Cont…

The fluvial and morainal deposits appear to be the most frost stable sediment types in the area. However, it is possible that as the ice sheet receded, ice blocks were left behind and buried by glaciofluvial sediment near the morainal deposits. The buried ice would then have been kept frozen within permafrost. Later, if permafrost thaws, the buried ice melts and steep-edged ponds and holes can form. This process is suspected to be active at the *Kettle* site discussed in section 7.2.5 and *Äshèyi Old Settlement* discussed in section 4.2.3. Therefore, although the glaciolacustrine deposits are generally the most frost susceptible, discrete ice-rich locations exist elsewhere depending on specific geological contexts.

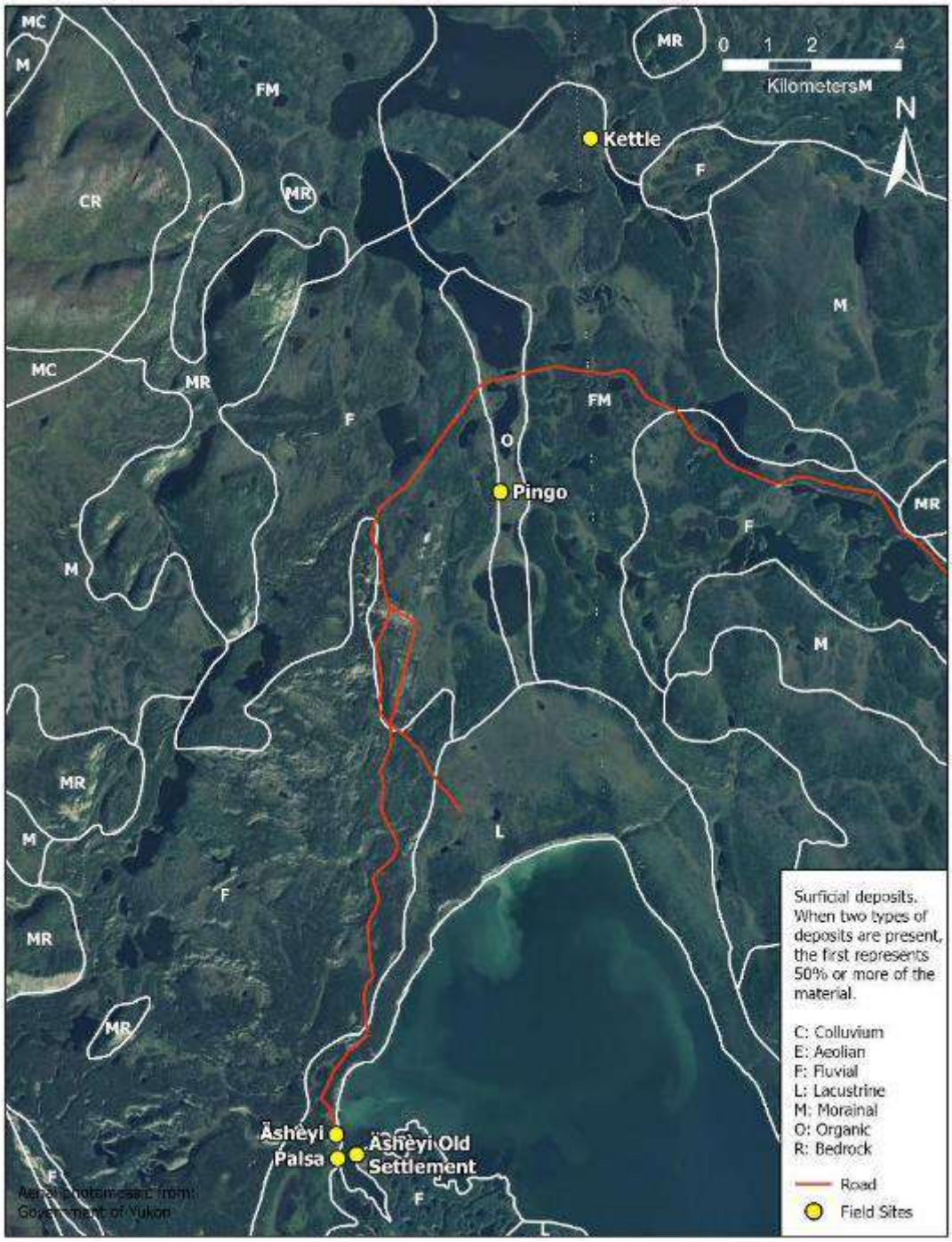

FIGURE 39 SURFICIAL DEPOSITS OF ÄSHÈYI AREA.

6.3 Äshèyi Road

Several sites were visited along Äshèyi Road during the summer of 2021. Four sites, shown in Figure 40, were surveyed. All the sites were documented using a UAV to produce orthomosaic imagery of the sites, and digital elevation models, including Chämì (old settlement) (section 6.3.1). The site called "culvert" (section 7.3.2) was investigated using shallow geotechnical drilling and ground temperature monitoring; while the site called "permafrost valley" (section 6.3.3) was investigated using shallow geotechnical drilling combined with an ERT survey and ground temperature monitoring. The site called "thermokarst" (section 6.3.4) was only surveyed using drone imagery.

FIGURE 40 LOCATIONS OF THE INVESTIGATED SITES ALONG ÄSHÈYI ROAD.

6.3.1 Chämì

The community expressed interest in having the research team visit Chämì, the old settlement, since it is site of cultural significance for the CAFN community. The site was jointly visited with community

representatives on August 4th, 2021. Following this trip, the YukonU team visited the site again on August 9th to plan the drone imagery survey; and returned on August 30th to conduct the drone survey.

During the field visits, both land features and cultural artifacts were assessed. The lake shore was given special attention. While there was erosion along some sections, it was primarily related to fluctuations in lake levels rather than permafrost thaw, as no frozen soil was observed on the cut banks (Figure 41A). No signs of permafrost degradation were observed on site or in the surrounding areas. All the old structures showed signs of aging and weathering, but their foundations were still flat and level on the ground, suggesting that no subsidence had occurred (Figure 41B, C, and D). This is a good sign because warmed structures, such as cabins, usually induce permafrost thaw below them, which results in structural damage and tilting such as the heritage buildings located in Dawson City.

The aerial imagery resulting from the drone survey allowed us to accurately locate the cultural artifacts (Figure 42), which are occasionally difficult to observe on the imagery because of the abundant vegetation present on site. Better observation can be obtained using a 3-D model produced from the aerial imagery (Figure 43).

To summarize, no permafrost-related hazards were observed. Erosion was observed along the bank of the lake, mostly related to lake level fluctuation and wave action. The site may be vulnerable to wildfires given the abundant vegetation.

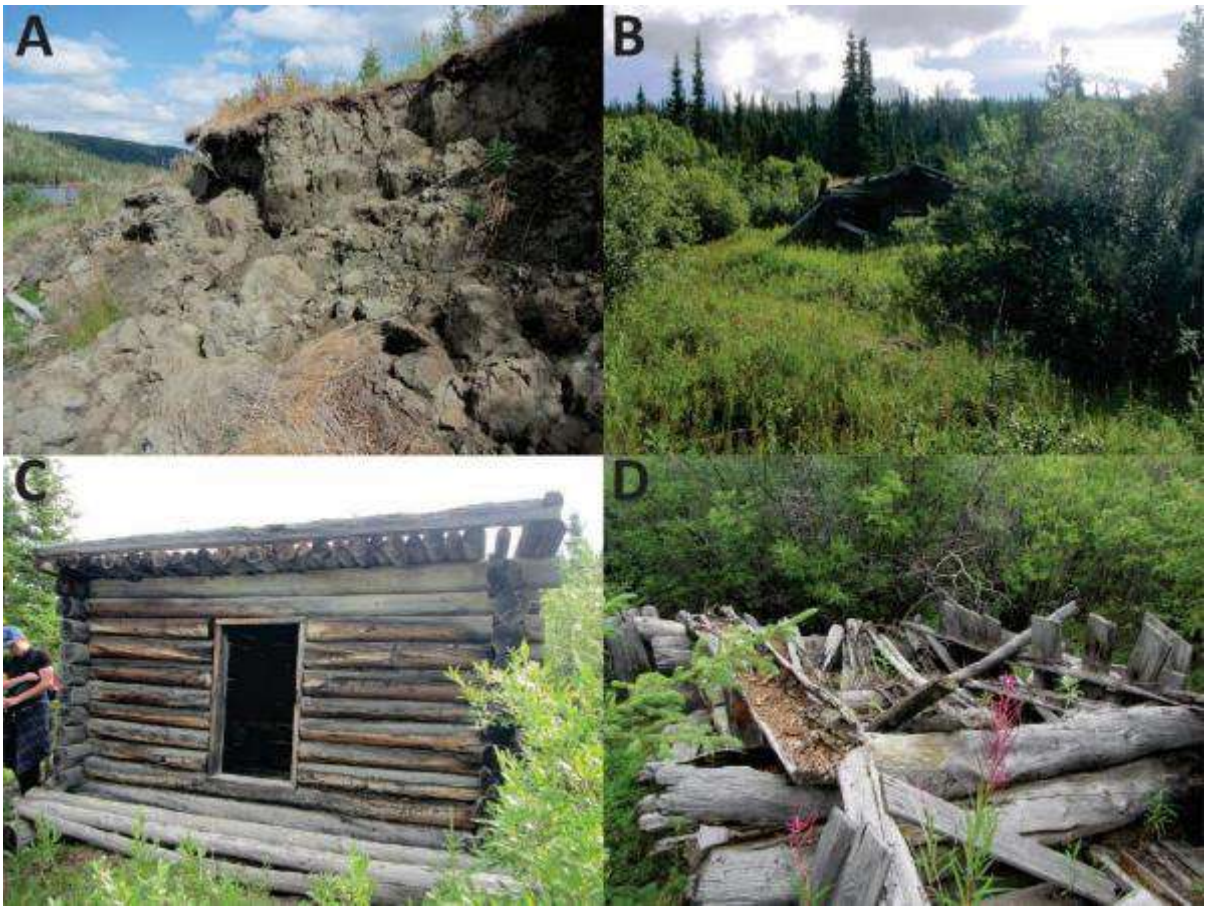

FIGURE 41 CHÄMÌ OLD SETTLEMENT SITE. A- ERODED BANK; B, C, & D- OLD CABINS.

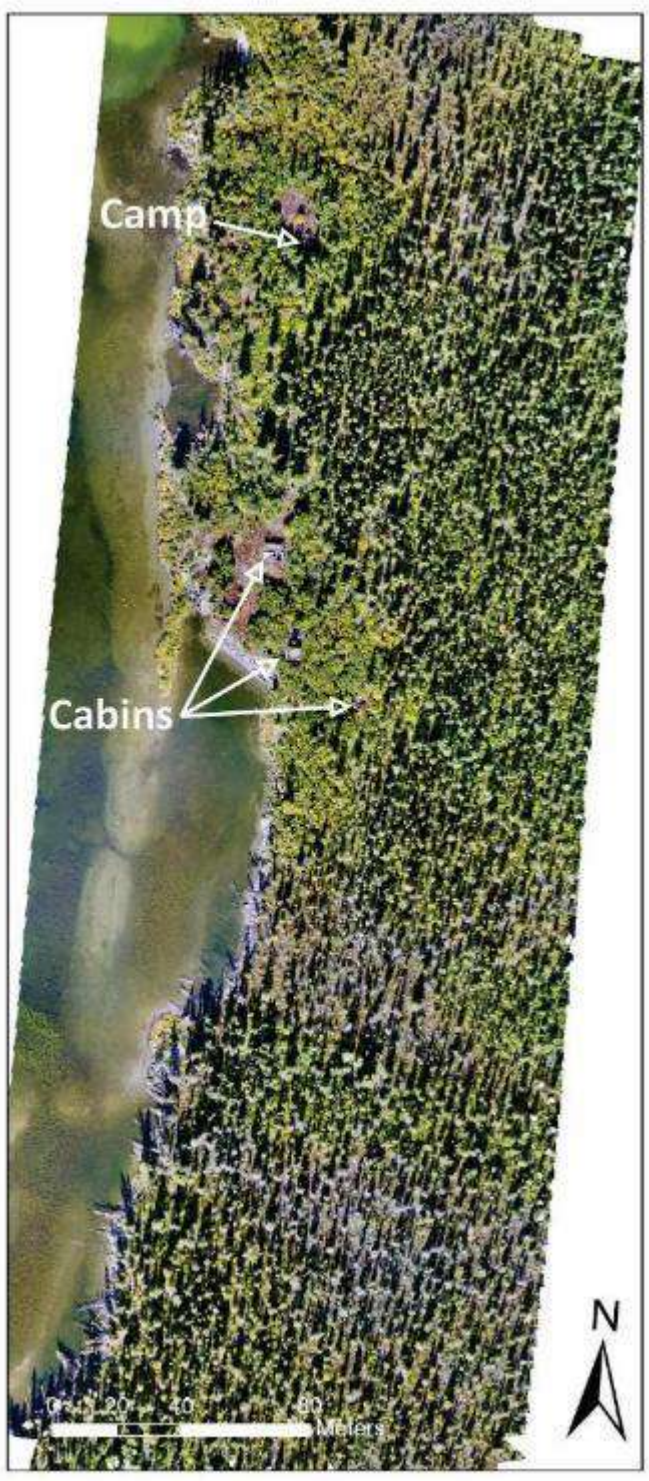

FIGURE 42 AERIAL VIEW OF CHÄMÌ OLD SETTLEMENT.

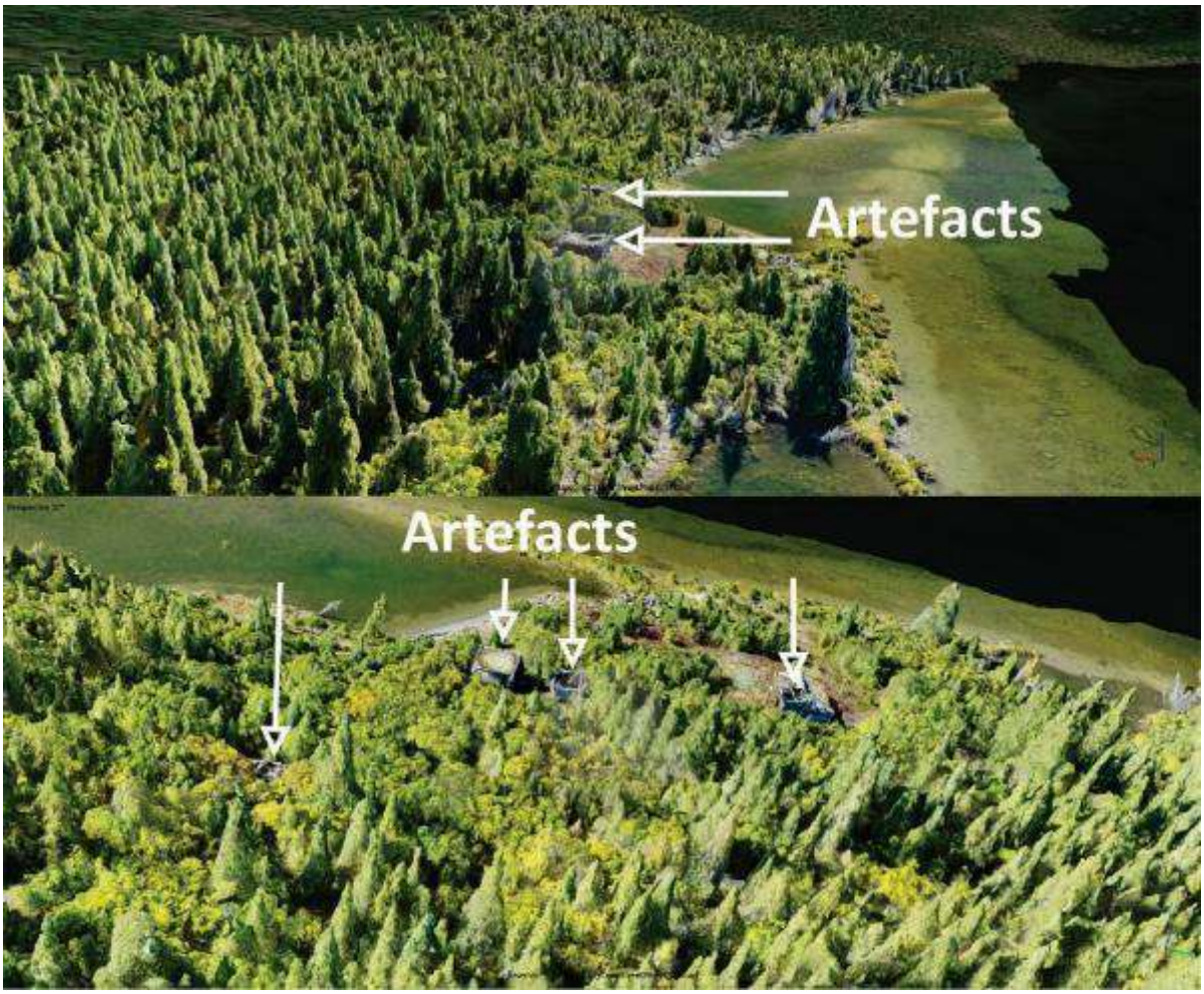

FIGURE 43 THREE-DIMENSIONAL MODEL OF CHÀMÌ OLD SETTLEMENT FROM DRONE IMAGERY.

6.3.2 Culvert Site

The site *Culvert* on Äshèyi Road is an area where a creek is flowing from an eastern hillslope under the road through a culvert. The site was selected because indicators of permafrost degradation such as subsidence, tilting trees, ground surface cracking, and organic sediment accumulating at the entrance of the culvert were present (Figure 44).

FIGURE 44 ÄSHÈYI ROAD, CULVERT SITE.

The site was assessed using shallow drilling with coring, ground temperature monitoring and aerial drone imagery (Figure 45). In addition to the culvert entrance area, the aerial imagery revealed additional degradation on the left side of the field, about 60 m from the road. This suggests that permafrost is widespread in this area.

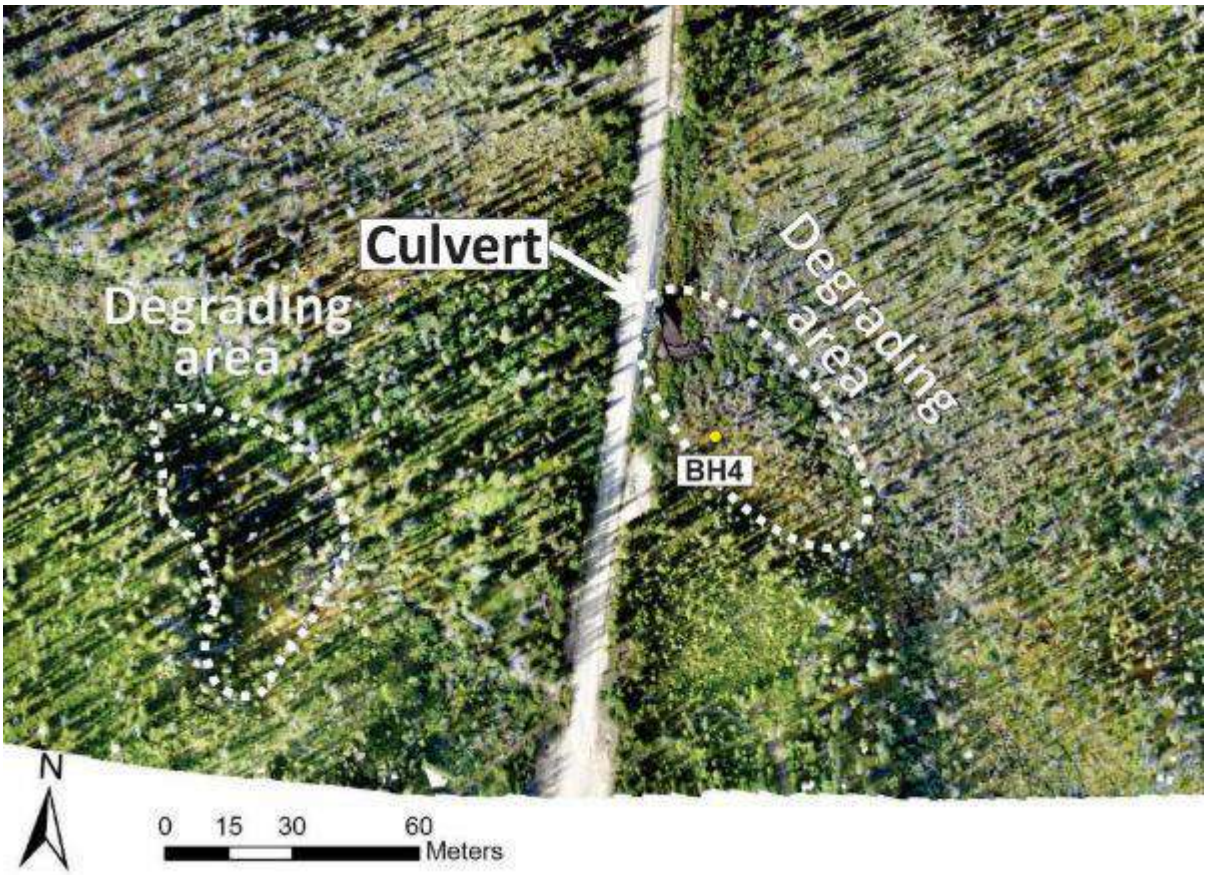

FIGURE 45 AERIAL IMAGERY OF ÄSHÈYI ROAD, CULVERT SITE. TILTING TREES AND DARK ORGANIC SEDIMENT ACCUMULATING AT THE ENTRANCE OF THE CULVERT ARE DUE TO PERMAFROST THAW.

The borehole AIS_BH04 (*Culvert*) was drilled near the creek flowing through the culvert, in a dryer, more elevated location than the culvert. This location was chosen to represent natural conditions without the degradation seen at the culvert. The cores were collected down to a depth of 3.84 m. The thaw front was encountered at a depth of 31 cm at the time of drilling (August 10th, 2021), below an unfrozen organic layer (Figure 46). From 31 cm to 170 cm, an organic silty layer is present, which also includes a tephra layer (volcanic ash) between 70 and 80 cm. From 170 cm, silty sand interlaced with organics layers extends to a depth of 290 cm. Below this, the sediment becomes siltier down to a depth of 384 cm, which was the end of the borehole. The ground ice cryostructure is microlenticular with volumetric excess ice content ranging from 3 to 45%. Overall, the borehole has a mean volumetric excess ice content of 24%. The cumulated ice content represents a potential subsidence of 0.9 m if permafrost were to thaw.

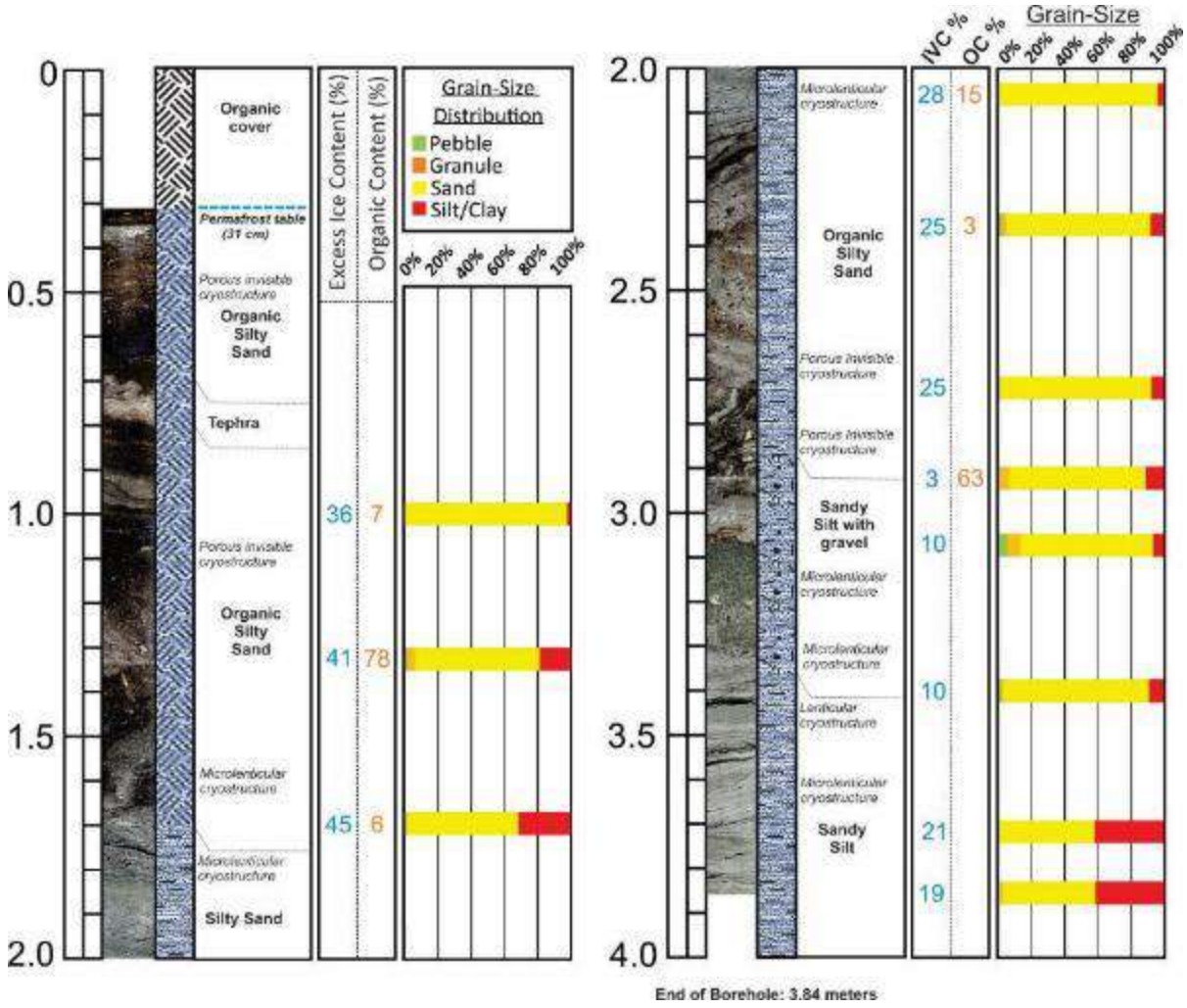

FIGURE 46 BOREHOLE LOG OF AIS_BH04 (*CULVERT*) WITH SOIL TEXTURE, ORGANICS AND GROUND ICE CONTENT.

The borehole AIS_BH04 Culvert was lined with PVC piping and instrumented with two 4-channel Hobo loggers to record ground temperatures at 0, 0.5, 1.5, 2.0, 2.5, 3.0, 3.5 and 3.8 m depths. The recording started August 10th, 2021, and the data were downloaded September 27th, 2021, providing 1 ½ month of monitoring. Figure 47 presents hourly ground temperature records of AIS_BH04 on August 17th, August 31st, and September 14th, 2021, at 12pm. The records show that the permafrost is close to or at 0°C. The active layer thickness is 0.5 m. Such warm permafrost can be considered close to thawing.

Figure 48 presents ground temperatures from BH4 recorded from August 10th to September 27th, 2021. The recording period is short but shows that the freeze back of the active layer was almost complete by the end of September.

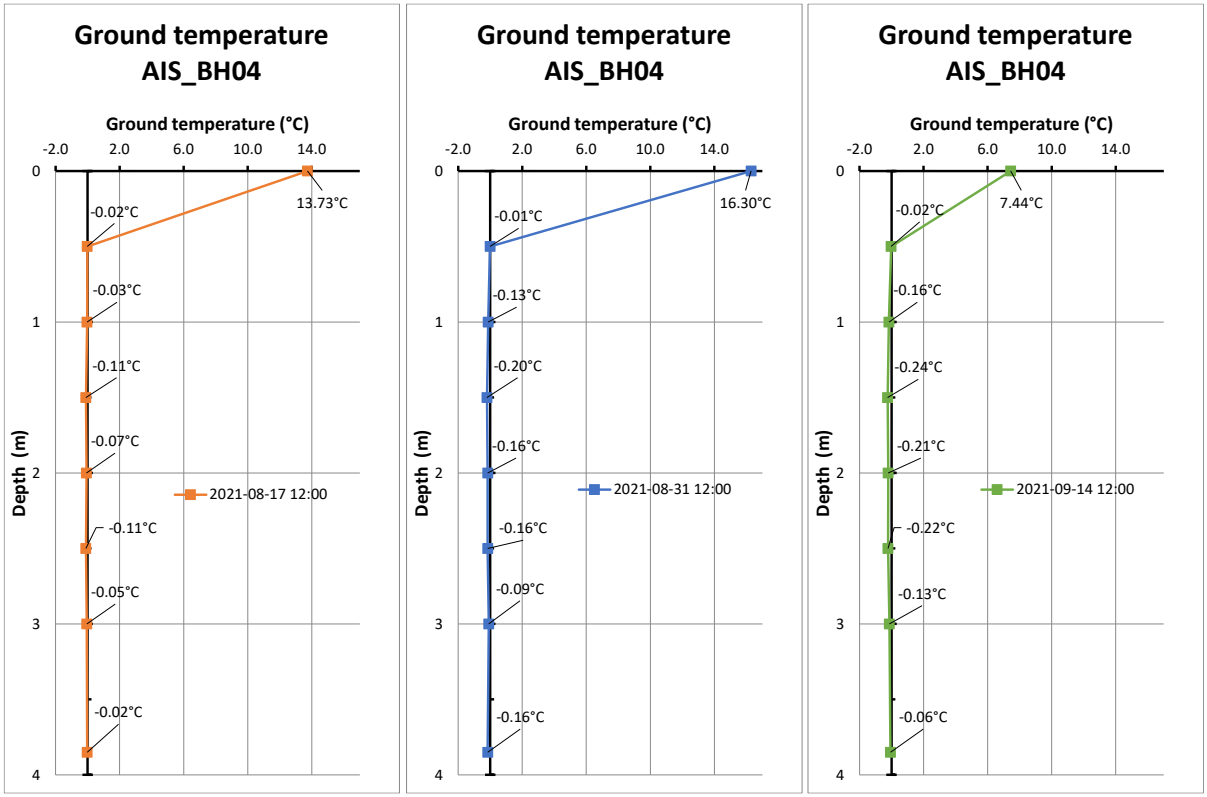

FIGURE 47 GROUND TEMPERATURE FOR AIS_BH04 (*CULVERT*) ON AUGUST 17TH, AUGUST 31ST, AND SEPTEMBER 14TH, 2021, AT 12PM.

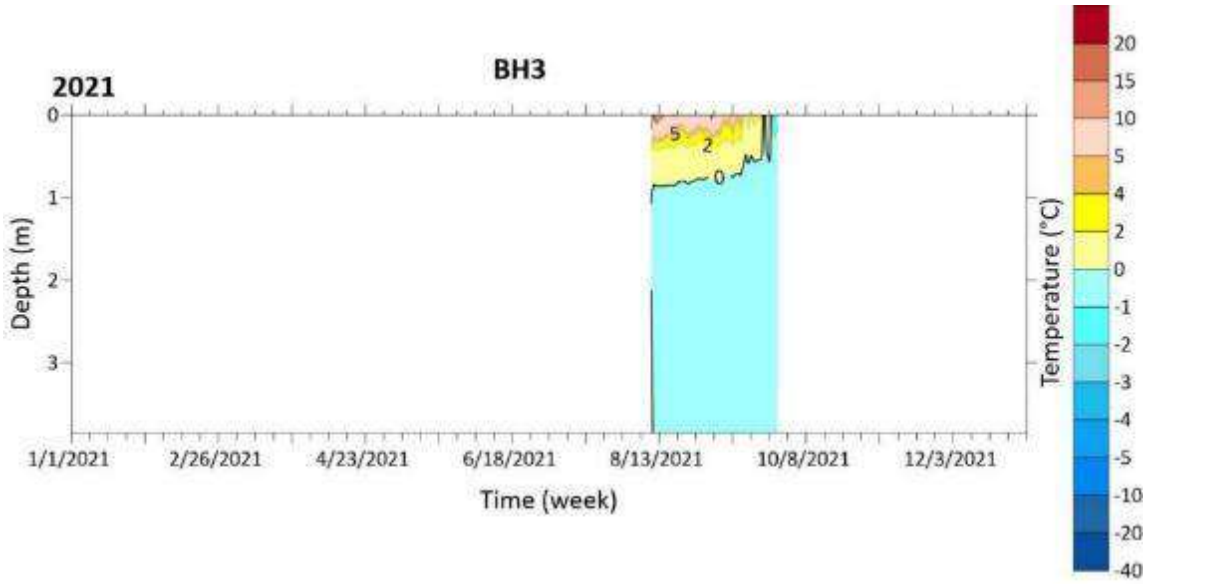

FIGURE 48 GROUND TEMPERATURE OF AIS_BH04 (*CULVERT*) FROM AUGUST 10TH TO SEPTEMBER 27TH 2021.

6.3.3 Permafrost Valley Site

The site *Permafrost Valley* on Äshèyi Road comprises a lowland area and a hillslope in a valley. At the bottom of the valley is a wetland where permafrost mounds coexist with thermokarst ponds resulting from the thaw of these mounds. This site was relatively easy to access compared to other similar terrain in the area that was only observable from afar.

The permafrost mounds are large, exceeding 100 m in width, and are more that 2 meters in height. Often, water is accumulating at the foot of the mounds such as in Figure 49. The wetlands surrounding the mounds consist of grasslands with ponds (Figure 50), and the hillslope is a dry, wooded area with lichen on the ground (Figure 51). A general aerial view of the site is presented in Figure 52.

FIGURE 49 A PERMAFROST MOUND IN THE VALLEY OF *PERMAFROST VALLEY* WITH A POND AT ITS FOOT.

FIGURE 50 WETLANDS AT *PERMAFROST VALLEY*. DEGRADING PERMAFROST MOUNDS WITH TOPPLING TREES ARE VISIBLE IN THE BACKGROUND.

FIGURE 51 HILLSLOPE AT *PERMAFROST VALLEY*.

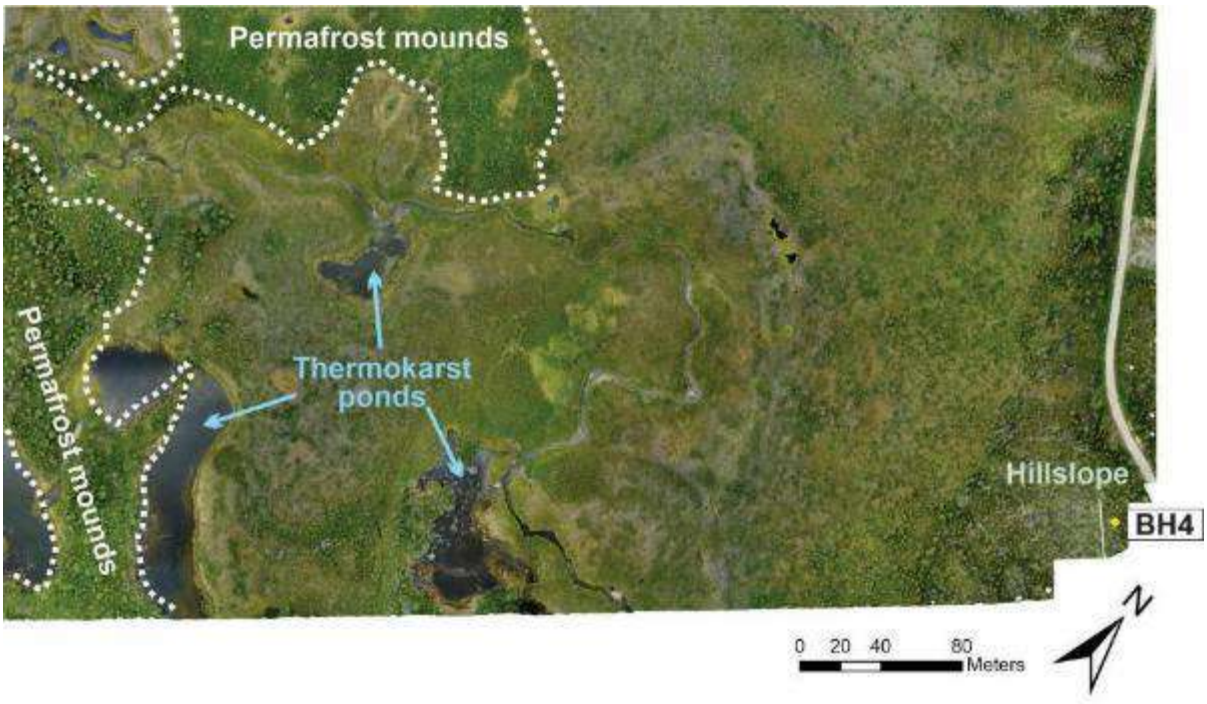

FIGURE 52 AERIAL IMAGERY OF *PERMAFROST VALLEY*.

A 3D model was produced from the drone imagery to better observe the area (Figure 53). The model shows a degrading permafrost mound and provides a good example of landscape changes that occur when permafrost thaws in environments like this one. The edges of the mound are collapsing, producing steep ridges, and revealing bare soil. As the ground subsides, lakes form, the shoreline of which represent the former boundaries of the mound (Figure 54).

FIGURE 53 THREE-DIMENSIONAL VIEWS OF *PERMAFROST VALLEY*. A- WETLAND WITH PERMAFROST MOUNDS AND THERMOKARST LAKES; B- HILLSLOPE NEAR THE ROAD AND BOREHOLE AIS_BH03 AND A 160 M ERT PROFILE.

FIGURE 54 THREE-DIMENSIONAL VIEWS OF A DEGRADING PERMAFROST MOUND IN THE WETLAND OF *PERMAFROST VALLEY*. A- PERMAFROST MOUND SURROUNDED BY A THERMOKARST LAKE RESULTING FROM THE THAW OF THE MOUND; B- COLLAPSING EDGE OF THE DEGRADING PERMAFROST MOUND.

Borehole AIS_BH03 was drilled on the hillslope, about 20 m west of the road. The cores were collected down to a depth of 4.10 m. The thaw front was encountered at a depth of 42 cm at the time of drilling (August 9th, 2021). The unfrozen layer consists of 20 cm of organic cover followed by 22 cm of silty sand (Figure 55). From 42 cm to 220 cm, the sediment is silty sand with a layer of tephra (volcanic ash) at about 110 cm. In general, the sediment is ice-rich with suspended cryostructures. From 220 cm to 410 cm (the end of the borehole), the sediment is finer, sandy clayey silt, and the ice content is lower with more microlenticular and lenticular cryostructures. The volumetric excess ice content ranges from 3 to 64%, with ground ice content decreasing with depth. Overall, the borehole has a mean volumetric excess ice content of 25%. The cumulated ice content represents a potential subsidence of 1 meter if permafrost were to thaw.

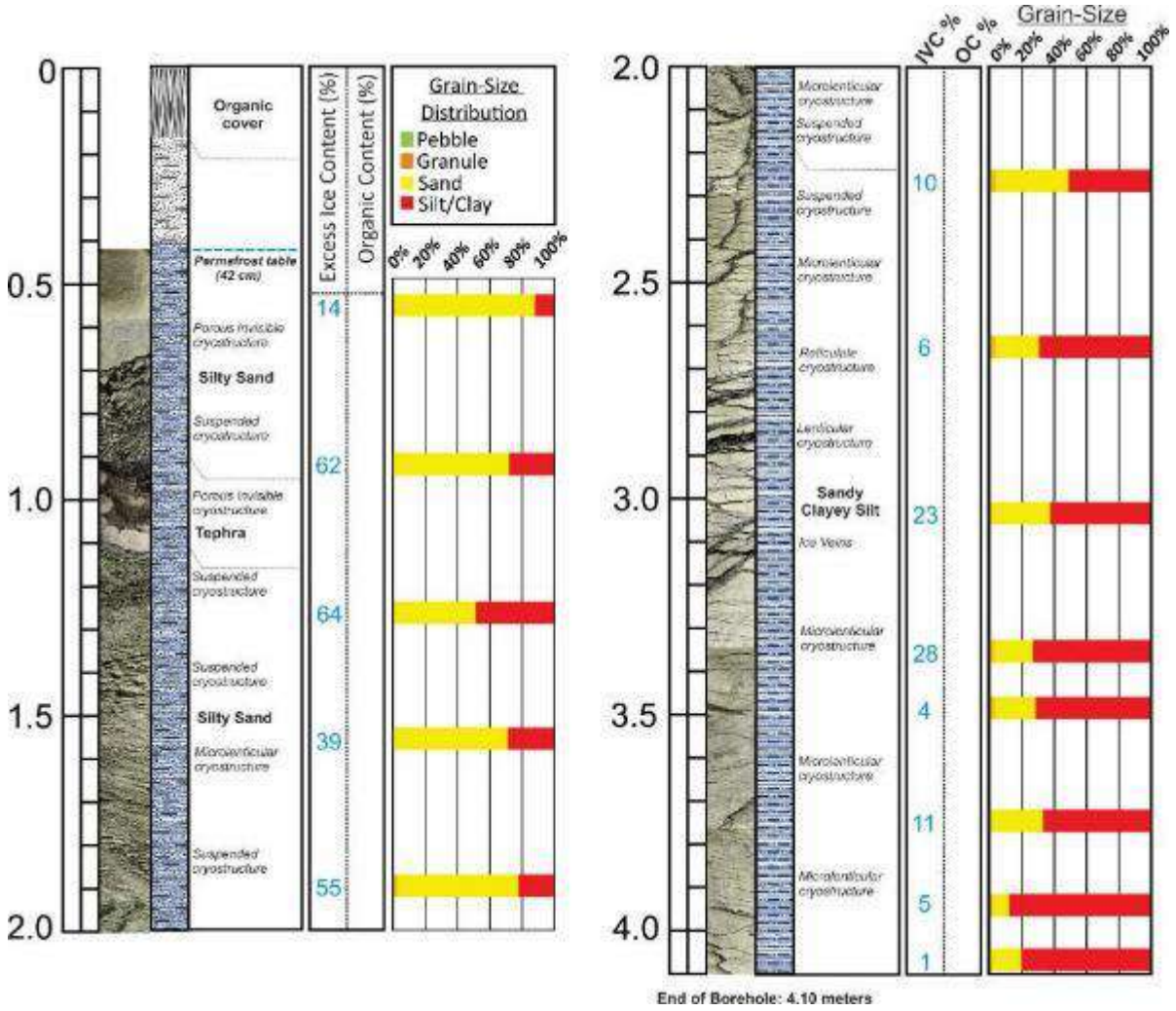

FIGURE 55 BOREHOLE LOG OF AIS_BH03 (*PERMAFROST VALLEY*) WITH SOIL TEXTURE, AND ORGANICS AND GROUND ICE CONTENT.

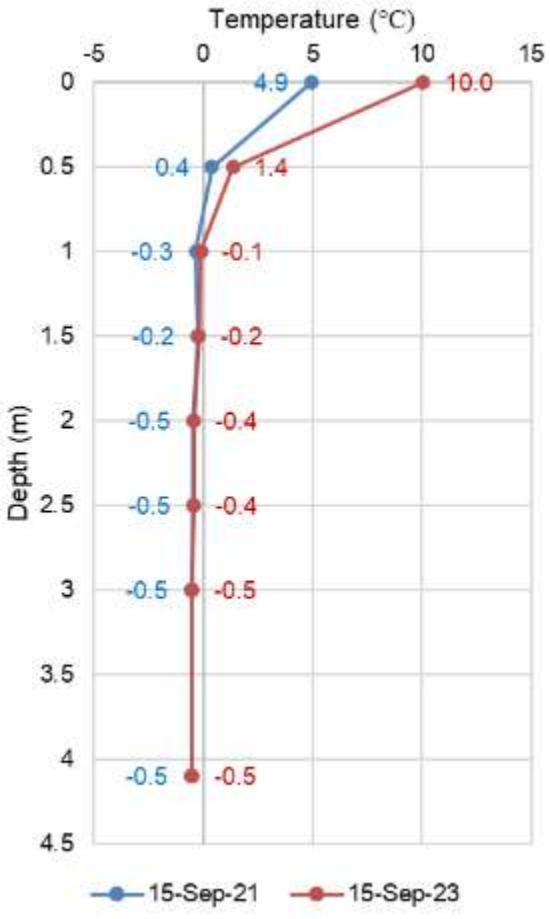

FIGURE 56 GROUND TEMPERATURE AT AIS_BH03 (*PERMAFROST VALLEY*) ON SEPTEMBER 15TH, 2021 AND SEPTEMBER 15TH, 2023 AT 12PM.

The borehole AIS_BH03 at *Permafrost Valley* was lined with PVC piping and instrumented with two 4-channel Hobo loggers to record ground temperatures at 0, 0.5, 1.5, 2.0, 2.5, 3.0, and 4.1 m depths. Recording spans from August 10th, 2021, to February 28th, 2024. Figure 56 presents hourly ground temperature records from AIS_BH03 on September 15th, 2021, and September 15th, 2023, at 12pm. The records show that maximum active layer thickness was 0.75 m in 2021 and 1 m in 2023. Ground temperature below the active layer has not changed between 2021 and 2023. The temperature of the deepest permafrost in the borehole is around -0.5°C on September 15th, 2021, and 2023. This is very warm, but cooler than at the Culvert site where permafrost is degrading.

Figure 57 presents ground temperatures from AIS_BH03 recorded from August 10th, 2021, to February 28th, 2024. A large gap in the record exists because the logger died from excessive power consumption. The logger settings were adjusted to remedy the issue in the future. Fully ascertaining thermal patterns over time with the existing data is not possible due to this gap. However, we can see that freeze-back of the active layer was almost complete by the end of September in 2021 and almost complete by mid-October in 2023. These freeze-back timings are normal for most permafrost in the region.

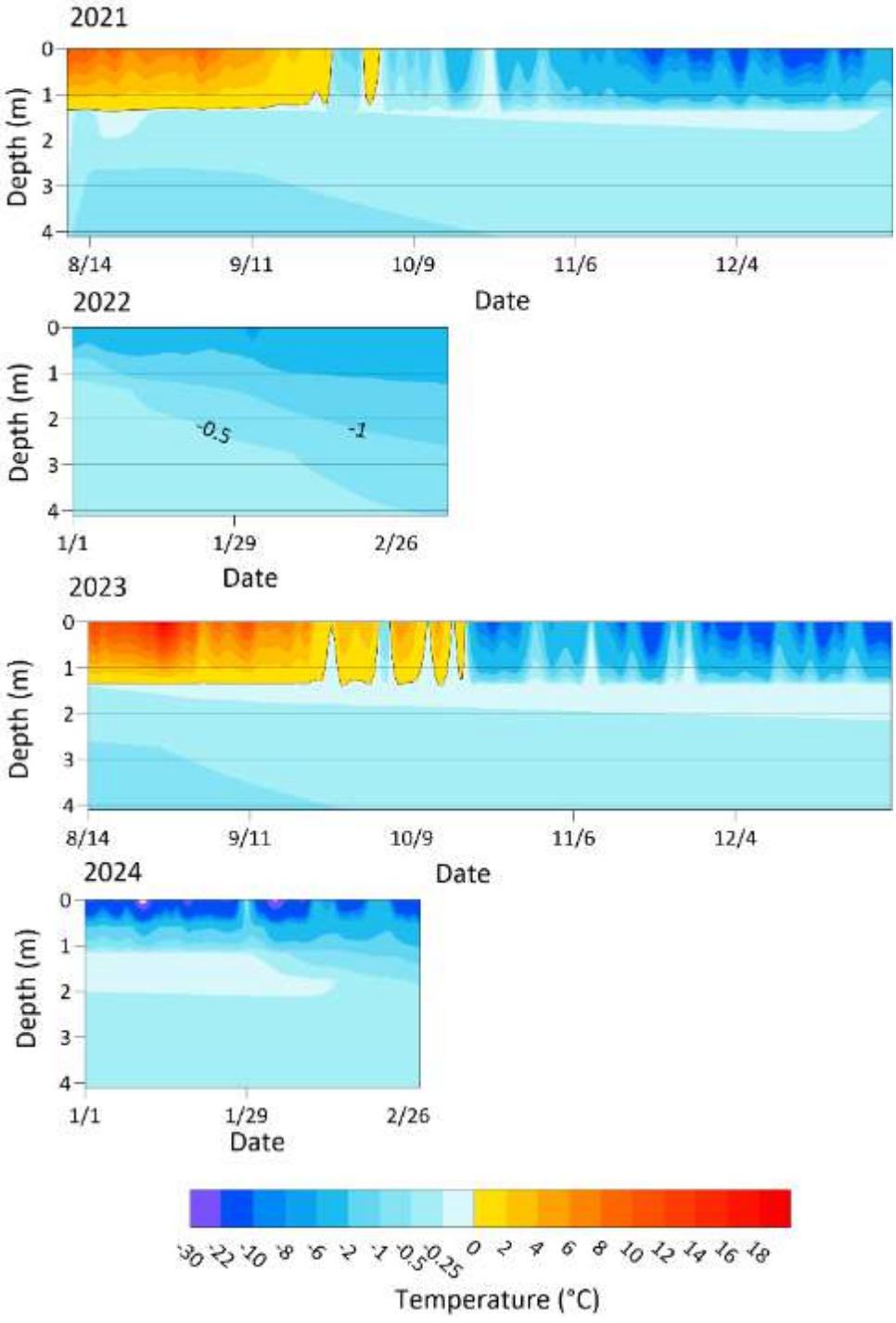

FIGURE 57 GROUND TEMPERATURE OF AIS_BH03 (*PERMAFROST VALLEY*) FROM AUGUST 10TH, 2021 TO FEBRUARY 28TH, 2024. THE LARGE GAP IN THE DATA OCCURRED BECAUSE THE LOGGER RAN OUT OF POWER DUE TO TOO FREQUENT DATA RECORDING AND A ROAMING BLUE TOOTH SIGNAL.

To assess permafrost distribution on the hillslope, a 160-m ERT survey was conducted in the wooded area, passing 6 meters west (downslope) of BH3 using a dipole-dipole array. The ERT profile of this survey is presented in Figure 58. The dipole-dipole profile suggests that permafrost is widespread across the profile with highly resistive areas (blue) representing frozen ground and less resistive areas (red) representing unfrozen ground. The low resistivity areas are restricted to the top of the profile, i.e., the active layer, except for two spots at 100 m and 125 m along profile, which could be attributable to ground water flow. Within the permafrost areas (marked with "P" in Figure 58), some even more resistive areas are present. These areas likely represent ground with higher ice content (marked by "ice" in Figure 58), such as between 120 and 140 m along the transect below 10 m in depth.

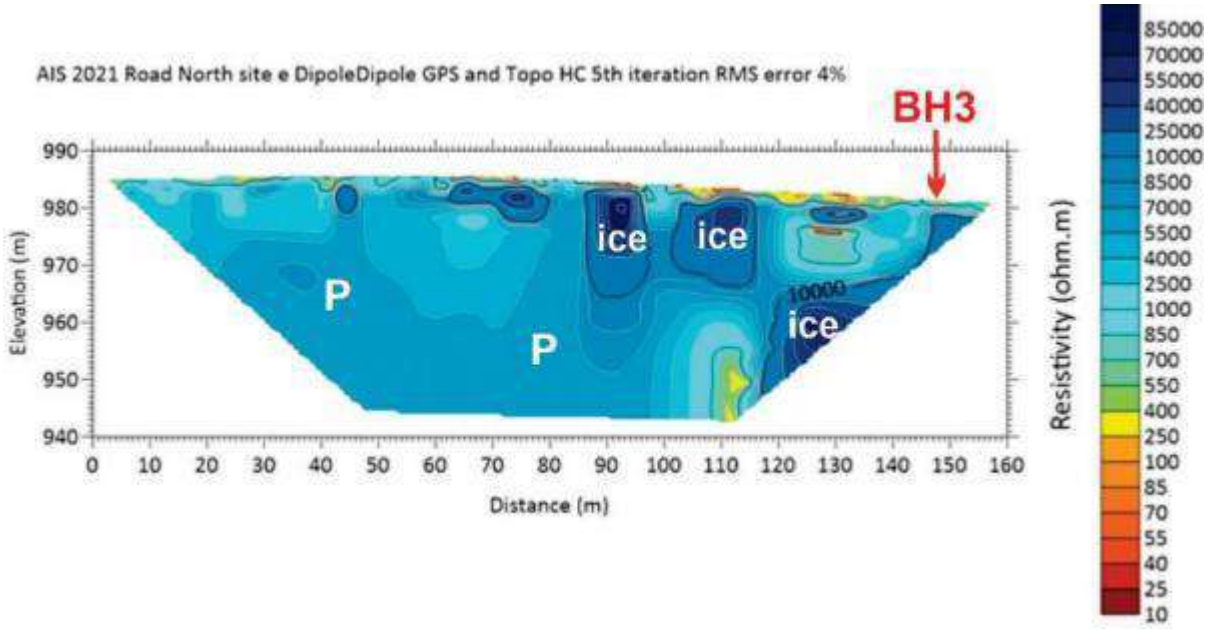

FIGURE 58 ELECTRICAL RESISTIVITY PROFILE AT *PERMAFROST VALLEY*. "P" MARKS POTENTIAL PERMAFROST AREAS, "ICE" INDICATES POTENTIAL ICE-RICH AREAS, AND "UNFROZEN" THE NON-PERMAFROST ZONES SUCH AS THE ACTIVE LAYER.

6.3.4 Thermokarst Pond Site

The third study site on Äshèyi Road – *Thermokarst Pond* – is an area where a pond is expanding, leading to collapsing edges, and sinking trees. *Thermokarst Pond* is located on the east side of the road (Figure 59, Figure 60). Thermokarst ponds are created by ground subsidence due to thawing ground ice in permafrost leading to water accumulation, which often drives further ground ice melt and subsidence around the edges of the pond. The proximity of the site to the road suggests the site is possibly a former borrowing pit, a pit where earth material is taken for construction purposes. If this is the case, removal of the thermally protective top layer of soil likely triggered the ground ice thaw deeper in the soil.

The north-facing ridge at the site shows a relatively gentle slope (Figure 59B), while the west-facing and south facing ridges of the pond have steep slopes that are 3 to 6 m high and also have trees that are leaning and toppling (Figure 59C, D, and E). The south-facing ridge shows soil exposure where a tephra layer is visible, and the organic material is tumbling downslope (Figure 59F). These behaviours suggest that the pond is actively expanding to the west and south via ground ice melt and subsidence.

The imagery provided by the drone survey and three-dimensional models made therewith (Figure 60, Figure 61, Figure 62) show the thermokarst depression contains a western and eastern pond, divided by a small, vegetated ridge running north-south. The imagery and models also show that the eastern pond contains the greatest abundance of fallen trees and is flanked by the some of the steepest embankments of fresh soil exposures on its eastern edge. This suggests that the greatest rate of thermokarst expansion has thus far been generally eastward.

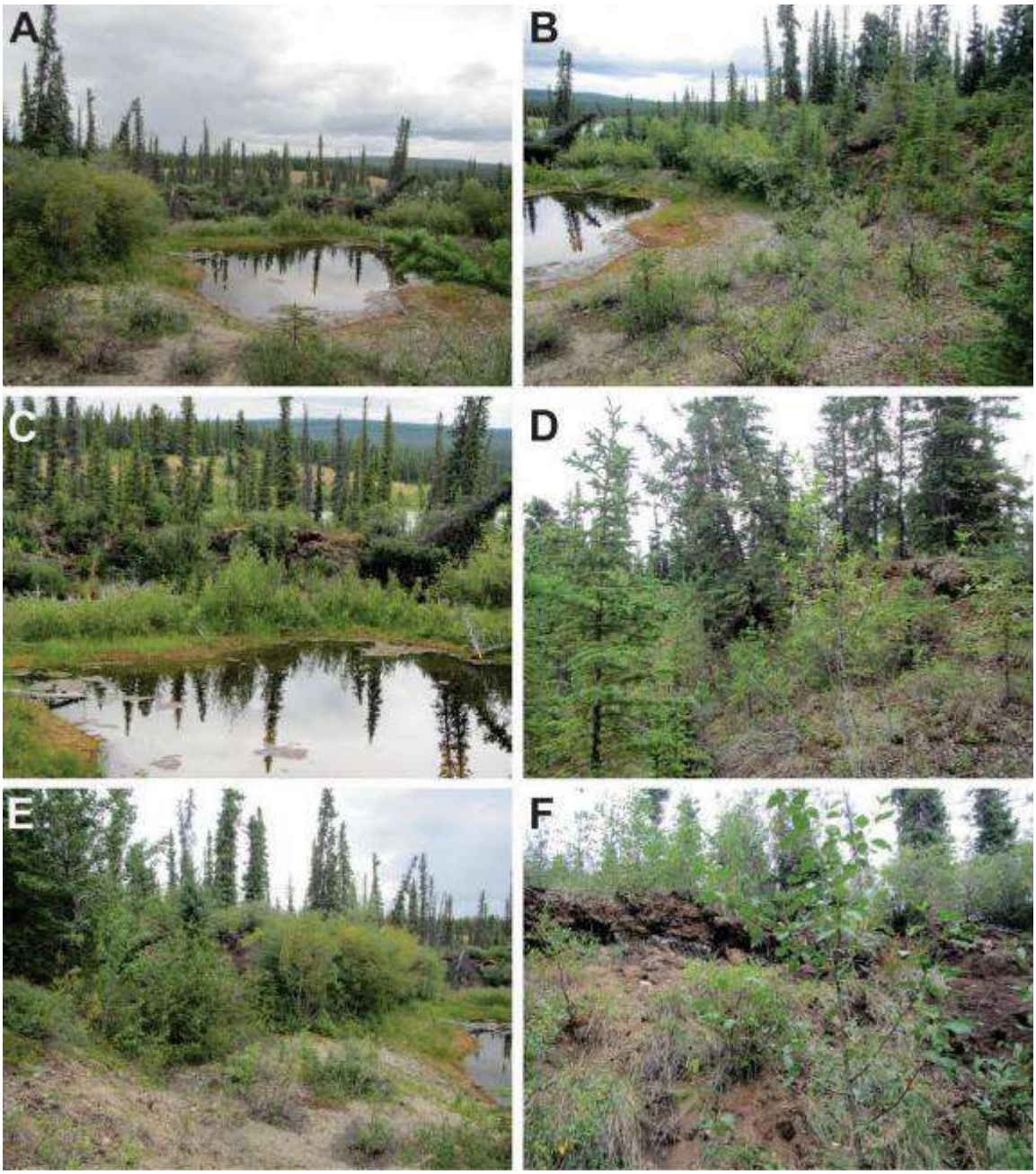

FIGURE 59 *THERMOKARST POND* SITE. A-GENERAL VIEW OF THE POND; B- NORTH-FACING RIDGE OF THE POND; C- WEST-FACING RIDGE OF THE POND, D- SOUTH-WEST-FACING RIDGE OF THE POND; E- SOUTH-FACING RIDGE OF THE POND; AND F- BLUFF ON SOUTH-FACING RIDGE OF THE POND.

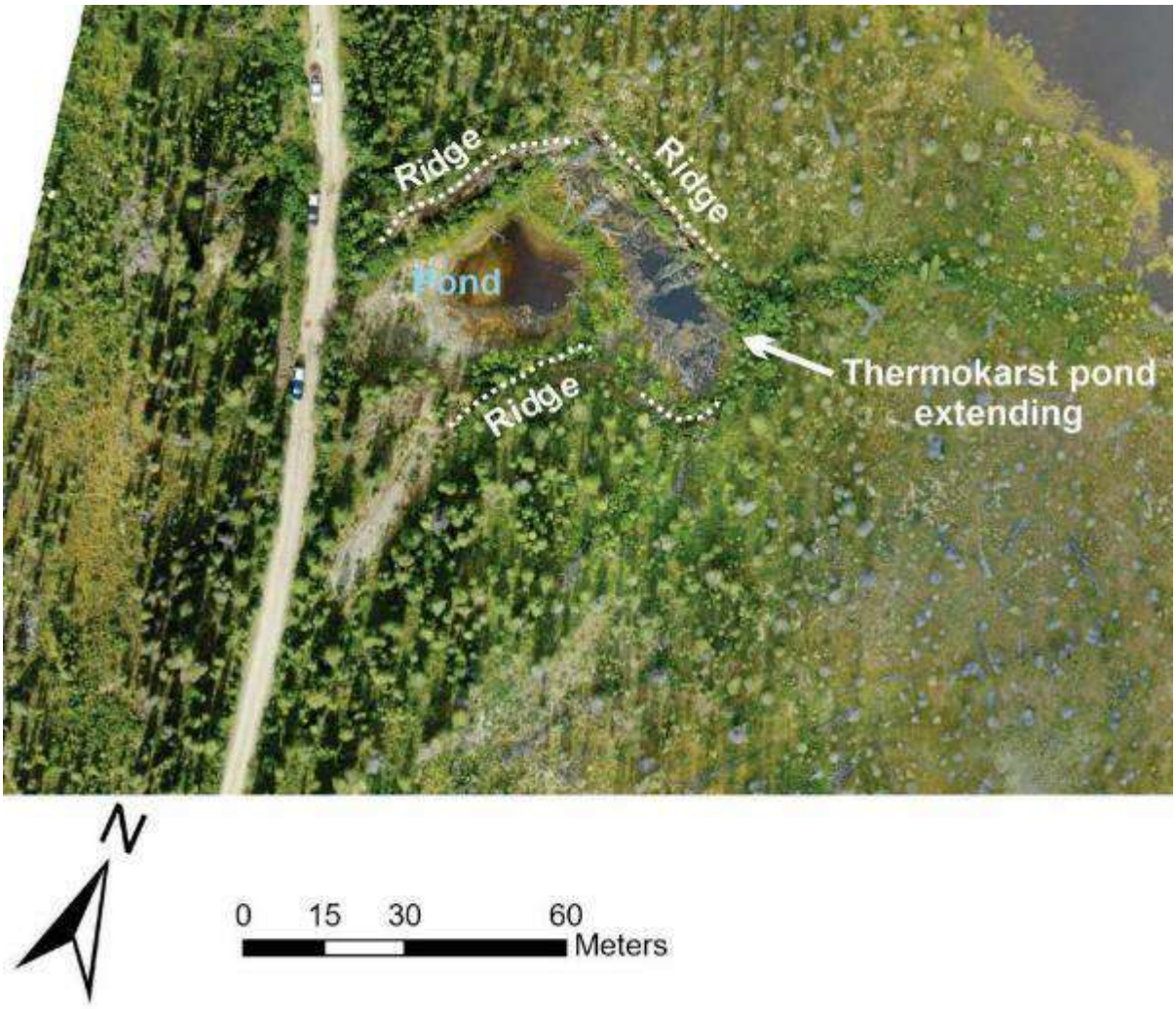

FIGURE 60 AERIAL IMAGERY OF *THERMOKARST POND*. STEEP EDGES (RIDGES) ARE FORMING, AND TREES ARE COLLAPSING WHILE THE POND IS GROWING ESPECIALLY TO THE EAST.

FIGURE 61 THREE-DIMENSIONAL REPRESENTATION OF *THERMOKARST POND*, FROM DRONE AERIAL IMAGERY. STEEP EDGES (RIDGES) ARE FORMING, AND TREES ARE COLLAPSING WHILE THE POND IS GROWING.

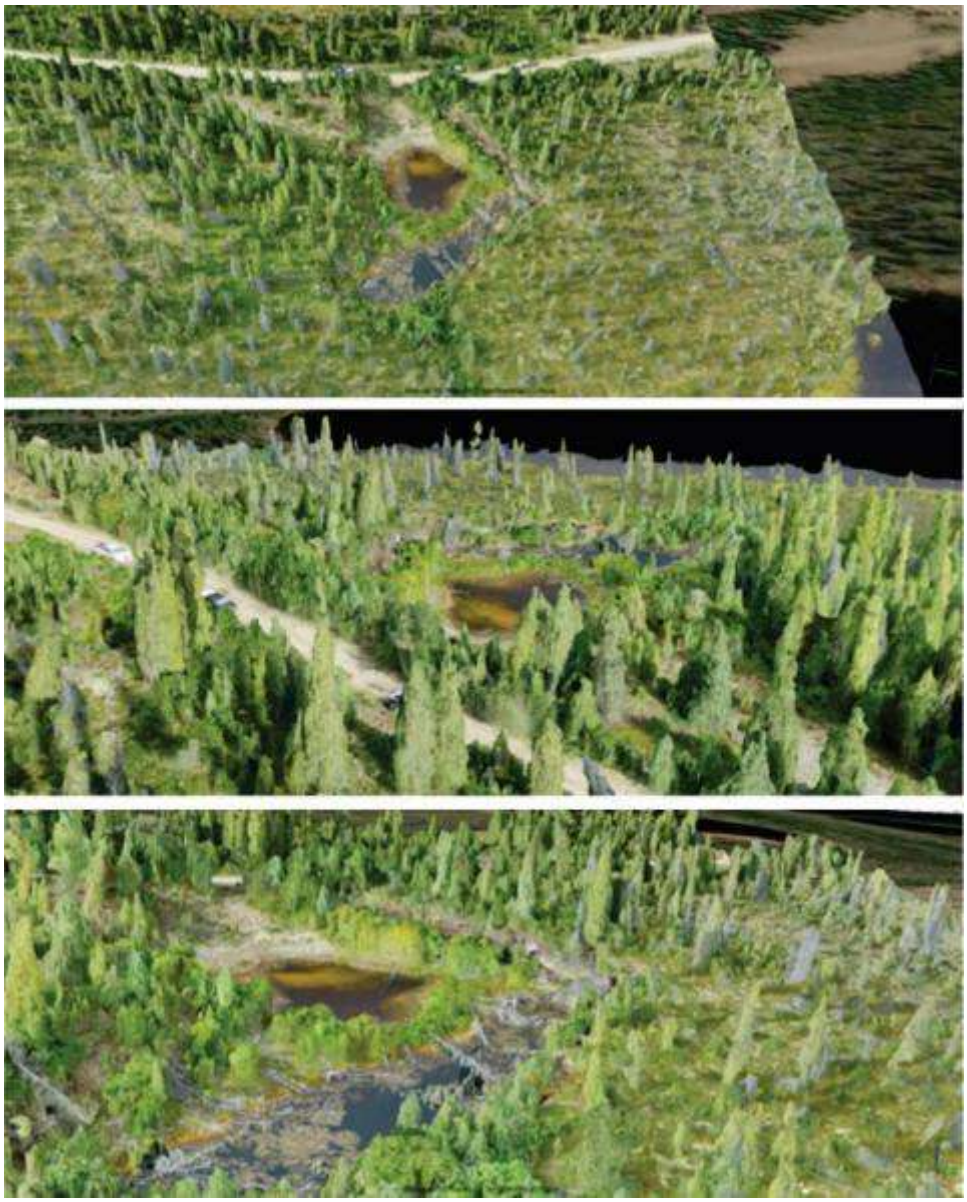

FIGURE 62 MULTIPLE 3D REPRESENTATIONS OF *THERMOKARST POND*, FROM DRONE AERIAL IMAGERY.

6.3.5 Summary of Sites along Äshèyi Road

Field investigations along the Äshèyi Road allowed for the identification of different permafrost environments, including some where degradation was observed. Like in the Äshèyi village area, the underlying geology appears to have the most influence on permafrost properties.

The Äshèyi Road passes through various environments with differing surficial geology, including morainal, lacustrine, and fluvial deposits, and bedrock (Figure 63).

Morainal deposits tend to be relatively frost stable. This is because the coarse-grained texture of the morainal deposits is less conducive to producing large amounts of excess ice via cryosuction. The Chämì site, discussed in section 6.3.1, is located on morainal glacial deposits (Figure 63), and none of the heritage buildings displayed any damage that could be attributed to permafrost thaw. No signs of permafrost degradation were observed on site or in the surrounding areas.

The lowlands of *Permafrost Valley*, discussed in section 6.3.3, are located on lacustrine sediment (Figure 63). At this site, the fine-grained sediment is frost-susceptible and frost-heave mounds have been created as segregated ice formed in the ground. Now that permafrost is degrading, subsidence occurs, and the mounds are progressively replaced by thermokarst ponds. Other observations along the lake shore showed subsidence and other similar signs of permafrost thaw and degradation. Permafrost was also present in the hillslope of *Permafrost Valley*, in a morainal deposit, though no signs of degradation were observed. The borehole log showed a ground ice content that decreased with depth, making the first two meters of the profile the most thaw sensitive.

Culvert and *Thermokarst Pond*, discussed in sections 7.3.2 and 6.3.4 respectively, are located on fluvial deposits (Figure 63). At these sites, the sediment also has a fine texture, and permafrost degradation was clearly noticeable, as the area seems to be becoming increasingly wetter. It is suspected that buried glacier ice is present at the Thermokarst pond site. This hypothesis is supported by field observations and the fact that this fluvial deposit is surrounded by glacial deposits.

The Äshèyi Road is mostly built on morainal deposits, which generally are more frost-stable than the fluvial (river) deposits. However, because the permafrost in the morainal deposits at these sites happen to host warm, high excess ice, general care should be taken not to greatly disturb the ground or vegetation regardless of ground type. The portions of the road that cross fluvial and lacustrine deposits are likely to be impacted by permafrost thaw based on the investigated sites.

6.4 K'ùa Mān (Kloo Lake)

Several sites were visited in the K'ùa Mān (Kloo Lake) area in summer 2019. Three sites were surveyed, which are shown in Figure 64. All the sites were documented using a UAV to produce ortho-mosaic imagery of the sites, and digital elevation models. The *K'ùa East* site (section 6.4.1) was surveyed using ERT while the *K'ùa West* site (section 6.4.2) was investigated using shallow geotechnical drilling and ground temperature monitoring, as well as ERT. The *K'ùa Old Village* site (6.4.3) was surveyed using ERT, in addition to the UAV imagery.

FIGURE 64 LOCATIONS OF THE SITES INVESTIGATED IN THE K'ÙA MĀN AREA.

6.4.1 K'ùa East Site

The *K'ùa East* site is located east of the road leading to the K'ùa Mān boat launch (Figure 64). It is in a wooded area and was selected because it is generally representative of this area (Figure 65). A shallow borehole was attempted on August 2nd, 2019, but the drill gear broke almost immediately. The thaw front was located at a depth of 70 cm. The top organic layer was 20 cm thick, followed by a mix of gravelly silt with cobbles. The location of this failed borehole is shown in Figure 56.

To assess permafrost distribution at *K'ùa East*, a 150-m ERT survey was conducted on the hillslope, crossing the wooded area and ATV trails. At this site, three types of ERT configurations were used: Dipole-dipole, Schlumberger, and Wenner. The ERT profiles of this survey are presented in Figure 66. Though they have different depths, the three surveys show similar results. All the profiles suggest that permafrost is relatively shallow, reaching no more than 10 m in depth. Highly resistive areas, represented by green and blue on the profiles, represent cold, frozen ground. Some even higher resistivity zones are present, for example a large one between 40 and 80 m along the profile and the small one between 100 and 110 m. These areas likely represent ground with higher ice content (marked by "ice" in Figure 66) Low resistivity areas, represented by the yellow to red on the profiles, are present at the top of the profiles (the active layer), but also below 10 m depth, which suggests that permafrost is not present below this depth.

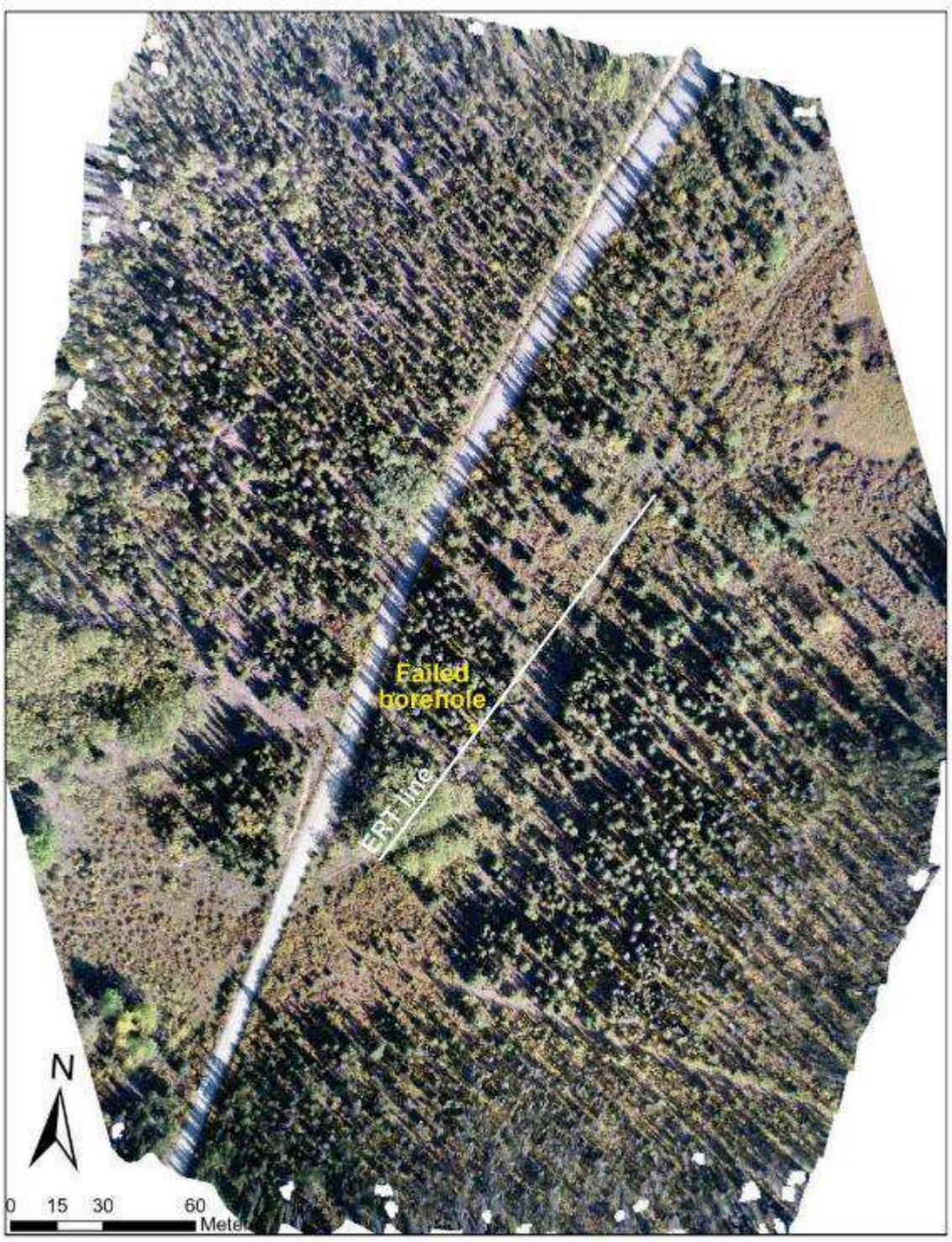

FIGURE 65 AERIAL IMAGERY OF THE *K'ÙA EAST* SITE.

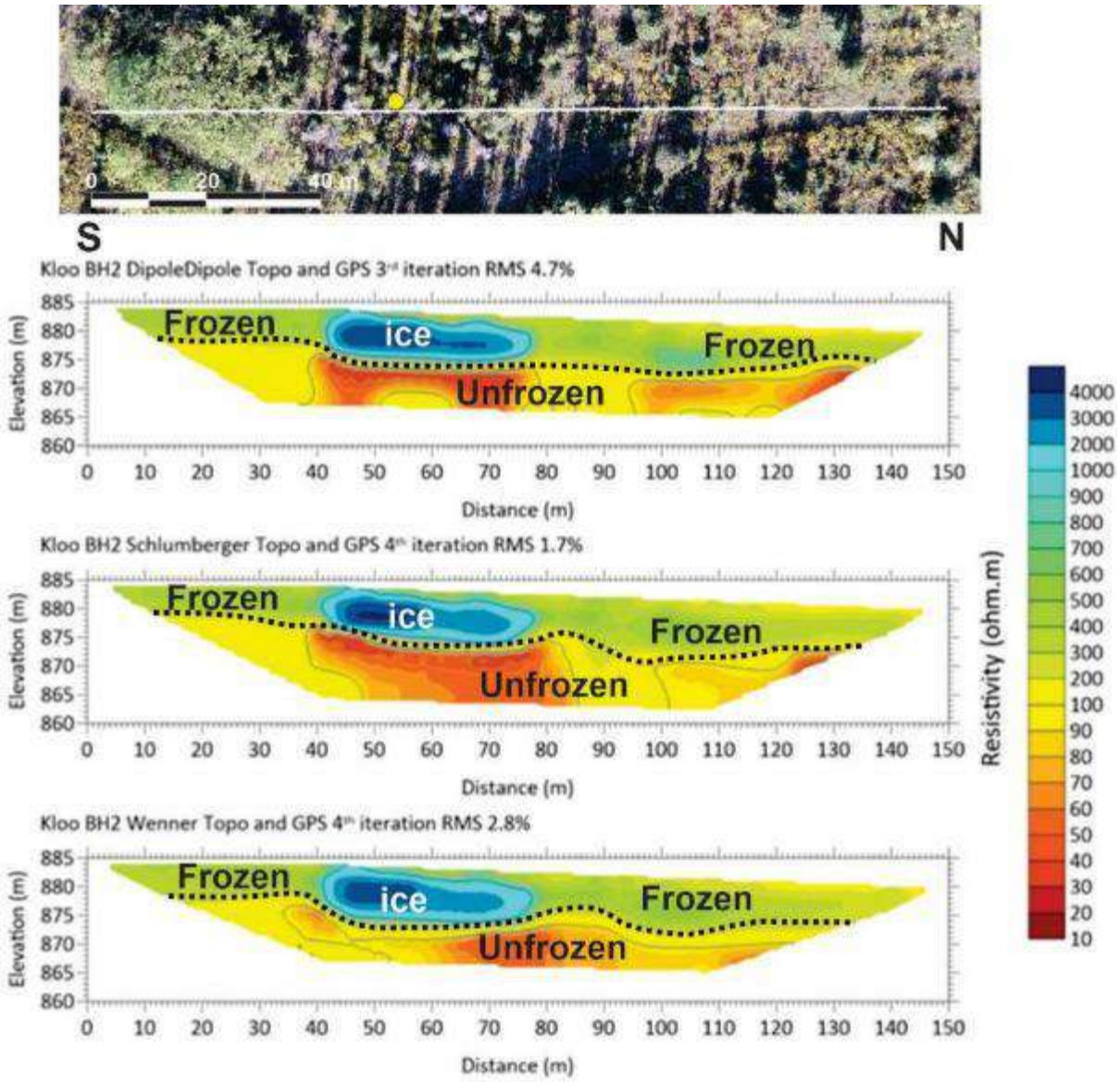

FIGURE 66 ELECTRICAL RESISTIVITY PROFILES FROM THE *K'ÙA EAST* SITE. THE BLACK DOTTED LINE REPRESENTS AN APPROXIMATE BOUNDARY BETWEEN FROZEN AND UNFROZEN MATERIAL WHILE "ICE" INDICATES POTENTIAL ICE-RICH AREAS.

6.4.2 K'ùa West Site

The *K'ùa West* site is located the trail leading to the old K'ùa settlement, about 1.4 km west of the village, and 3.3 km North of the Alaska highway (Figure 64). It is in a wooded area on the west side of the trail, while the eastern side is a wetland with ponds (Figure 67). The site was chosen because of the numerous signs of degradation, such as ponds and wetlands present in the area. A shallow borehole was drilled on August 2nd, 2019, and a ERT surveys were conducted, parallel to the trail and using the borehole location as a mid-point (Figure 67).

The borehole KLOO_BH01 was drilled at *K'ùa West* on a low-elevation permafrost mound. The cores were collected down to a depth of 1.35 m. The thaw front was encountered at a depth of 33 cm at the time of drilling (August 2nd, 2019). The unfrozen layer consisted entirely of organic cover (Figure 68). From 33 cm to 135 cm, which was the end of the borehole, the sediment is sandy silt with gravel. The sediment is ice-rich with crustal, microlenticular, and suspended cryostructures. The volumetric excess ice content ranges from 16 to 46%. Overall, the borehole has a mean volumetric excess ice content of 36%. The cumulated ice content represents a potential subsidence of 0.37 m if permafrost were to thaw.

KLOO_BH01 was lined with PVC piping and instrumented with one 4-channel Hobo logger to record ground temperatures at 0, 0.3, 0.6 and 1.35 m depths. The recording started August 5th, 2021. Data were last downloaded September 27th, 2021, providing about 26 months of data, more than two complete years. Figure 69 presents the trumpet diagram of ground temperatures for KLOO_BH01, using a 12-month record from January 1st to December 31st, 2020. The minimum and maximum monthly mean temperatures at 1.35 m, the deepest sensor, are -3.33°C and -0.39 °C respectively, with a mean annual ground temperature of -1.36 °C. The maximum monthly ground temperature curve suggests that the active layer thickness is 0.6 m.

Figure 70 presents ground temperatures for KLOO_BH01 recorded from August 2019 to September 2021. The graph shows that active layer thickness reached about 80 cm in 2019, about 82 cm in 2020, and about 90 cm in 2021. This increase of the active may reflect yearly variations in climate where 2020 and 2021 had snowy winters and warmer than average summers.

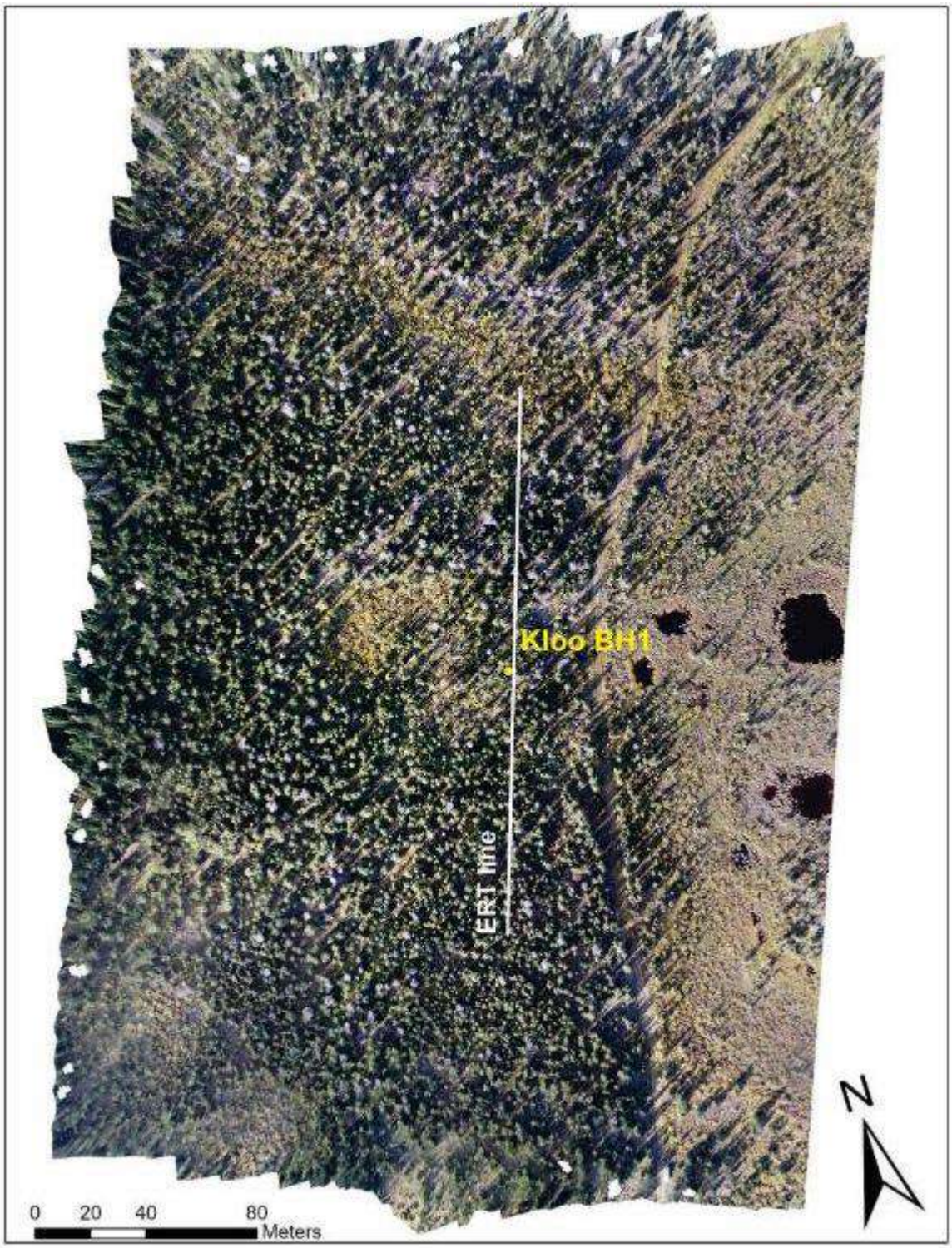

FIGURE 67 AERIAL IMAGERY OF THE K'ÙA WEST SITE.

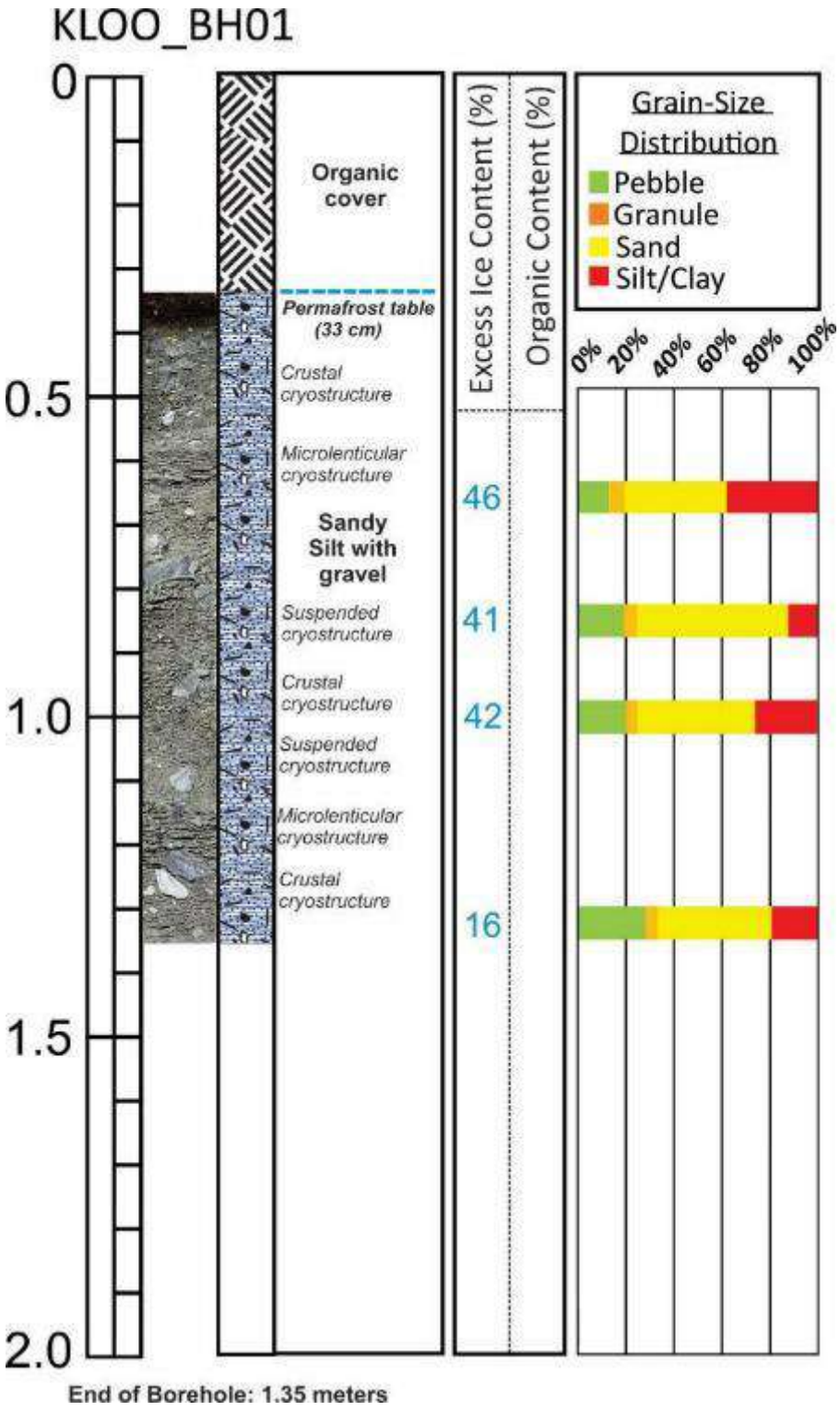

FIGURE 68 BOREHOLE LOG OF KLOO_BH01 SHOWING SOIL TEXTURE, AND ORGANICS AND GROUND ICE CONTENT.

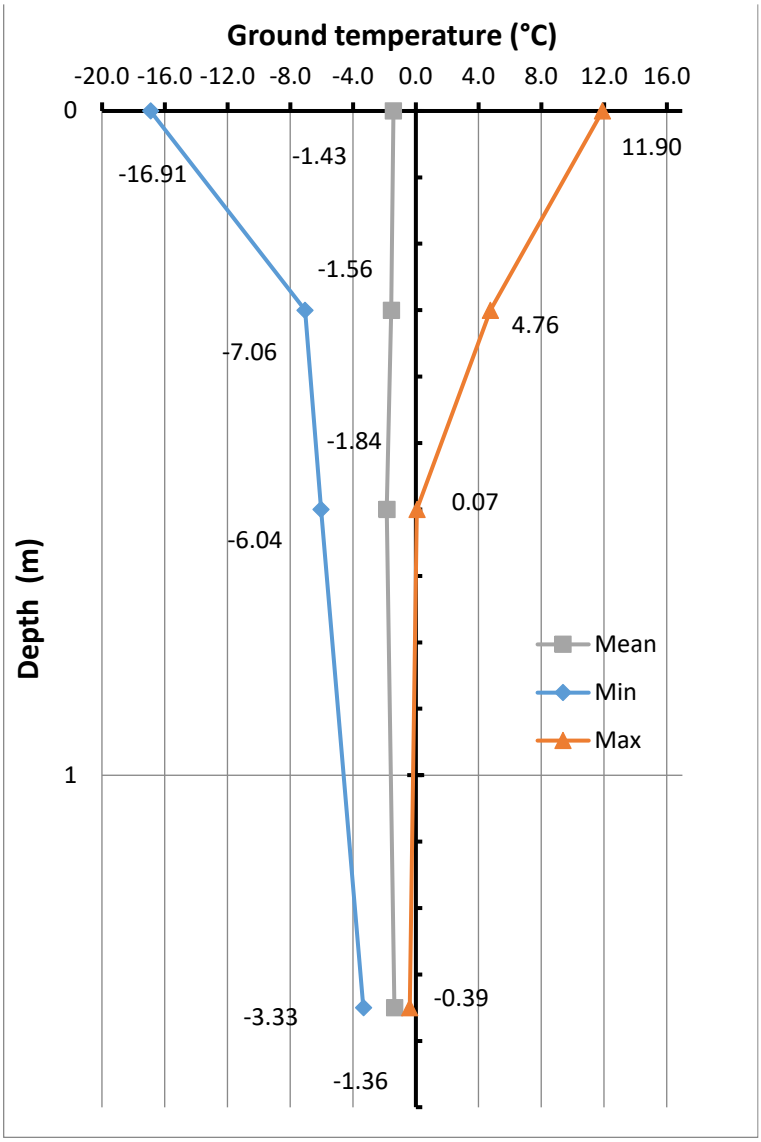

FIGURE 69 GROUND TEMPERATURE PROFILE FOR KLOO_BH01 FOR THE YEAR 2020.

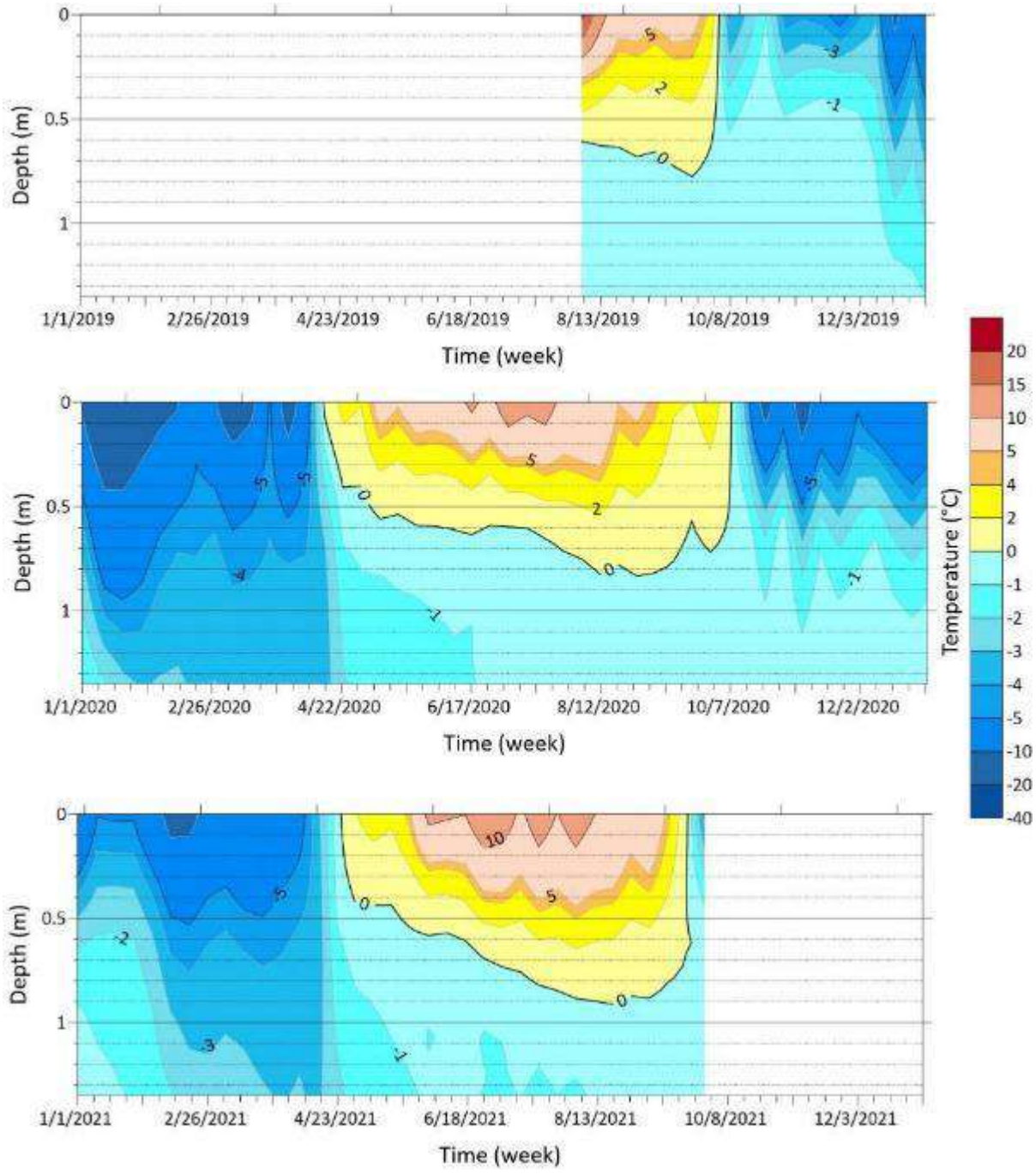

FIGURE 70 GROUND TEMPERATURE OF KLOO_BH01 FROM AUGUST 2019 TO SEPTEMBER 2021.

To assess permafrost distribution at *K'ùa West*, a 200-m ERT survey was conducted, parallel to the trail and using the borehole location as a mid-point (Figure 67). At this site, two types of ERT configurations were used: dipole-dipole and Wenner. The ERT profiles of this survey are presented in Figure 71. Though they have different depths, the two surveys show similar results, but the dipole-dipole seems more detailed. Both profiles suggest that the base of permafrost is deeper than at the *K'ùa East* site, reaching about 20 m depth. Highly resistive areas, represented by the blue sections of the profiles, represent cold, frozen ground. Some higher resistivity (dark blue) zones are present in the dipole-dipole profile, likely representing ground with higher ice content. Low resistivity areas, represented by green to red sections on the profiles, are present at the top of the profiles (the active layer), but also below the approximate permafrost base, shown by with a black dotted line in Figure 71. The lowest resistivity zone occurring in the unfrozen areas might represent groundwater flow.

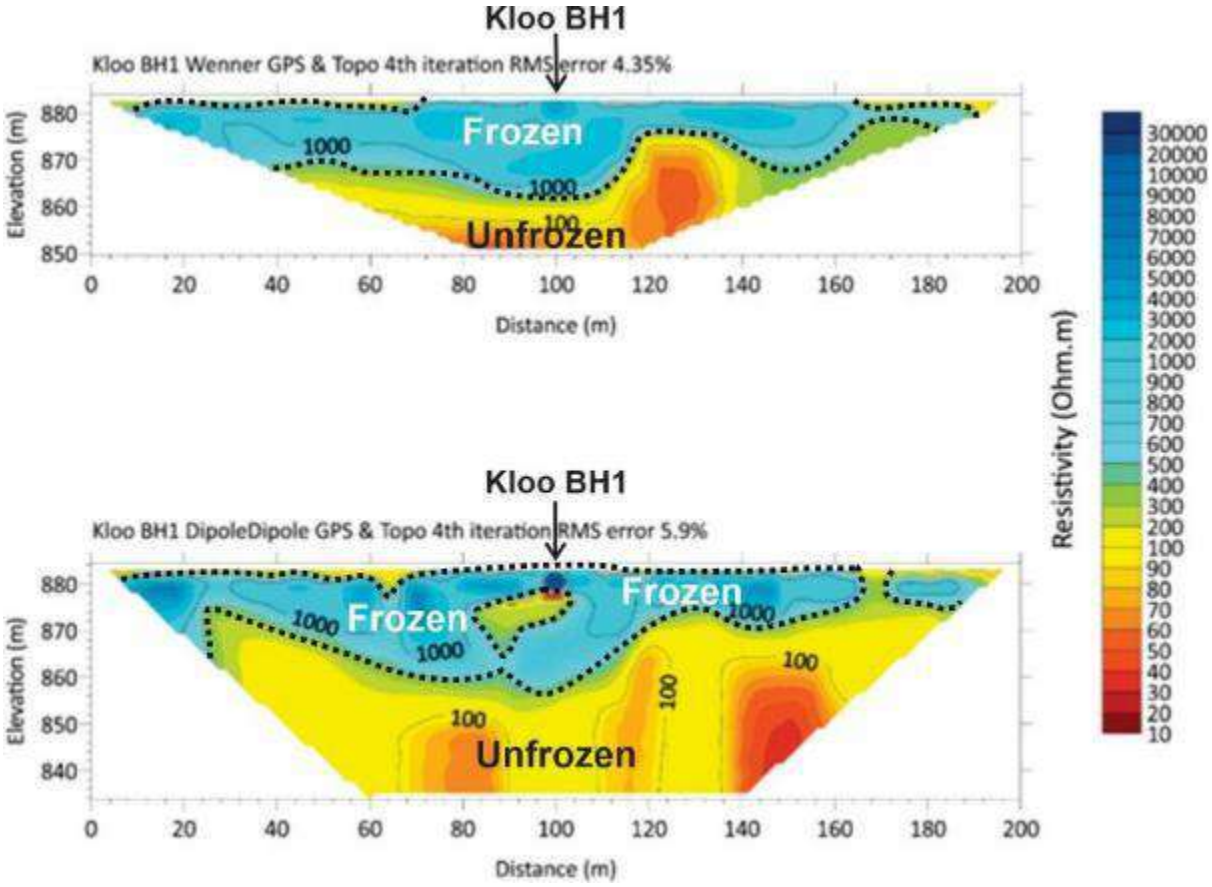

FIGURE 71 ELECTRICAL RESISTIVITY PROFILES FROM THE *K'ÙA WEST* SITE. THE BLACK DOTTED LINE REPRESENTS AN APPROXIMATE BOUNDARY BETWEEN FROZEN AND UNFROZEN MATERIAL.

6.4.3 K'ùa Old Settlement Site

The site *K'ùa Old Settlement* is a former settlement site of cultural significance to the community, much like the Äshèyi old settlement and the Chämì settlement. The site is inaccessible by trail and was reached by boat and surveyed August 4th, 2019.

At the time of the visit, several heritage cabins were identified, and their locations were used as boundaries for the survey area. Several areas were highly vegetated (Figure 72). A drone flight was done over the area to better observe the permafrost conditions. An orthomosaic of this area is shown in Figure 73. The observations carried out with the imagery had two main objectives: first, to identify and locate heritage buildings on site; and second, to observe and locate signs of permafrost and/or degradation.

Five heritage sites were identified (numbered 1 to 5 in Figure 73 and Figure 74). No indicators of permafrost presence or degradation were observed on the drone imagery. Additional observations can be obtained using a 3-D model produced from aerial imagery (Figure 74). Finally, further observations were made from satellite imagery that suggested that permafrost might be present at this site, as numerous lakes and ponds, likely resulting from thermokarst processes, are observable in the surrounding areas (Figure 75).

FIGURE 72 CABINS AT *K'ÙA OLD SETTLEMENT* SITE, SURROUNDED BY VEGETATION.

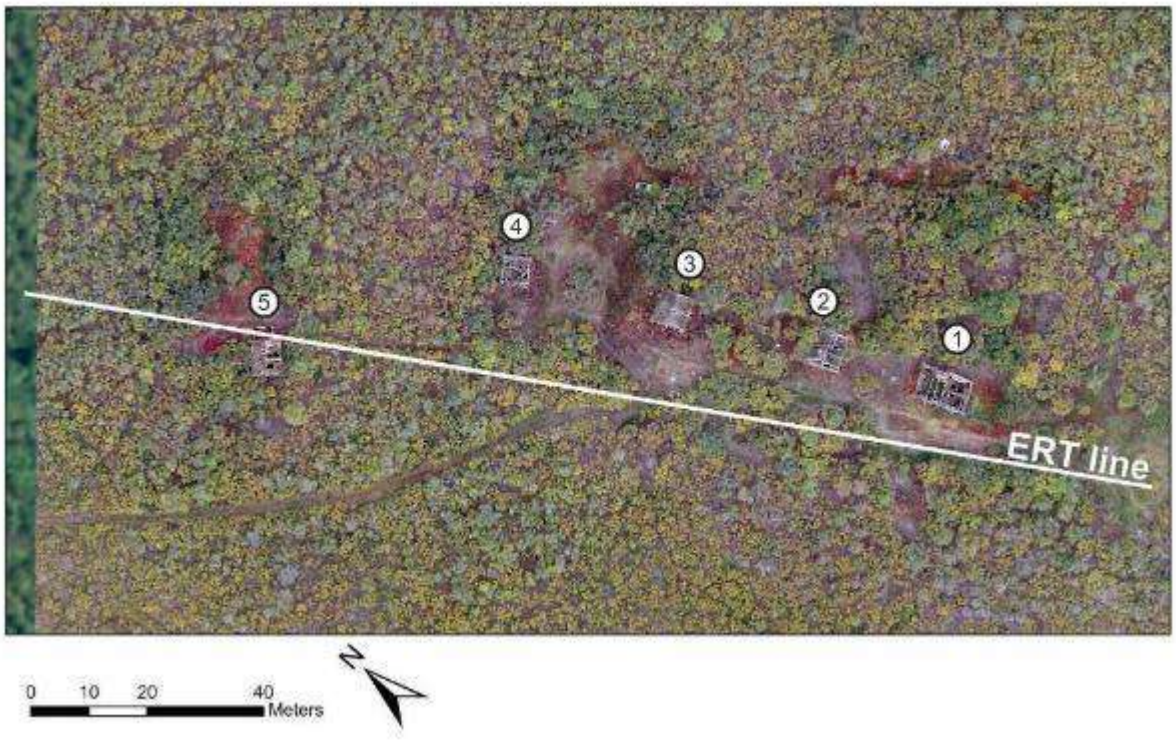

FIGURE 73 AERIAL IMAGERY OF THE *K'ÙA OLD SETTLEMENT* SITE. HERITAGE BUILDINGS ARE IDENTIFIED BY A NUMBER FROM 1 TO 5.

During the field survey, the ground surface was probed at several locations with a frost probe. The thaw front was not found, which suggested that if permafrost were present, it was at more than 2 m depth. Because of how deep the permafrost would be, it was not possible to drill with the YukonU portable drill. Therefore, to assess permafrost distribution in the old K'ùa village, a 200-m ERT survey was conducted along a line passing in-between the heritage cabins (Figure 73), using dipole-dipole and Wenner arrays. The ERT profiles of this survey are presented in Figure 76. The dipole-dipole and Wenner surveys both suggest that permafrost, with high resistivity (blue), is present below a mainly 10 m thick, low resistivity (red), unfrozen layer at the time of the survey. The dipole-dipole survey, having a greater depth of investigation than the Wenner array, also shows an unfrozen layer starting at about 25 m depth. Some even more resistive areas are present (darker blue). These areas likely represent ground with higher ice content (marked by "ice" in Figure 76), such as between 120 and 150 m along the transect. Such ice-rich areas might be responsible for the thermokarst pond observed in the area (Figure 75).

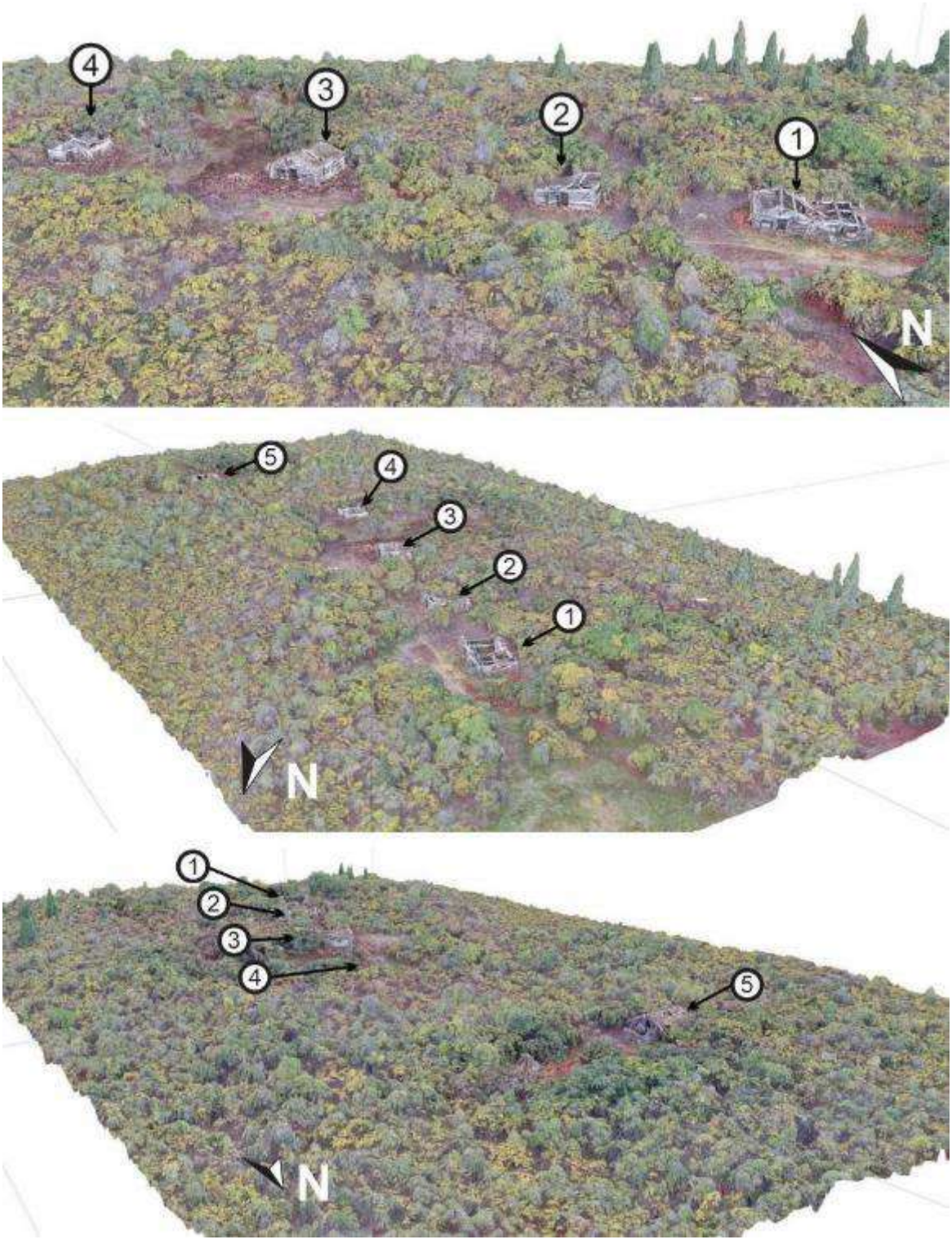

FIGURE 74 THREE-DIMENSIONAL MODEL OF THE OLD K'ÙA SETTLEMENT FROM DRONE IMAGERY.

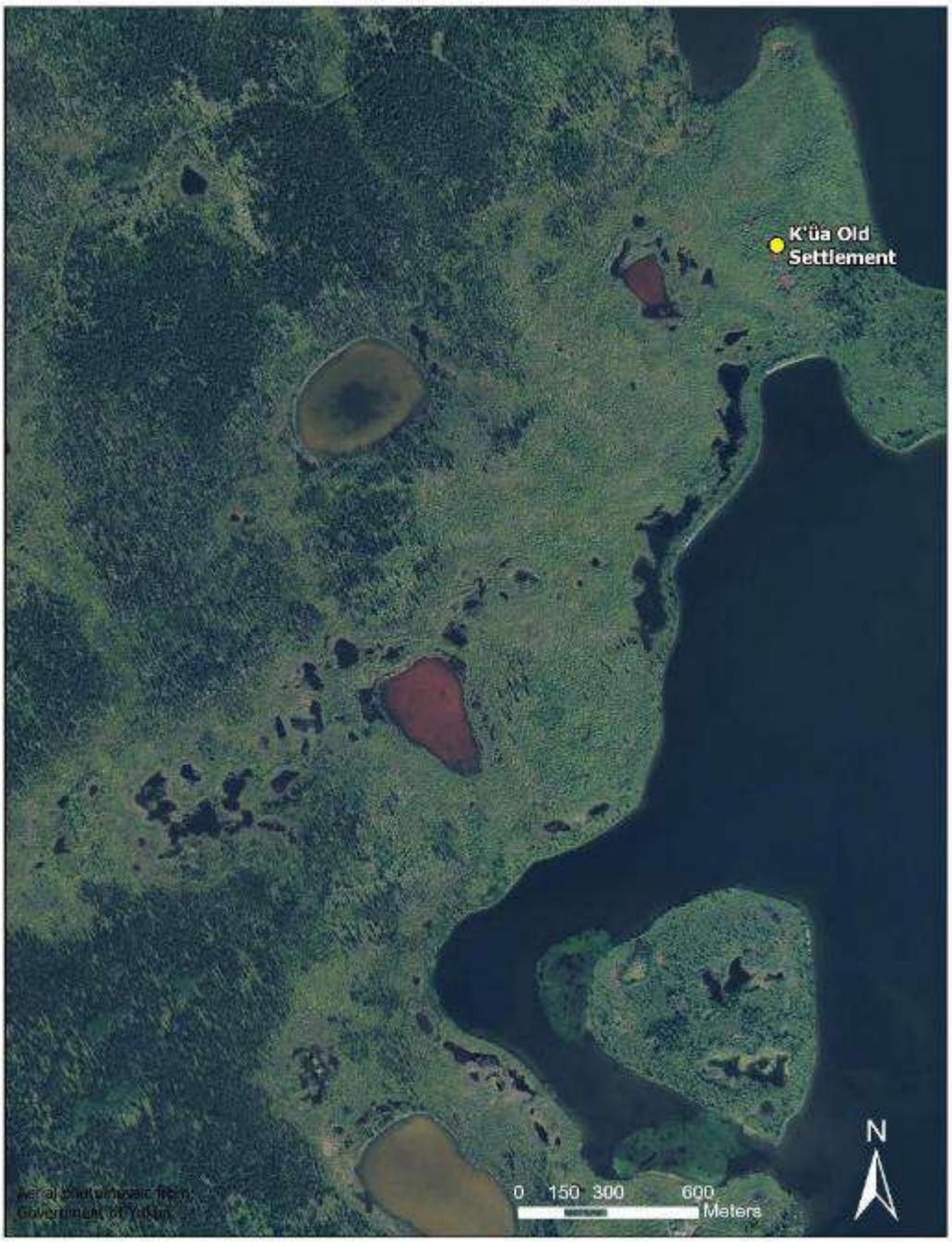

FIGURE 75 SATELLITE VIEW OF THE OLD K'ÙA VILLAGE AREA.

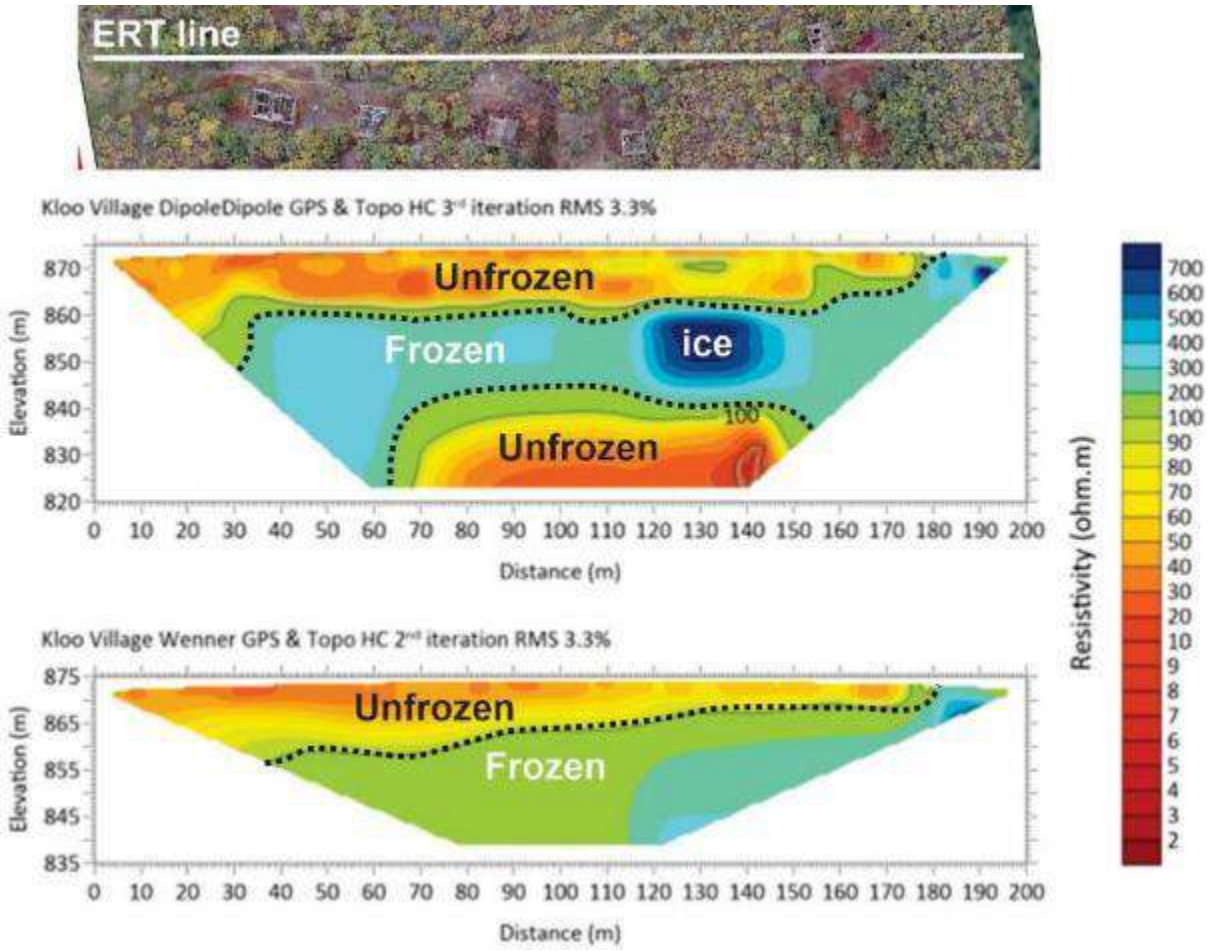

FIGURE 76 ELECTRICAL RESISTIVITY PROFILES FROM *K'ÙA OLD SETTLEMENT*. THE BLACK DOTTED LINE REPRESENTS AN APPROXIMATE BOUNDARY BETWEEN FROZEN AND UNFROZEN MATERIAL. "ICE" INDICATES POTENTIAL ICE-RICH AREAS.

6.4.4 Summary of Sites in the K'ùa Mān Area

The investigation of permafrost characteristics in the K'ùa Mān area were conducted in relatively homogeneous environments compared to the Äshèyi and along Äshèyi Road. Much like for these areas, this is due to the underlying geology.

While the K'ùa Mān area contains various types of terrain, ranging from water-laid to glacial and aeolian deposits, all the study sites are in lacustrine deposits of various thicknesses overlying morainal material (labeled LM in Figure 77).

The investigations at the *K'ùa East* and *K'ùa West* sites, discussed in sections 6.4.1 and 6.4.2 respectively, show that permafrost is relatively thin at these sites (between 5-10 m thick), and mostly contained in the lacustrine deposit. The sediment contained a coarser fraction than the permafrost cores sampled in the Äshèyi and Äshèyi Road areas, translating the influence of subjacent glacial deposit.

Though it has a similar geological context, the situation is different at *K'ùa Old Settlement*, as discussed in section 6.4.3. At this site, permafrost is present deeper in the profile, and geophysical surveying suggests that ground-ice could be present below 10 m depth.

The presence of multiple ponds and lakes of various sizes in the study area suggests that thermokarst processes (permafrost thaw followed by subsidence and increase in site wetness), were, or still are active in the area. These thermokarst processes are driven by the melt of ground ice which is present either at shallow depths in the lacustrine sediment, or deeper in the ground, linked to the glacial deposits, where buried ice could be present.

In general, the K'ùa Mān area could be considered thaw sensitive at two timescales. In the short term, where ice-rich layers of permafrost are located at relatively shallow depths, and in the longer term, where ice-rich clusters are present at greater depths, where it will take more time for the thaw front to reach.

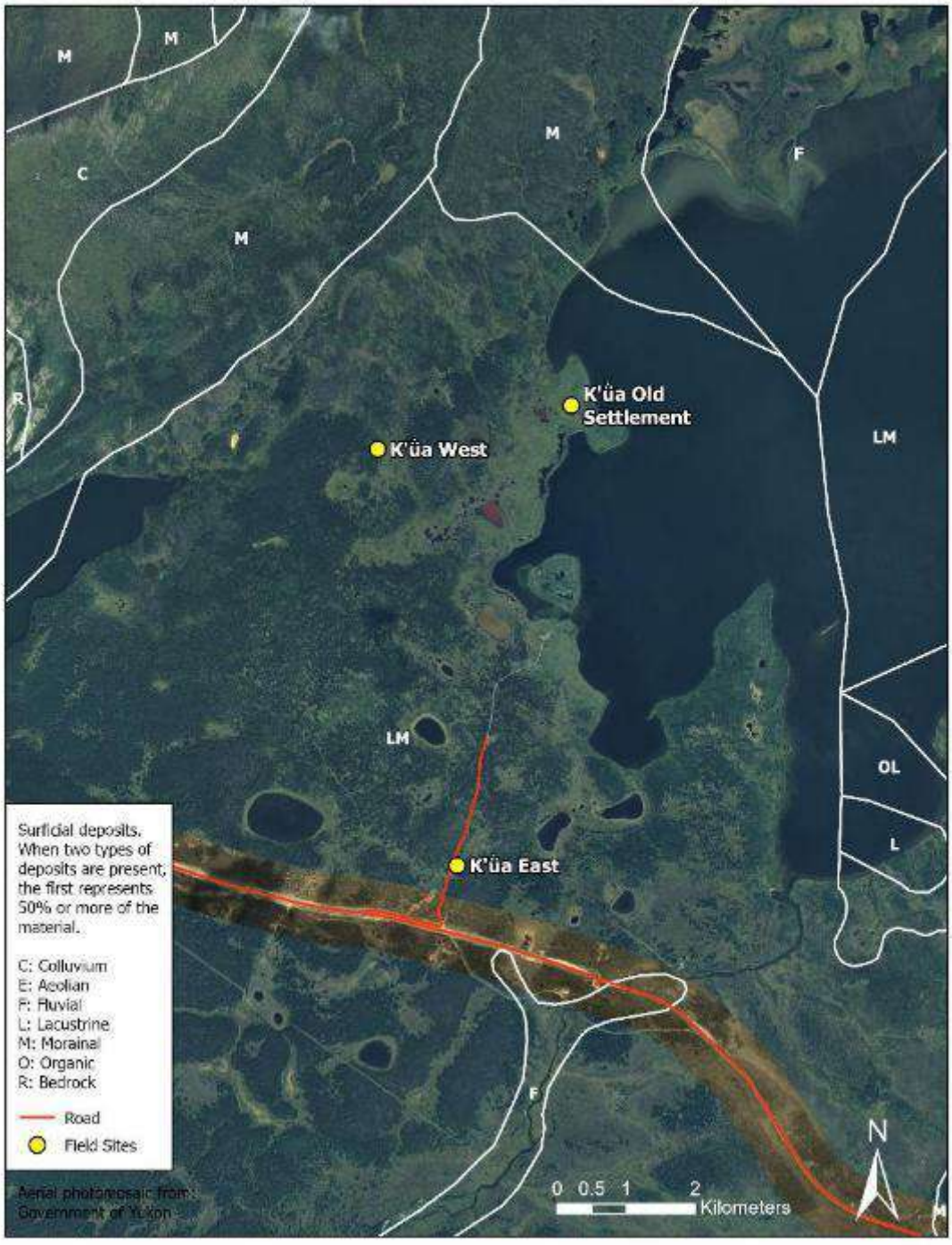

FIGURE 77 SURFICIAL DEPOSITS OF K'ÙA MĀN AREA.

6.5 Dakwäkäda (Haines Junction)

Permafrost conditions were surveyed at settlement land parcels R25B (Sites 1 and 2), C3B (Site 3), C4B (Site 4), and C2B (Site 5) in the Dakwäkäda area at the request of the CAFN community because these areas were slated for development. The locations of these sites are presented by the map in Figure 78. These sites were selected because they were suspected of having high ground ice content that could threaten future development plans. Survey activities in these parcels are discussed in detail in Sections 4.5.1 – 4.5.5, respectively.

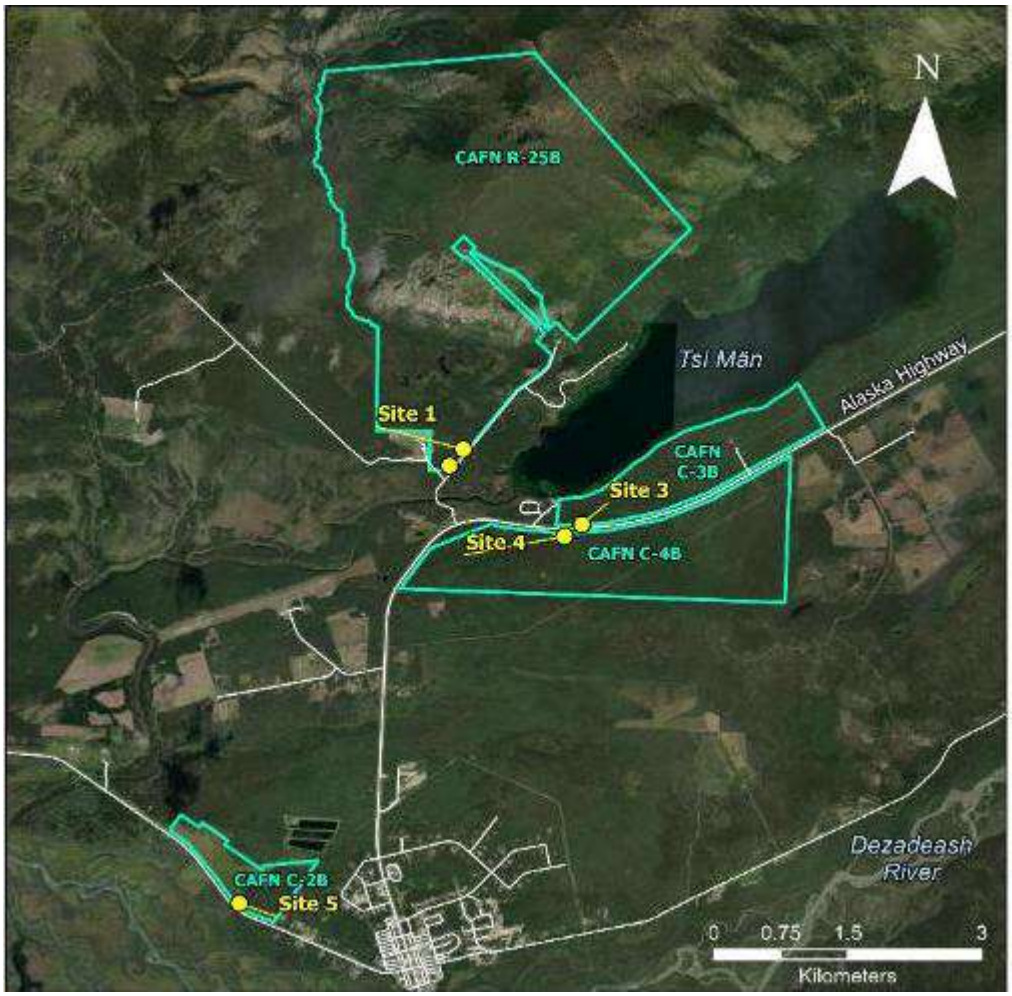

FIGURE 78 DAKWÄKÄDA ASSESSMENT REGION MAP. TURQUOISE POLYGONS AND LABELS ARE SETTLEMENT LAND PLOTS.

6.5.1 R25B (Sites 1 and 2)

Sites 1 and 2 are both located off the western side of Pine Lake Road in the R25B settlement land parcel in moderately open flat forest. At Site 1 a borehole was drilled in a closely forested spot with 15 cm of mossy surface organics and a thaw depth of 45 cm on July 29th, 2022. A thaw depth of 85 cm was observed on July 26th and approximately 25 m to the southwest of the borehole. At Site 2 thaw depth was 125 cm on July 26th approximately 26 m northwest of the road. ERT surveys were conducted at Sites 1 and 2 on July 27th, 2022.

The sediment profile at Site 1 is finer-grained (muddy sand and sandy mud) lower down and is coarser grained (sandier mud and sand) in the upper part (Figure 79). This is typical of ancient glacial lake sediments topped by river, stream, and wind deposits that formed following lake drainage. Thin, alternating light and dark-coloured bands in the finer material lower down represent seasonal variations in sediment deposition called varves that are also indicative of lake sediments.

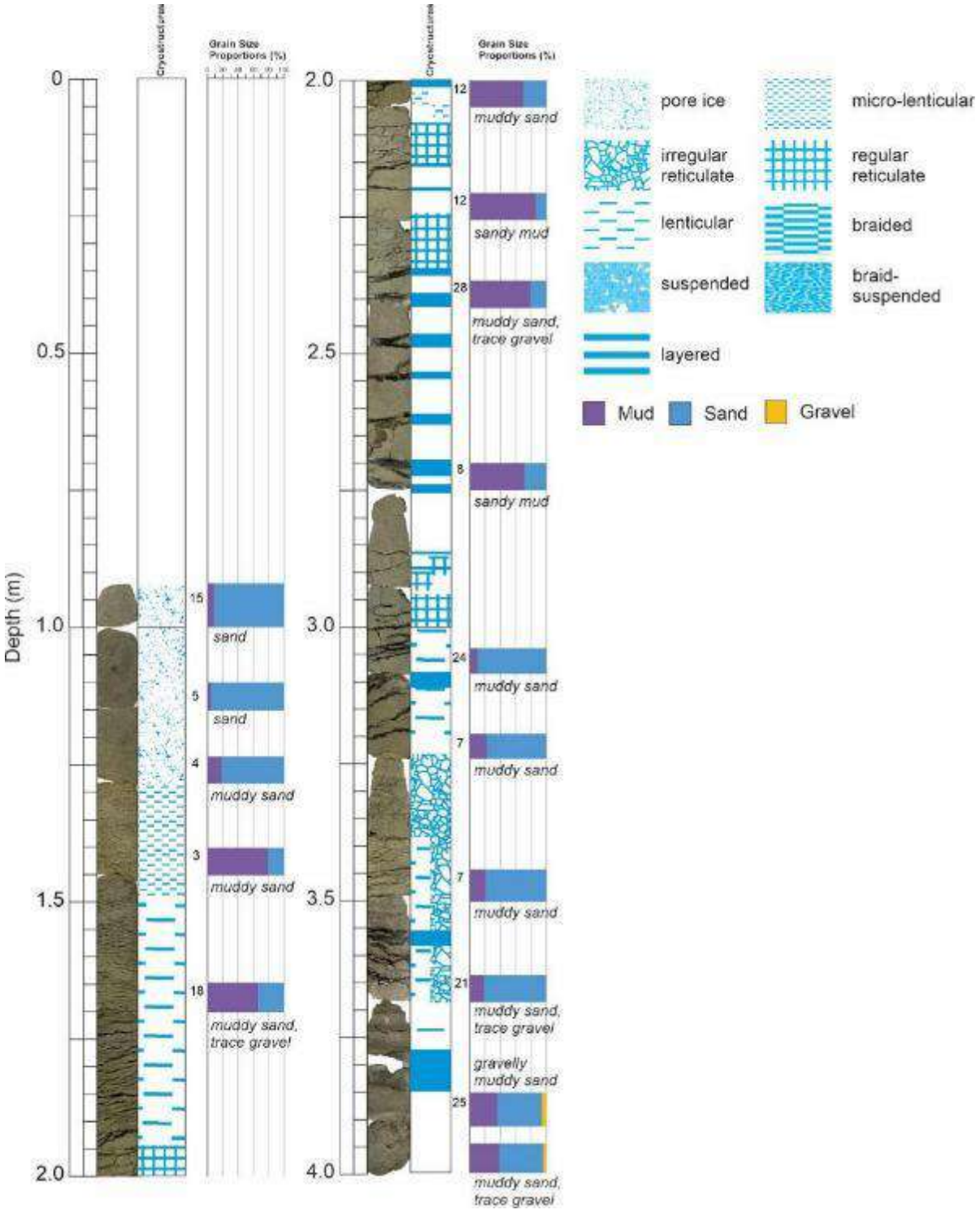

FIGURE 79 GEOTECHNICAL LOG FOR BOREHOLE R25B_BH01. BLACK REGIONS IN THE CORE PHOTO ARE ICE. "MUD", AS USED HERE, MEANS A MIXTURE OF CLAY AND SILT.

Excess ice content ranges between 3-28% with an average around 13.6%. Ice contents deeper in the core were, on average, higher than in the upper part of the core. A thaw subsidence model presented in Figure 80 demonstrates that approximately 43 cm of ground subsidence should be expected if the entire soil column were to thaw.

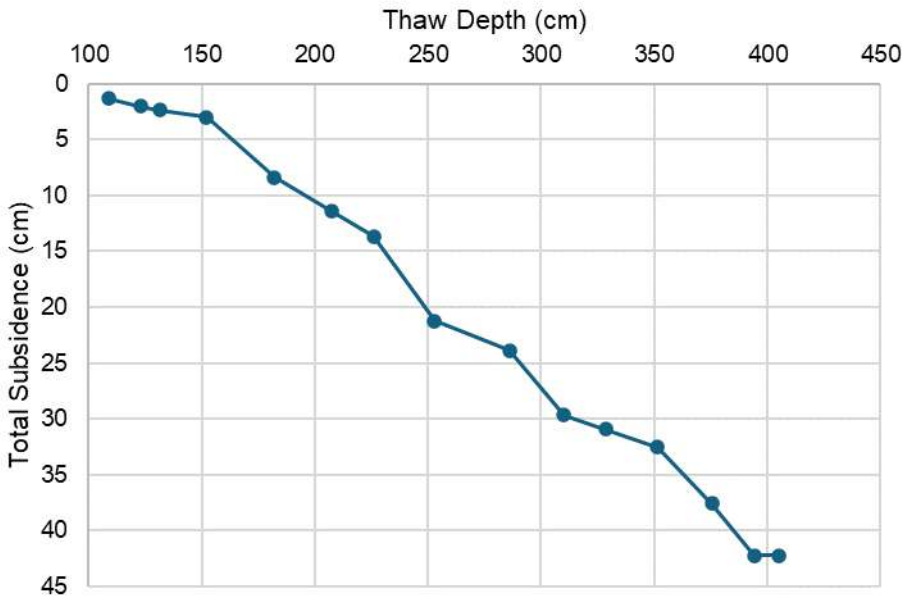

FIGURE 80 CUMULATIVE THAW SUBSIDENCE MODEL FOR R25B_BH01.

Figure 81 shows ground temperature data collected between October 2022 and February 2024 in the borehole R25B_BH01. A large gap in the data set in the summer of 2023 was caused by the logger running out of power because of a roaming blue tooth signal. This was remedied during data collection in Fall 2023. The profile shows that the active layer was ~1m thick in 2022 and ~1.25m thick in 2023, and freeze-back began slightly later in 2022 than in 2023. Permafrost is very warm – warmer than -0.25°C for most of the summer. The warm spot in December 2022 might be indicative of ground water flow; however, it is more likely an artifact of the interpolation process used by the plotting program caused by ground temperatures being at 0°C.

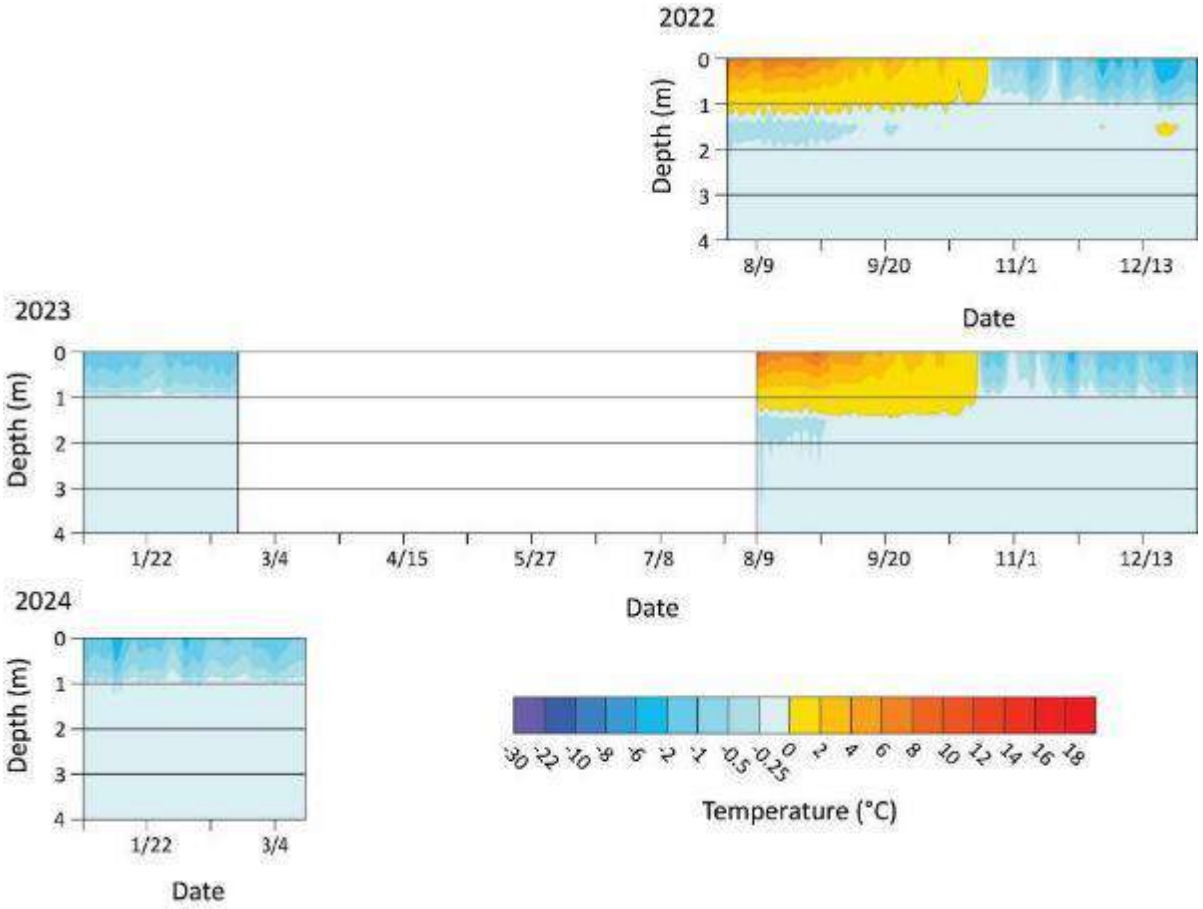

FIGURE 81 TIME SERIES OF SURFACE AND GROUND TEMPERATURE AT R25B_BH01 SPANNING BETWEEN OCTOBER 2022 AND MARCH 2024. THE DATA GAP IS A RESULT OF TOO FREQUENT DATA RECORDING AND A ROAMING BLUETOOTH SIGNAL, CAUSING THE LOGGER TO RUN OUT OF POWER.

ERT dipole-dipole surveys were conducted at Site 1 (Figure 82) and Site 2 (Figure 83) to examine the lateral extent of the soil and ice properties observed in borehole R25B_BH01. These ERT profiles, in addition to the ground temperature data, show that maximum thaw depth spatially varied between 1–4 m depth in the area at the time the surveys were conducted. Much of the frozen ground is likely ice-poor based on low resistivity values, except for a localized region at Site 1 approximately 32 m wide and 6 m thick on the northwest side of the ERT profile (dark blue regions, Figure 82). The southeast end of the Site 1 ERT profile exhibits lower resistivity values, indicating the ground is more ice-poor. The active layer on the southeast side is thicker, potentially because the forest is more open (less underbrush and trees further spaced apart), providing less ground shading. At Site 2, resistivity values do not go above 300Ωm, indicating that much of the ground likely does not contain ground ice. The extremely low resistivity values at Site 2 in the upper 2–3 m are likely organics and sediment with a high moisture content.

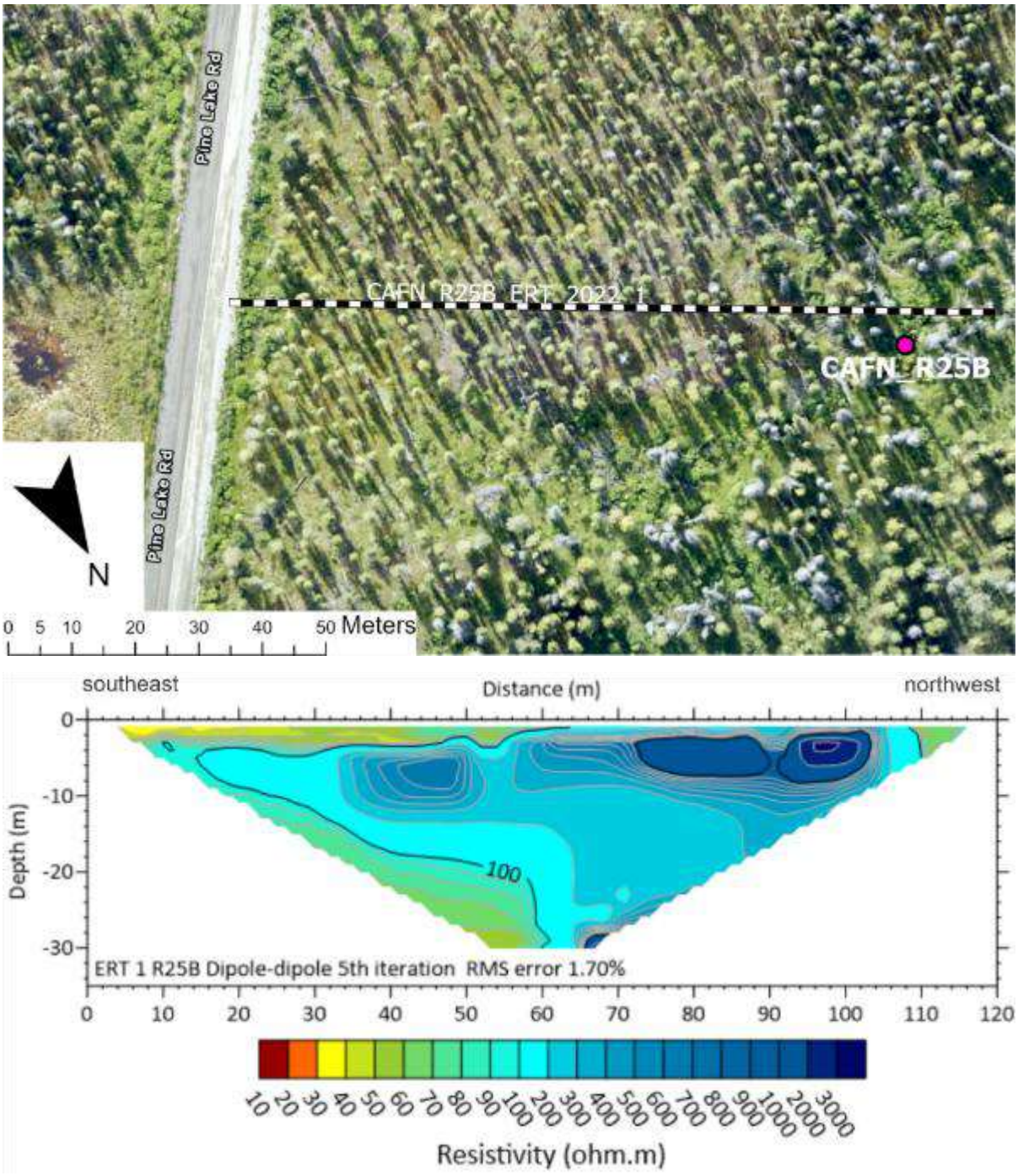

FIGURE 82 DAKWÀKÀDA SITE 1 SHOWING THE LOCATION OF THE ERT DIPOLE-DIPOLE SURVEY (DASHED LINE; JULY 27, 2022) AND BOREHOLE (PINK; JULY 29TH, 2022). THE APPROXIMATE BOUNDARY BETWEEN FROZEN AND UNFROZEN MATERIAL IS INTERPRETED TO BE AT APPROXIMATELY 1000Ωm.

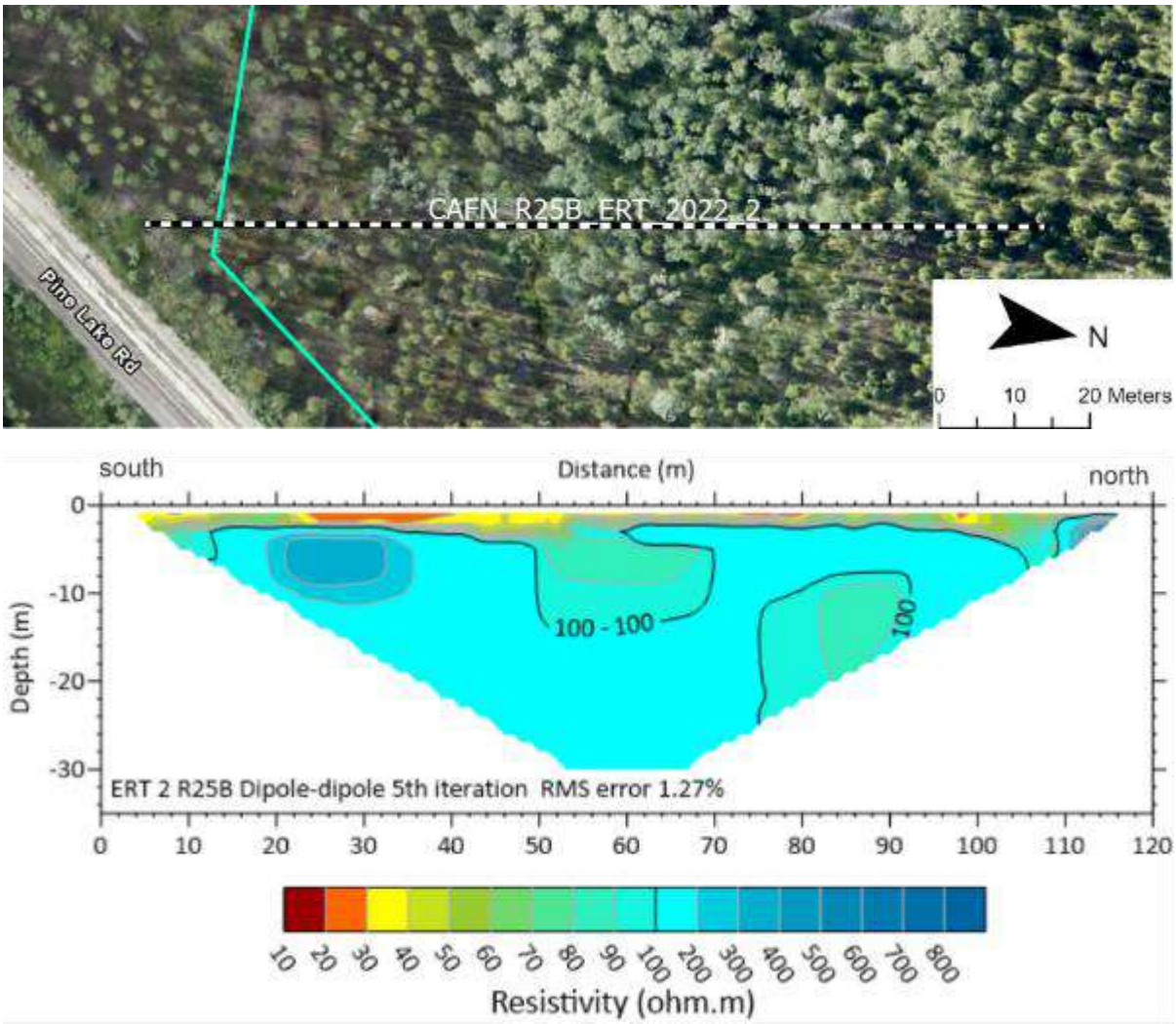

FIGURE 83 DAKWÄKÄDA SITE 2 MAP SHOWING THE LOCATION OF ERT DIPOLE-DIPOLE SURVEY (DASHED LINE). GROUND ICE LIKELY DOES NOT EXIST IN THIS SURVEY, JUDGING BY THE LOW RESISTIVITY VALUES.

On August 8th, 2023, recent vegetation removal and churned up soil from heavy machinery was found between Sites 1 and 2 (Figure 84). Loss of vegetation, disturbance of surface organic horizon, and creation of divots where water can pool means thermal degradation of ground ice is expected to occur here if patches of ice-rich ground are present.

FIGURE 84 AREA OF FOREST CLEARED IN SUMMER OF 2023. SITE 1 AND 2 ERT PROFILE EXTENTS ARE IN SHOWN IN PURPLE.

6.5.2 C3B (Site 3) and C4B (Site 4)

Sites 3 and 4 are located close to the shoulder of the Alaska Highway and within the forest southeast of Pine Lake Campground (Figure 78 and Figure 85). An ERT dipole-dipole survey was conducted at each site on July 28 and July 29, 2022, respectively, to determine ground ice extent and geometry (Figure 85). Thaw probing further back from the road was also conducted on July 26th, 2022.

The resistivity of the ground in both profiles is relatively higher than at Sites 1 and 2. This is indicative of higher ground ice presence. Alternating layers of resistivity in the upper 5 m are probably due to differences in soil moisture. Seasonal frost can create a similar layer-cake resistivity geometry in the upper metre of soil, but August is too late in the summer to expect any remaining seasonal frost.

The top of frozen ground at Site 3 is approximately 5 m depth across the profile. Low resistivity values at the base of the profile indicate the ice-rich soil layer is approximately 16–19 m thick. A region of particularly high ground ice content is present between approximately 6–16 m depth (dark blue region, Figure 85B).

At Site 4, frozen ground starts at approximately 7 m depth. A region of particularly high ground ice content is present between about 43–64 m distance and about 9–18 m depth (dark blue region, Figure 85C). Another is observed further east on the profile, and slightly deeper. High resistivity values around 25 m depth indicate the ground ice is present at deeper depths than at Site 3.

These regions of particularly high ground ice content interpreted from both profiles are more likely segregated ice rather than massive, buried glacier ice. This is because 1) the landscape closely surrounding the sites does not show evidence of past or current kettle lake development, despite ground temperatures in the region being very warm, and 2) higher resistivity values (in the 10,000s – 100,000s) are more typical of massive ground ice.

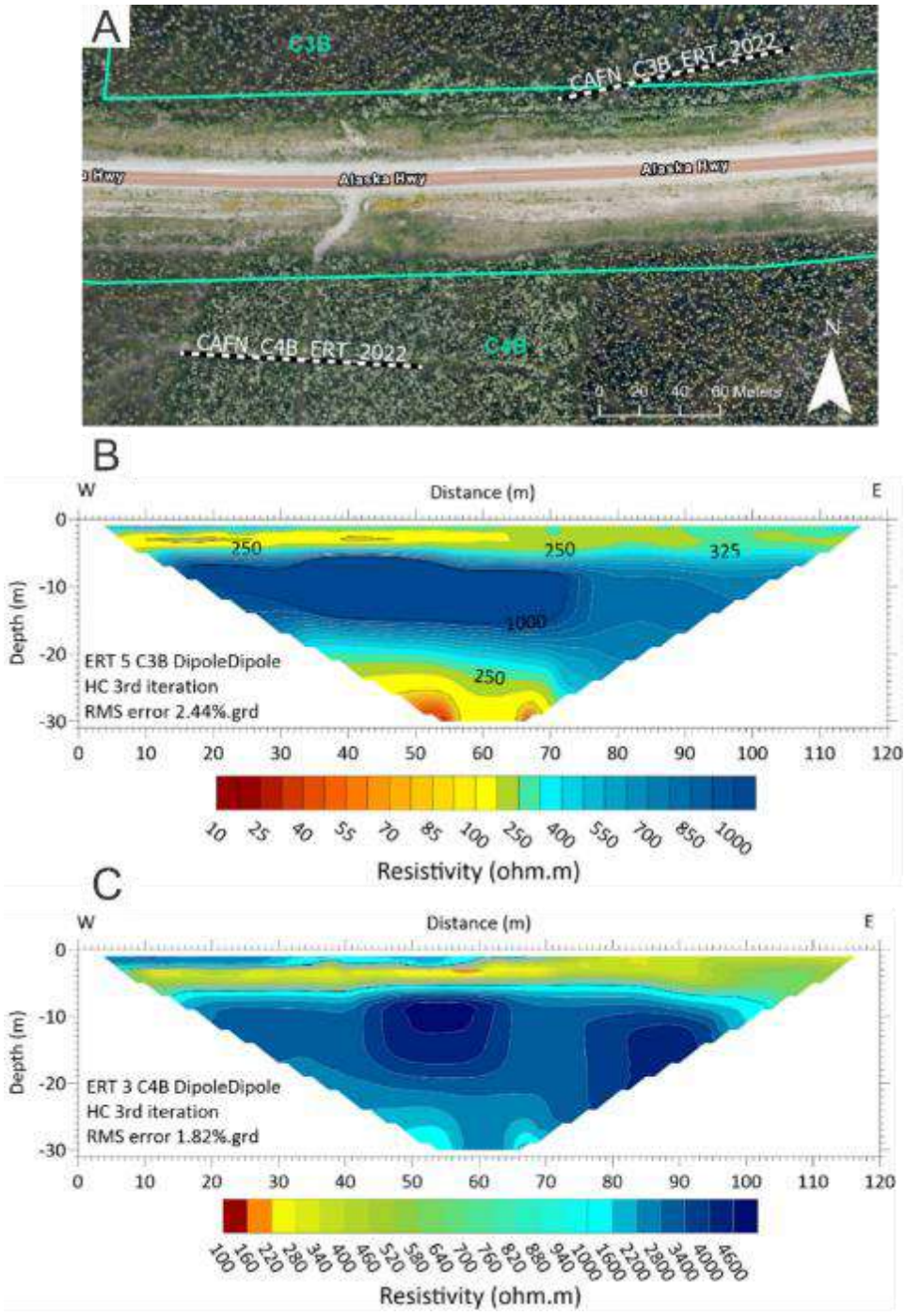

FIGURE 85 A) MAP OF SITE 1 (CAFN_C3B_ERT_2022) AND SITE 2 (CAFN_C4B_ERT_2022). B) ERT DIPOLE-DIPOLE SURVEY OF SITES 3. C) ERT DIPOLE-DIPOLE SURVEY OF SITE 4.

6.5.3 C2B (Site 5)

Site 5 is located on settlement land parcel C2B southwest of Dakwäkäda (Figure 78 and Figure 86B). Resistivity values are overall very low (Figure 86B), indicating the ground is not ice-rich if ice is present at all. Without drilling a borehole to compare physical ground properties with the resistivity values, we cannot say with certainty that there is ground ice at this site. Ground ice degradation created by clearing surface vegetation and other surface disturbances often creates a sharp and sub-vertical resistivity change in the ERT, associated with a sharp change in ground ice content. No such boundary exists in the Site 5 profile where the surface clearing begins. This indicates ground ice is likely not present. Instead, resistivity differences are more likely due to differences in sediment stratigraphy and liquid moisture content.

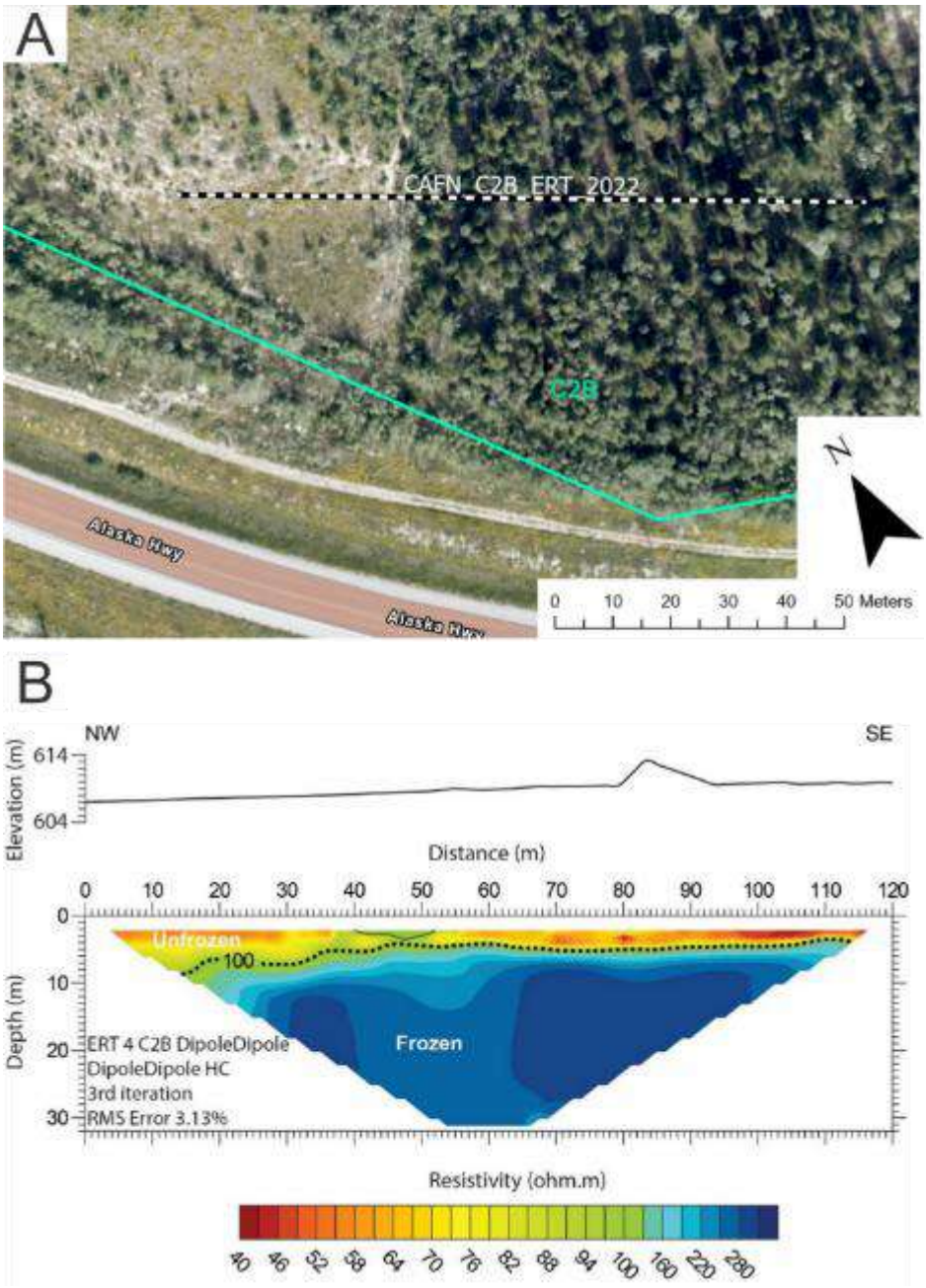

FIGURE 86 A) MAP OF SITE 5 ERT DIPOLE-DIPOLE SURVEY (CAFN_C2B_ERT_2022). B) SITE 5 ERT DIPOLE-DIPOLE SURVEY IN THE C2B SETTLEMENT LAND PARCEL CONDUCTED ON JULY 29, 2022.

6.5.4 Summary of Sites in the Dakwàkàda Area

A borehole was drilled, ground temperature station installed and ERT dipole-dipole surveys conducted to assess the ground thermal conditions and the presence and distribution of ground ice in the Dakwàkàda area at locations of interest to CAFN for future development. Ground temperatures in southern Yukon are usually very warm (very close to 0°C). The ground temperature station installed in borehole R25B_BH01 (Site 1) near Pine Lake is consistent with this knowledge. Site 2-4 are also located mainly in forested areas, similar to Site 1. For these two reasons, their ground temperatures are probably very similar to Site 1. Ground ice exists thanks to shading provided by forest, so likely does not exist under land that was deforested in the past, such as on the west side of Site 5. Sites 1 and 2 appear to contain low ground ice content, except for very localized patches. Areas with thinner forest cover likely have very little ground ice content, as inferred from Site 1. The greater ground ice content at Sites 3 and 4 compared to Sites 1 and 2, as well as the difference in ground ice thickness between Sites 3 and 4, exemplifies the high spatial variability of ground ice content within a sporadic permafrost environment. Overall, permafrost and associated ground ice appear stable at the sites examined. However, given the very warm temperatures, this could easily change if the vegetation and ground surface is disturbed by deforestation and heavy machinery. The recently deforested patch between Sites 1 and 2 should be monitored by the community for signs of ground ice thaw – primarily uneven surface subsidence.

6.6 Shadhäla (Champagne)

There are three sites in the Shadhäla area: *Alaska Highway* site, *Dump* site, and *Champagne Road* site (Figure 87). The *Alaska Highway* and *Champagne Road* sites were chosen because they were representative of the terrain in this area – generally flat or sloping at a very low angle, heavily forested with interspersed wetlands. Permafrost cores were extracted and ground temperature stations installed at the *Champagne Road* and *Alaska Highway* sites on August 11th, 2023, and ERT dipole-dipole surveys conducted on August 10th and 11th, 2023, respectively. An ERT survey was also conducted at the *Dump Site* on August 9th, 2023, after the community expressed concern over the state of the ground in the vicinity of the dump. Ground temperature data were collected from the *Alaska Highway* and *Champagne Road* sites during subsequent visits.

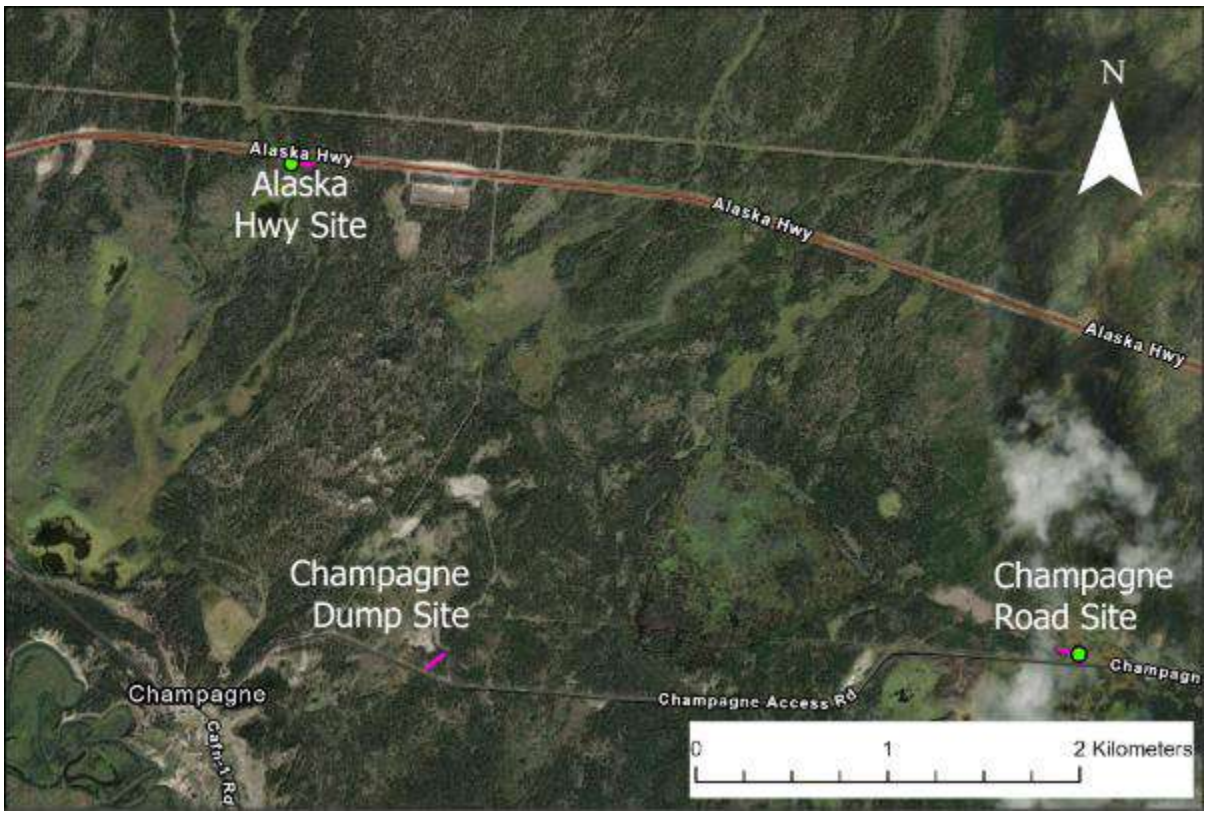

FIGURE 87 INVESTIGATION SITE MAP FOR THE SHADHÄLA AREA. GREEN DOT: BOREHOLE. PINK LINE: ERT SURVEY.

6.6.1 Alaska Highway Site

The *Alaska Highway* site is located just within the woods off the south embankment of the Alaska Highway at kilometre 1514 (Figure 87). The site is raised but adjacent to lower lying wetlands immediately to the west (Figure 91A). Core collection and ERT surveying were conducted on August 11th, 2023. At this time the thaw depth was 26 cm. The surface organic layer at the drilling location was 45 cm thick, under which dry mud was encountered and sometimes made drilling difficult. This resulted in small gaps in our core record (Figure 88). A ground temperature station was installed in the borehole on August 12th with sensors at 0, 0.5, 1 and 1.5 m depth.

The sediment profile coarsens upwards from clay and silt-rich sediment to sandier sediment with some pebbly gravel (Figure 88). This sequence is interpreted to have developed from an ancient glacial lake (clay and silt) into an environment characterized by wind and river sediment deposition. Adding up the thickness of the major observable ice structures yields a conservative theoretical ground subsidence of approximately 42 cm, 10.4% of the total core length. This is very similar to the average excess ice content of 12.4%. Thaw subsidence modelling using the measured excess ice values (Figure 89) yields a smaller estimate of 28 cm.

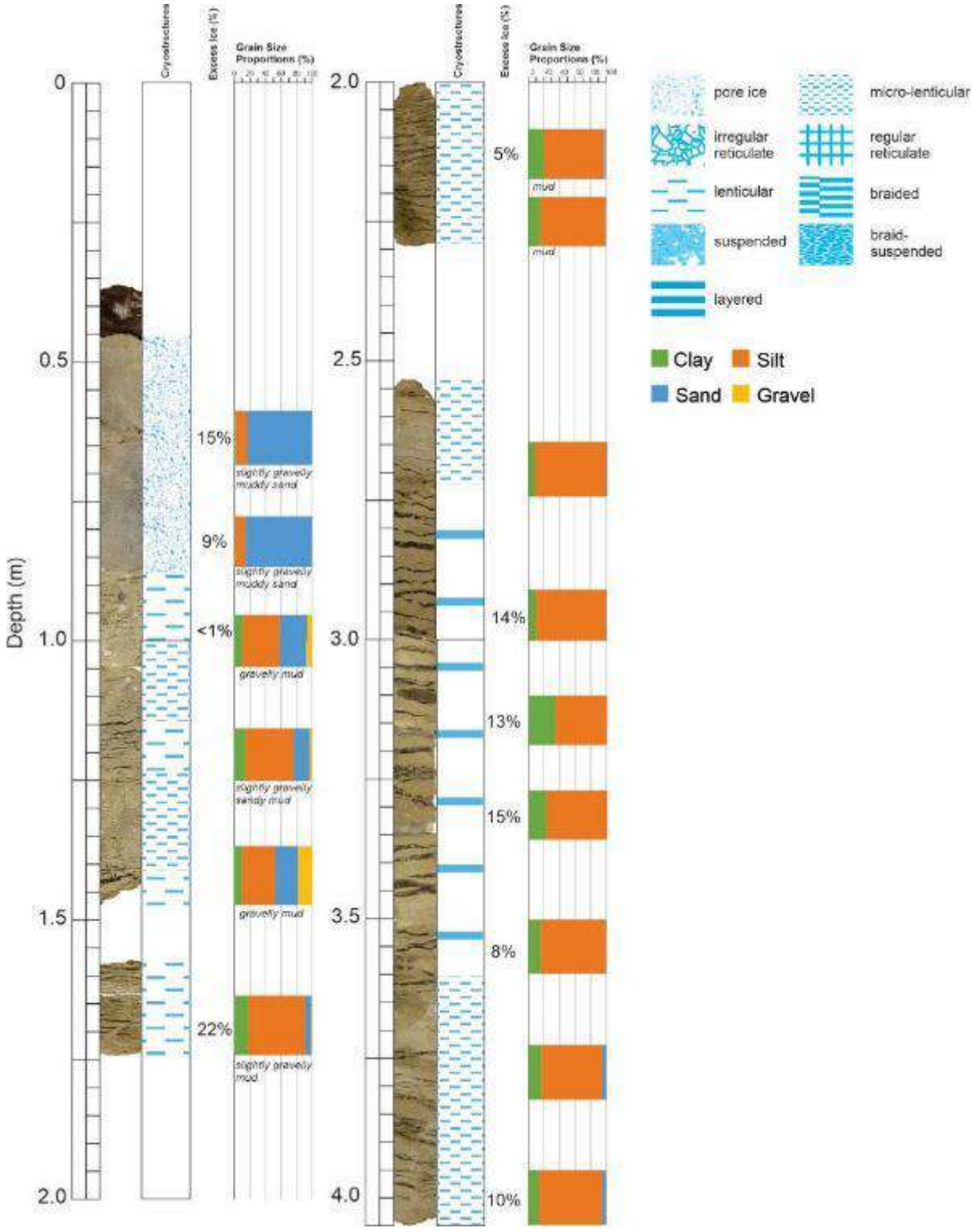

FIGURE 88 GEOTECHNICAL LOG OF BOREHOLE R43B_BH01 (ALASKA HIGHWAY SITE).

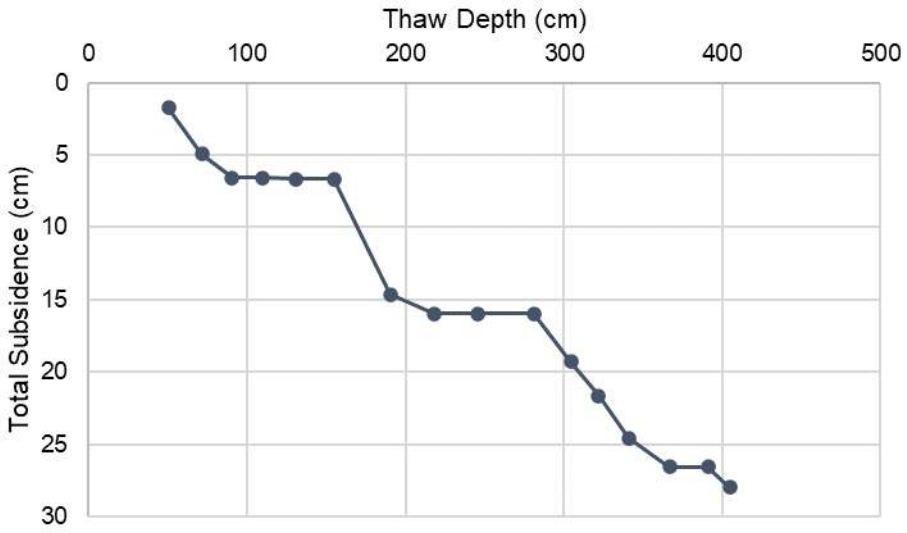

FIGURE 89 CUMULATIVE THAW SUBSIDENCE MODELLING USING EXCESS ICE CONTENT FROM BOREHOLE R43B_BH1 (ALASKA HIGHWAY SITE).

On August 12th, 2023 a ground temperature station was installed in the borehole following drilling. Ground temperature data were collected on February 28th, 2024. Figure 90 shows a time series of this temperature data, which indicates that maximum active layer thaw depth in 2023 was approximately 90 cm depth in late August and freeze-back finished by late October, with some intermittent periods of re-thawing in mid-winter. The winter cold wave was still moving downwards into the ground when the last data were gathered in February 2024, re-cooling the ground.

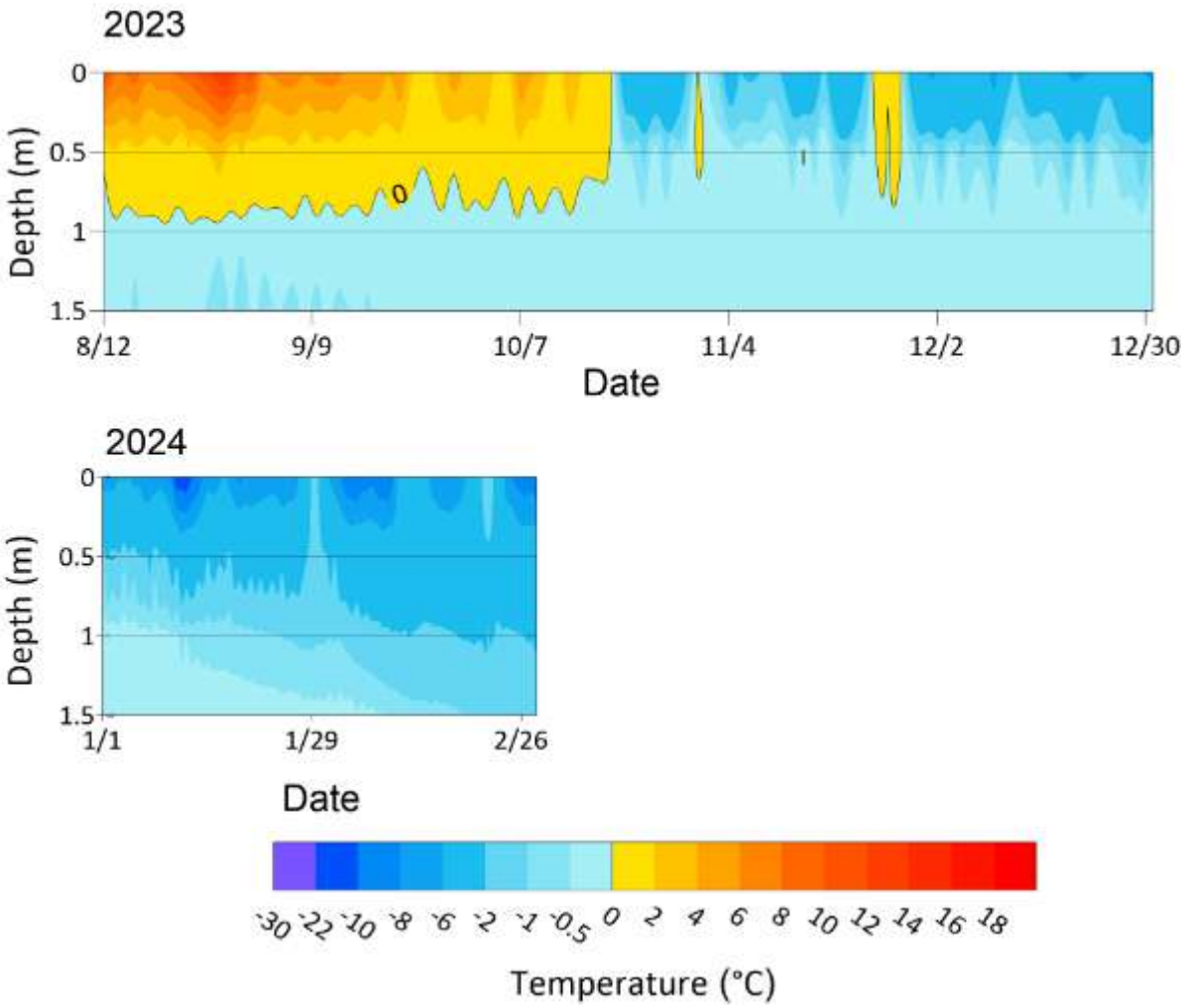

FIGURE 90 GROUND TEMPERATURE IN THE BOREHOLE R43B_BH01(ALASKA HIGHWAY SITE) SPANNING AUGUST 12TH, 2023 TO FEBRUARY 28TH, 2024.

The ERT dipole-dipole survey conducted at the Alaska Highway Site is shown in Figure 91. Higher resistivity values (blue, Figure 91b) are mainly prevalent on the western end of the survey down to a depth of approximately 18 m. Because the borehole was too shallow to determine the exact sediment type at this depth, the sediment is potentially lake-derived low-resistivity clayey silt, similar to the lower half of the core (R43B_BH01). If this is the case, then the higher resistivity values are likely due to the presence of ground ice. Some higher resistivity values are also observed in the center of the profile down to a depth of approximately 7 m. However, because these resistivities are relatively lower than observed to the west. This possibly means there is only a very small amount of ground ice here, or there is no ground ice, but the sediment contains more coarse material. Beneath 7 m, resistivity is low, indicating a lack of ground ice. The eastern end of the profile does not contain ground ice, as indicated by the considerably lower resistivity (dark reds). These values are more typical of moist, wet sandy soil or dry, clay-rich soil.

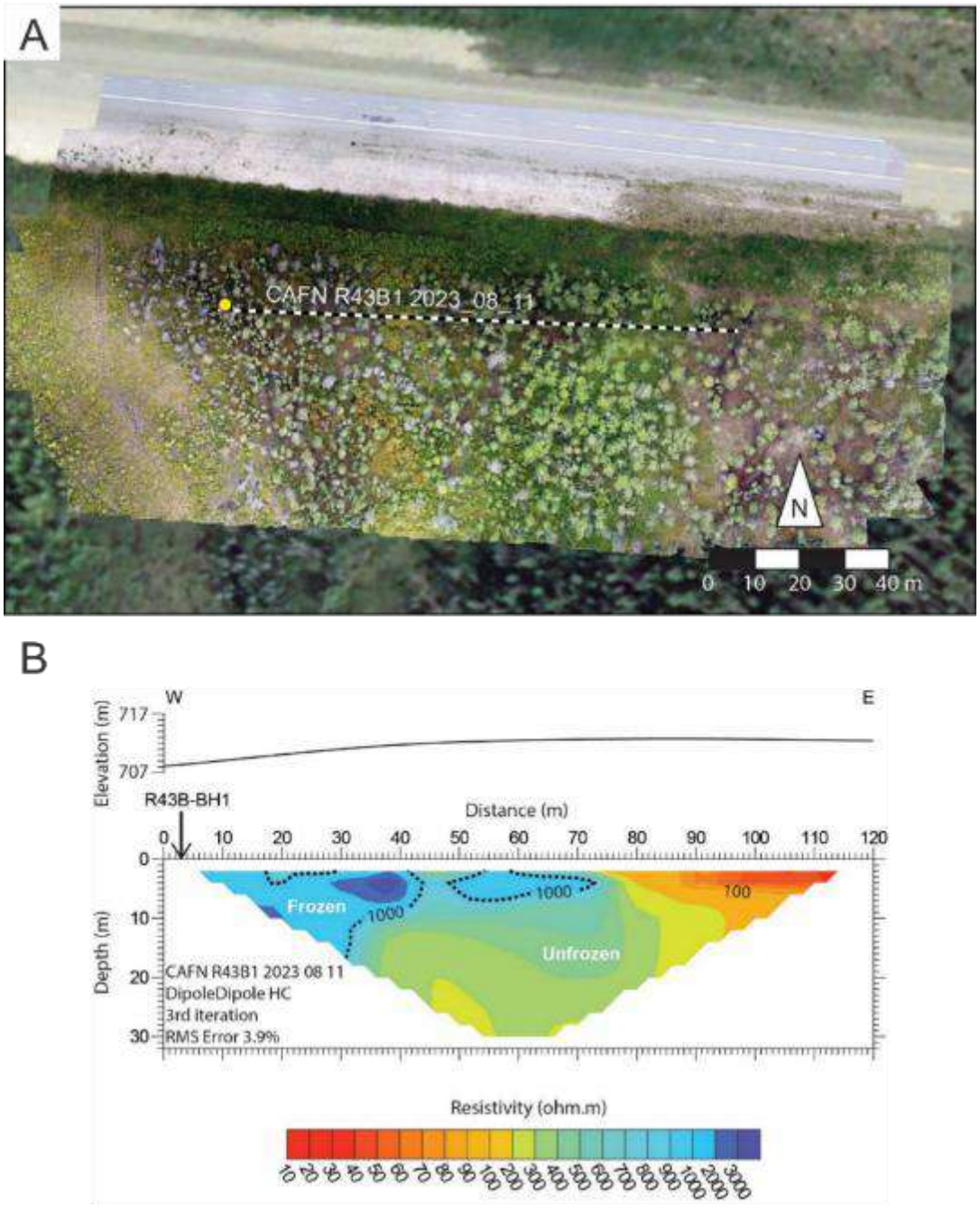

FIGURE 91 ERT DIPOLE-DIPOLE SURVEY OF THE ALASKA HIGHWAY SITE. THE APPROXIMATE BOUNDARY BETWEEN FROZEN AND UNFROZEN GROUND IS INTERPRETED TO BE ~1000ΩM.

6.6.2 Champagne Road Site

The *Champagne Road* site was accessed by an ATV trail on the north side of Champagne Road (Figure 87). An ERT dipole-dipole survey was conducted on August 10th, 2023 to determine the presence and depth of permafrost. The borehole was drilled and a ground temperature station installed on August 11th, 2023 with sensors at depths of 0, 0.5, 1, 1.5, 2, 2.5, 3, 3.4 m. The borehole is located on a mound raised approximately 0.5 m above a marsh to north and a pond to the south. The ERT profile follows the length of this mound, crosses the ATV trail, and continues along a wider area of raised terrain on the west side of the trail.

Drilling was very difficult because the predominantly clayey silt sediment under the mound was very dry. Consequently, the core samples came out as amorphous clods, so a stratigraphic log was not produced.

Ground temperature data were collected on February 28th, 2024. The temperature time series presented by Figure 92 shows that the maximum 2023 thaw depth is approximately 110 cm. Freeze-back was complete by around October 15th. Temperatures below the active layer in February are still very warm – less than 0.5 degrees below 0°C. Although the maximum depth of seasonal temperature variation was not reached, this indicates that the permafrost is warm. The winter cold wave continued propagating downward into the ground around February 1st, 2024.

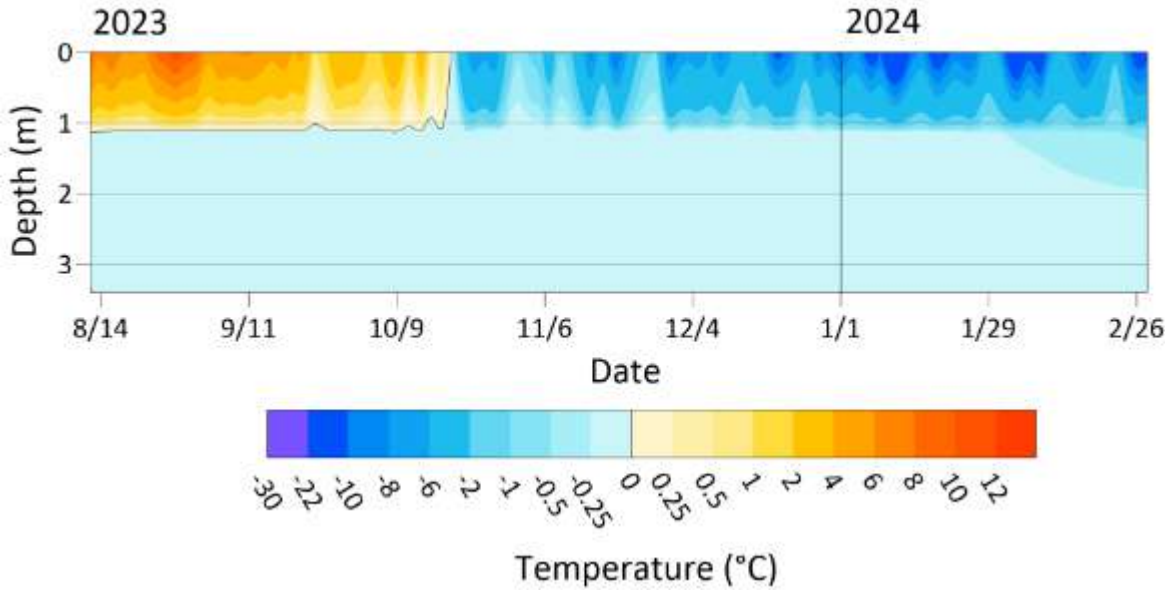

FIGURE 92 TIME SERIES OF GROUND TEMPERATURE IN BOREHOLE R43B_BH03 FROM AUGUST 12TH, 2023 TO FEBRUARY 28TH, 2024.

To the east of the ATV trail, low resistivity values were observed where the borehole is located (Figure 93, black arrow). This was expected given the dry conditions. Relatively higher resistivity values of ~700–800 Ωm are indicative of some ground ice 35–40 m distance along the profile and at 2–4 m depth. This ice is associated with a wider section of the mound. Below ~4 m depth, very low resistivity values are

indicative of high pore water content, likely a talik (a body of unfrozen ground surrounded by permafrost), owing to the thermal effects of the adjacent marsh and pond. The ATV trail is centered at 50 m distance along the profile and does not contain ground ice, as indicated by the very low resistivity values. West of the ATV trail, similar resistivity patterns were observed, except for slightly higher values at depth, potentially due to the lack of ponding water to the north and south.

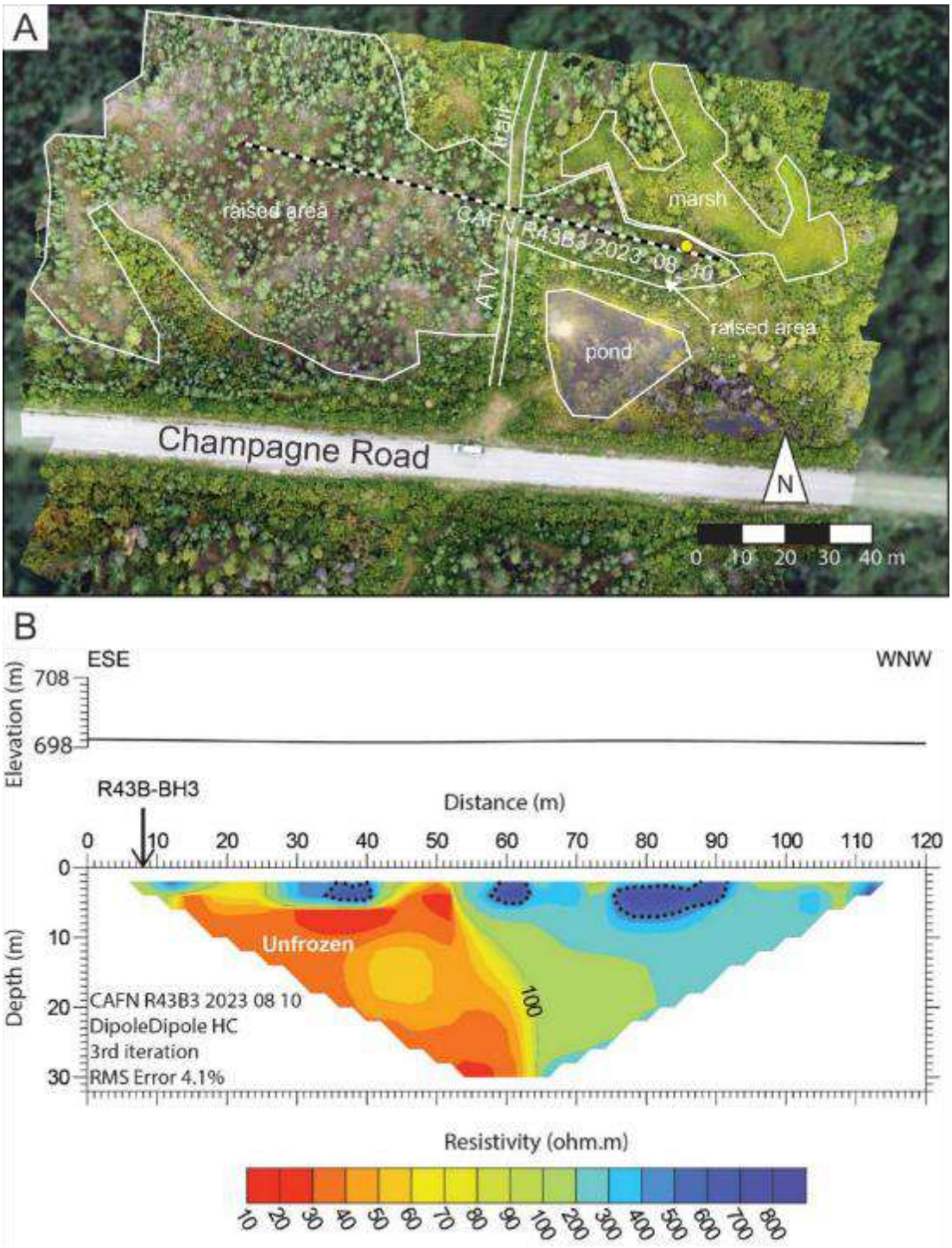

FIGURE 93 *CHAMPAGNE ROAD* SITE MAP AND ERT SURVEY PROFILE. DOTTED LINES INDICATE REGIONS THAT ARE FROZEN. YELLOW DOT ON THE MAP INDICATES THE LOCATION OF THE BOREHOLE.

Because permafrost here at this site is warm, it is more thermally vulnerable. However, except for the small pockets of ground ice (indicated by the higher resistivity spots in the ERT profile), dry, elevated surfaces of the local topography are potentially physically stable due to the very minor or absent ground ice content.

6.6.3 Shadhäla Dump Site

An ERT dipole-dipole survey was conducted immediately south of the Shadhäla Dump (Figure 87) on August 9th, 2023, to determine if ground ice was present. Localized high resistivity values (Figure 94B, dark blue regions) could indicate the presence of ground ice. A shallow hole was dug at the NE end of the survey to assess potential drilling conditions, which revealed the shallow subsurface consisted of very dry gravelly, silty material. Although this dry coarse sediment prevented us from drilling a borehole to validate ERT observations, it also means the high resistivity region on the northeast side of the ERT profile is potentially due to the gravel rather than ground ice.

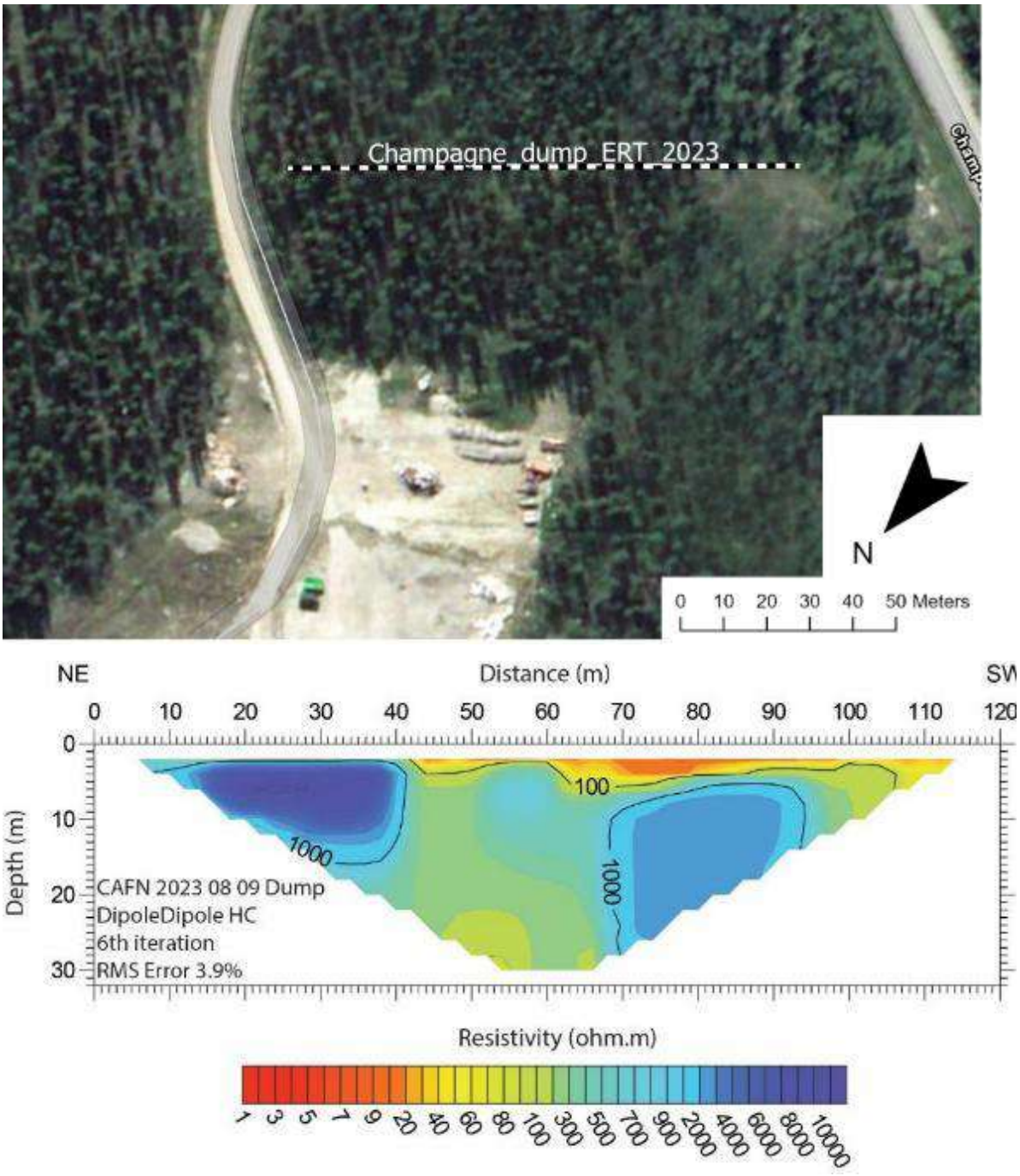

FIGURE 94 ERT DIPOLE-DIPOLE SURVEY PROFILE FOR THE SHADHÄLA DUMP SITE.

6.6.4 Summary of Sites in the Shadhäla Area

Boreholes, ERT dipole-dipole surveys, and ground temperature stations were installed at three sites in the area northeast of Shadhäla on August 11th–12th, 2023 to assess ground ice conditions. The stratigraphy at the sites generally consists of clay-silt lake sediments below with sandier, gravely river, stream, and wind-blown sediments on top. The Alaska Highway borehole had a maximum excess ice content of 15%, but modelling indicates this would cause between 28–42 cm of thaw subsidence if the upper 4 m of the sediment column were to thaw. Although the Champagne Road site was too dry to yield high quality permafrost cores for ice content analysis, the ERT survey indicated that there appear to be localized, small patches of ground ice within the upper ~4–8 m of soil and a talik underlying the eastern end of the survey. Despite high, localized resistivity regions in the Dump site ERT survey, a shallow survey pit revealed these are less likely produced by ground ice and more likely to be caused by dry, sandy, gravely sediment.

7. Sensitivity Mapping

Mapping for this project is based on field observations as well as surficial geology, vegetation changes, slope orientation, and slope steepness. Mapping and spatial analysis were completed using ArcGIS Pro.

7.1 Mapping Area

The mapping area encompasses areas of interest and concern for the community (Figure 95). Of these areas identified in pink in Figure 95, only the one closer to Dakwäkäda is outside of the mapping area. It was identified as a lower priority by the community and the time and resources available for this two-year project did not allow us to investigate this area. The Äshèyi Road mapping area starts on the east shore of Äshèyi Män and stops 12 km east of the road.

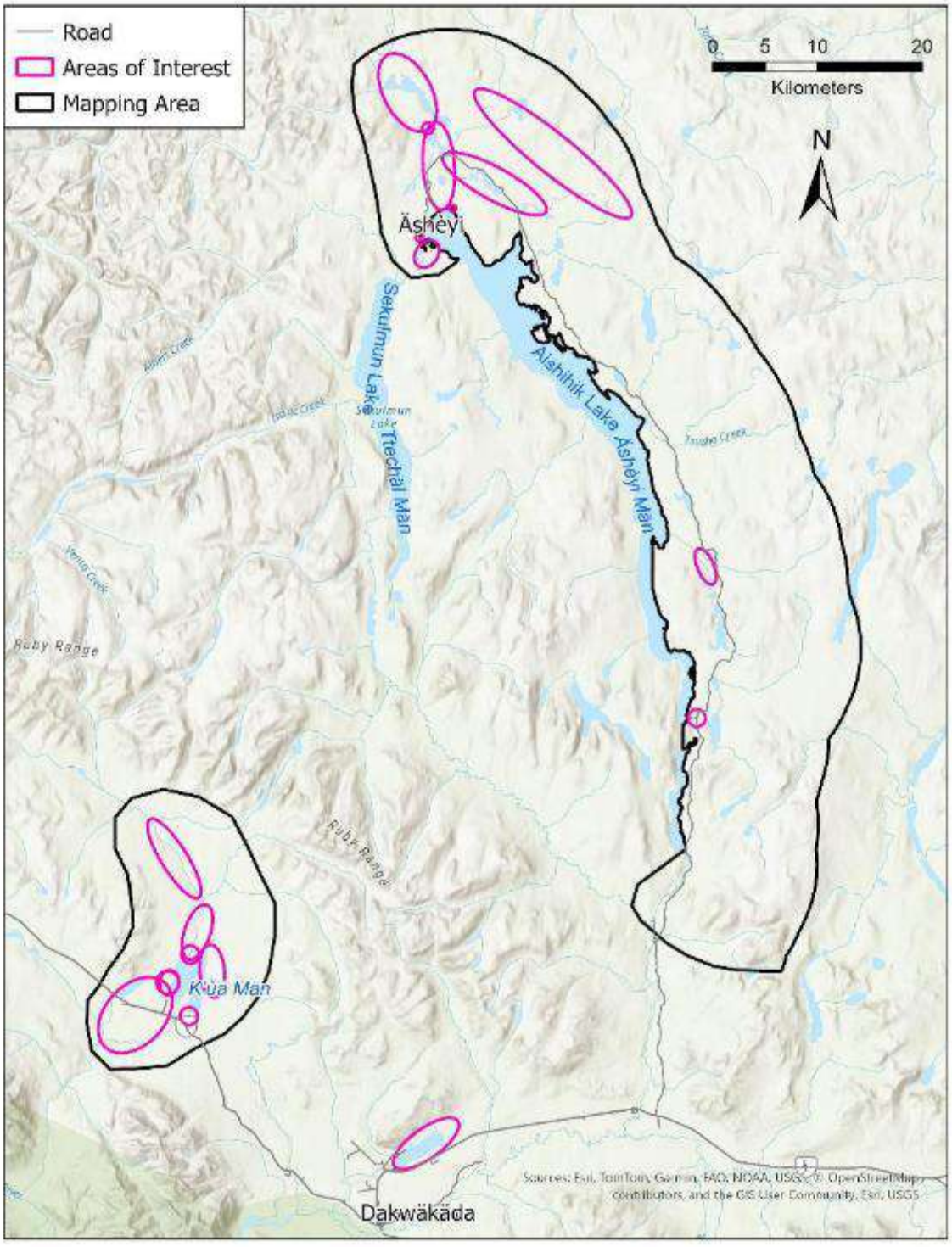

FIGURE 95 SENSITIVITY MAPPING AREA.

7.2 Field Investigations

Field investigations were conducted along the Äshèyi Road and at K'ùa Mãn. In total 33 sites were investigated: five sites were drilled, sampled and instrumented with ground temperature cables, aerial surveys were conducted at eleven sites, seven sites were surveyed with ERT and observations were recorded for the rest. These investigations provided information on characteristics and the current conditions of permafrost (see chapter 6).

7.3 Surficial Geology

Surficial geology materials and their associated soil textures and geomorphological processes were provided by Yukon Government at 1:100,000/1:125,000 scale.

The surficial geology was used to determine the likelihood of presence of permafrost and to attribute levels of sensitivity to disturbance related to permafrost thaw. The field investigation sites were overlayed with the surficial geology, the resulting selection gave a list of geomorphological processes and surficial materials that contain permafrost for the study area. Based on their known association with permafrost, the processes and surficial materials listed in Table 1 were then selected across the entire mapping area. An air photo validation was performed at this stage to validate or exclude certain polygons and ensure the best accuracy possible on the final map.

Levels of sensitivity to thaw were then attributed to each type of surficial deposit based on local field observations or known characteristics of the deposits related to permafrost and ice content. The classification was done on four levels: low, medium, high and very high. Polygons identified as having permafrost processes, or that overlapped with permafrost monitoring sites or identified landforms, were given a sensitivity label of very high. Levels of sensitivity for combinations of Material A (primary surficial material) and Material B (secondary surficial material), as indicated in the surficial geology dataset, were discussed individually, and are listed in Table 1. For certain combinations involving morainal deposits, a distinction was made based on the texture of the deposits. Any other combination of surficial deposits present in the dataset and not mentioned in Table 1 was classified as low sensitivity.

TABLE 1 SURFICIAL DEPOSITS CLASSIFIED BY SENSITIVITY LEVEL TO PERMAFROST AS PER THEIR PROCESSES, MATERIALS, AND TEXTURES.

Process	Material A	Material B	Texture	Sensitivity level
X – Permafrost	Any	Any	Any	Very high
Any other or none	Fluvial		Any	High

Any other or none	Fluvial	Morainal	Any	High
Any other or none	Fluvial	Organic	Any	Very high
Any other or none	Lacustrine		Any	High
Any other or none	Lacustrine	Morainal	Any	High
Any other or none	Morainal		Mixed fragments + mud	Low
Any other or none	Morainal		Mixed fragments + sand	Medium
Any other or none	Morainal		Sand + silt	Medium
Any other or none	Morainal		Boulder + cobble	Low
Any other or none	Morainal	Eolian	Any	Medium
Any other or none	Morainal	Bedrock	Any	Low
Any other or none	Morainal	Lacustrine	Any	Medium
Any other or none	Organic		Any	Very high
Any other or none	Organic	Fluvial	Any	Very high
Any other or none	Organic	Lacustrine	Any	Very high
Any other or none	Organic	Morainal	Any	High

7.4 Land Cover Change

Land cover or types of vegetation can be used in permafrost mapping as an indicator of presence of permafrost, as certain types of land cover better tolerate the ground conditions imposed by the presence of permafrost. For this project, not enough field observations were taken to classify the types of land cover in such a way. Instead, the changes in land cover over 30 years were analyzed and integrated into the mapping model as these changes can indicate the presence of degrading permafrost. Land cover data was provided by the Arctic-Boreal Vulnerability Experiment (ABoVE) in the form of a digital map layer. The dataset is an annual dominant land cover classification for the 1984-2014 period (Wang et al., 2019).

Annual classifications for the years 1984 and 2014 have been compared and analysed together to produce a land cover change layer that could be integrated into this project analysis. Indeed, some land cover change can be attributed to permafrost thaw (Vogt, 2021); in particular when the new type of land cover leads to more moisture and water ponding on the surface, and also when a certain type of land cover is replaced by another type composed of small plants. The land cover change layer shows a change over 30 years and includes both the type of vegetation that disappeared and the type of vegetation it was replaced with. Each pixel (resolution of 30m) was then classified according to a scale of low, medium and high, indicating how likely it is to attribute the change to permafrost thaw. The land cover was represented in 10 different classes, and 84 different types of land cover change were identified in the mapping area, Table 2 summarizes how the vegetation changes were classified.

TABLE 2 SUMMARY OF LAND COVER CHANGE CLASSIFIED BY THEIR LIKELIHOOD OF BEING CAUSED BY PERMAFROST

Type of change	Likelihood
Gain of moisture: water, shallow/littoral, fen, bog	High
Land cover type replaced by another composed of smaller plants; i.e. shrubs being replaced by herbaceous	Medium
Land cover type replaced by another composed of taller plants; i.e. shrubs being replaced by evergreen forest	Low

7.5 Slope Orientation (Aspect)

Slope orientation was calculated using a Digital Elevation Model (DEM) provided by Yukon Government with a spatial resolution of 16 m.

Like vegetation, slope orientation was used as an indicator for the probability of presence of permafrost. Terrain orientation ranges from 0° to 360° and was divided into 8 sectors, each having more or less weight depending on their sun exposure. The more sun exposure, the less likely the terrain has of containing permafrost. Therefore, a slope that is oriented north is much more likely to have permafrost than a south-facing slope. An eastern oriented slope is considered more likely to have permafrost than a west-facing slope because the sun's heat is cooler in the morning than in the afternoon. Values of 1 to 10, where 1 is the least likely to contain permafrost, were attributed to the eight different directions and a ninth class was added for flat terrain. Figure 96 shows how the weights were distributed.

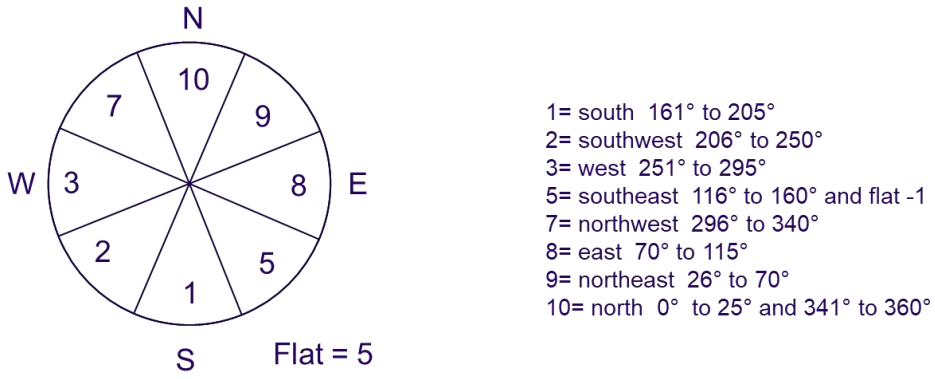

FIGURE 96 WEIGHTS ATTRIBUTED TO THE SLOPE ORIENTATION.

7.6 Slope Steepness

Slope steepness was calculated using a Digital Elevation Model (DEM) provided by Yukon Government with a spatial resolution of 16 m.

Slope steepness aggravates disturbances related to permafrost thaw. The steeper the slope the more likely it is to aggravate existing disturbances. Values of 1 to 10 were attributed, where 1 is the least likely to aggravate disturbances (Table 3).

TABLE 3 WEIGHTS ATTRIBUTED TO SLOPE STEEPNESS (BENKERT, ET AL., 2016)

Description of Surface	Slope Percentage	Slope Degree	Classified Value
flat to gently undulating	0-5	0-3	1
gentle slope	6-27	4-15	3
moderate slope	28-49	16-26	6
moderately steep slope	50-70	27-35	8
steep slope	>70	>35	10

7.7 Mapping Model

To simplify processing, the surficial deposits were converted from vector to raster in order to be in a compatible format with the land cover change, the slope orientation and the steepness layers. This was achieved using the *polygon to raster tool*. The outputs were given the same spatial resolution as the slope and were snapped to it to ensure pixel alignment.

The levels of sensitivity given to the surficial deposits and the levels of likelihood given to the land cover change were then converted into values ranging from 1 to 10 to match the range of values given to the two slope layers. The slope orientation and steepness were combined into one layer, therefore obtaining values from 1 to 100, which was then reconverted on a scale of 1 to 10.

The final model included three layers: surficial deposit was given a weight of 1, land cover change was given a weight of 0.25, and slope was given a weight of 0.5 (Figure 97).

The final map includes values ranging from 1 to 15.2 which were classified in three classes using first the natural breaks method and then rounded to the nearest half digit, producing the following classes:

- 1 to 3.5: Low
- 3.6 to 7.5: Medium
- 7.5 to 15.2: High

Finally, the final layer was simplified using the *boundary clean* tool, that smooths the boundaries between zones and therefore eliminates individual pixels isolated in larger zones.

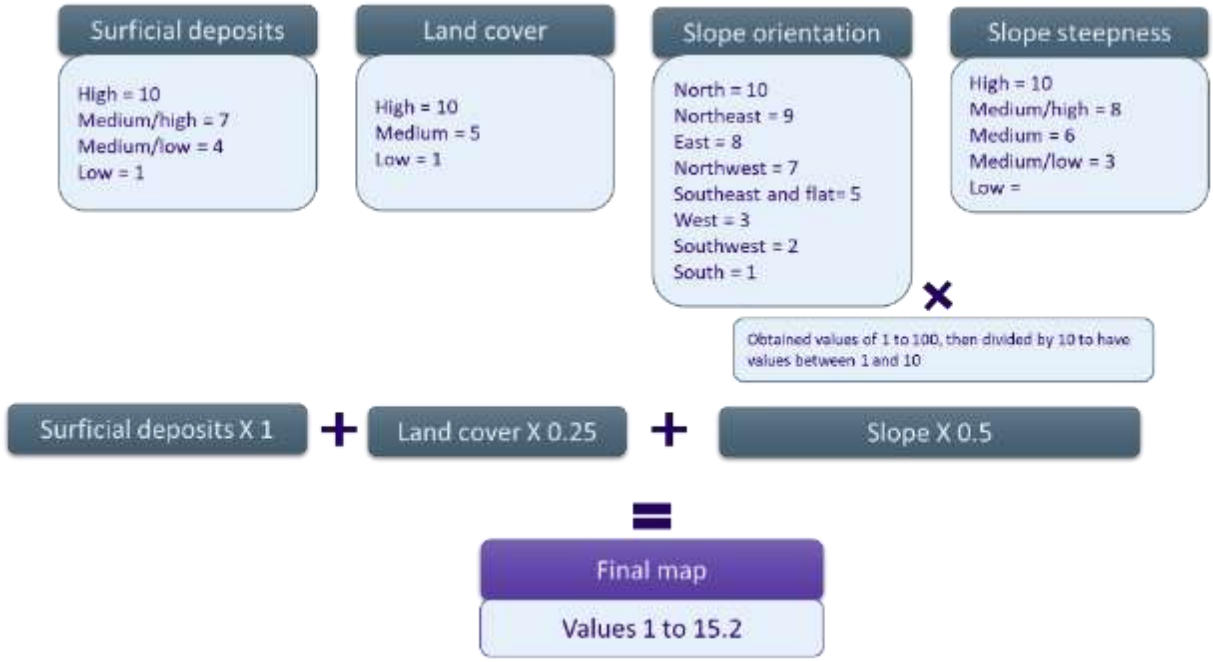

FIGURE 97 LAYERS AND WEIGHTS APPLIED TO THE FINAL MODEL.

7.8 Results

7.8.1 Surficial Geology Analysis

Surficial geology is one of the main factors influencing the distribution of permafrost and its sensitivity to thaw under a warming climate. As explained in the methodology, the first step was to classify the surficial deposits in classes representing permafrost sensitivity to thaw. Figure 4 shows the four classes: low, medium, high, and very high. The category with the most area is the low category, which represents 63% of the total area, followed by medium with 16%, very high with 12%, and finally high with 9%. Table 4 shows the categories and corresponding areas and percentages of total area.

TABLE 4 SENSITIVITY OF SURFICIAL DEPOSITS TO PERMAFROST THAW.

Geology	Km^2	%
Low	1195.5	63
Medium	310.4	16
High	167.6	9
Very high	232.1	12

The largest concentration of surficial deposits classified as very high (red polygons on Figure 98) is located in the K'ùa Mān area; directly around the lake, extending to the south and passing under the road. This indicates that the road in this sector is at risk of ground movements that could result in depressions or cracking. The deposits found in the area are primarily lacustrine associated with morainal, and fluvial sometimes associated with organic with permafrost processes. Many thermokarst lakes are present in this same area north of K'ùa Mān and also in the very high sensitivity elongated area further north. All study sites and permafrost stations around K'ùa Mān are located in the very high sensitivity area.

In the rest of the study area, along Äshèyi Road, the very high sensitivity is concentrated on the east shore of Äshèyi Mān and the following permafrost stations and study sites overlap with it: Permafrost Valley, Pingo, Äshèyi village, Palsa, and Äshèyi old village. Similarly to K'ùa Mān, the surficial deposits are primarily lacustrine, fluvial or morainal, with permafrost processes. Äshèyi village sits on lacustrine deposits with permafrost processes. The rest of the sites; Culvert, Thermokarst, and Kettle overlap with high sensitivity area, classified as Fluvial sometimes associated with morainal. The site Chämì, as in field observations shows no indication of presence of permafrost and therefore overlaps with a low sensitivity.

7.8.2 Land Cover Analysis

As mentioned in the methodology, the land cover changes can be used as an indicator of permafrost degradation. Unlike surficial deposits, these changes don't indicate the presence of permafrost itself but the fact that permafrost is degrading, therefore changing the ground and surface conditions, which triggers a change in plant species able to survive and grow in these new conditions. Two noticeable land cover changes in the study area are a gain of fens and shrubs. Wetlands classified as fens are very often linked with permafrost and many palsas can be found in these environments. Shrubification can also be an indicator of permafrost degradation when the shrubs replace taller vegetation. Figure 99 shows the land cover changes classified by their likelihood of being caused by permafrost. Of the entire study area, 13% has undergone a land cover change between 1984 and 2014; 7% have a low likelihood of being caused by permafrost, 2% a medium likelihood, and 4% a high likelihood, see Table 5.

TABLE 5 LIKELIHOOD OF LAND COVER CHANGES BEING CAUSED BY PERMAFROST.

Likelihood	Km^2	%
No change	1659.7	87
Low	139.0	7
Medium	36.9	2
High	70.1	4

The area where the most land cover change is observed is around K'ùa Mān, see Figure 99. This is also the area where the largest patches of change classified as having a high likelihood of being caused by permafrost can be observed. The study sites in this area are all surrounded by land cover change, predominantly classified as low or high, see Figure 100. For the changes classified as high they mainly correspond to herbaceous, sparsely vegetated, or shrubs being replaced by fen.

Another area where the amount of change is noticeable is between Äshèyi village and the pingo, see Figure 100. Large patches of change classified as high correspond to herbaceous, sparsely vegetated, or shrubs being replaced by fen. A similar amount of change is classified as low and correspond to herbaceous vegetation turning into shrubs. This area also has some change classified as medium which is mainly sparsely vegetated becoming herbaceous vegetation (corresponding partially to the airstrip).

The Äshèyi Road Sites 2 and 3 (Permafrost Valley and Thermokarst) are surrounded by change of all 3 classes with a slight dominance of medium likelihood corresponding to shrubs becoming herbaceous vegetation or forest becoming sparsely vegetated. There has been little change in landcover in the vicinity of the Äshèyi Road Site 1 (Culvert). Chämì is mainly surrounded by changes classified as low.

7.8.3 Slope Steepness and Aspect

Figure 101 shows a combination of the slope steepness and slope aspect (or orientation) as a colour gradient of probability to exacerbate the changes caused by permafrost thaw. The Palsa site and the Äshèyi old village site are the only ones overlapping with values of 2.7 out of a gradient of 1 to 10. All other study sites overlap with lower values. Table 6 indicates the slope steepness (values from 1 to 10, see table 3) and aspect for each study sites.

TABLE 6 VALUE OF SLOPE STEEPNESS AND ORIENTATION FOR EACH STUDY SITE.

Study site	Slope steepness	Slope aspect
Palsa	3	Northeast
Äshèyi old village	3	Northeast
Äshèyi village	1	East
Pingo	1	East
Kettle	1	Southwest
Thermokarst	1	Northwest
Permafrost Valley	1	Southwest
Culvert	3	Northwest
Chämì	3	West
K'ùa West	1	South
K'ùa East	1	West
K'ùa village	1	Southeast

7.8.4 Sensitivity Map

The sensitivity map is the result of the mapping model presented in the methodology. It is composed of three classes of sensitivity of the land to permafrost thaw. The more sensitive the land is the more changes in landforms, vegetation, and surface drainage can be observed. Table 7 shows that of the mapping area, 58% is classified as low sensitivity, 27% is classified as medium, and 15% is classified as high.

TABLE 7 SENSITIVITY TO PERMAFROST THAW FOR THE ENTIRE MAPPING AREA.

Sensitivity	Km^2	%
Low	1101.8	58
Medium	520.2	27
High	283.7	15

- Low sensitivity areas are unlikely to contain permafrost or only small patches present in surficial material that would be mostly unaffected by thaw.
- Medium sensitivity areas are likely to contain permafrost in patches that are or will be affected by thaw as climate warming continues.
- High sensitivity areas have a high probability of containing permafrost patches or even be entirely underlain by permafrost. Permafrost in these areas is present in surficial material that present a high sensitivity to thaw which leads to more significant landscape changes.

Figure 102 shows how the sensitivity levels are spread across the mapping area. With the surficial geology having the highest weight in the mapping model, its influence is clearly visible in this final map. The highest sensitivity areas are located around K'ùa Mān, Äshèyi Village, and on the east shore of Äshèyi Mān. The land cover change and slope layers bring some nuances to the medium and low sensitivity areas. For example, the area between Äshèyi village and the Pingo is predominantly classified as medium but scattered with small patches of high sensitivity. As expected, almost all the study sites overlap with high sensitivity, only the Äshèyi Road Site 1-Culvert and the Kettle site near Äshèyi are located areas of predominantly medium sensitivity, and Chämì is located in a low sensitivity area. This confirms that the mapping model is appropriate for the area as it supports the field observations.

Together with the Äshèyi village, the Äshèyi Road is the other at-risk infrastructure. There is a total of 122.8km of road in the mapping area and over half of it, 73.6km, overlaps with either medium or high sensitivity to permafrost thaw. These sections are represented as thick black lines on Figure 102. It includes the entire section of the Alaska Highway comprised within the mapping area, the first 9.5km of the Äshèyi Road from the south of the mapping area and multiple sections north of the Äshèyi Road Site 1 (Culvert). At these locations, ground movements such as cracks and depressions can be expected, likely requiring more frequent or important road maintenance than in other sections.

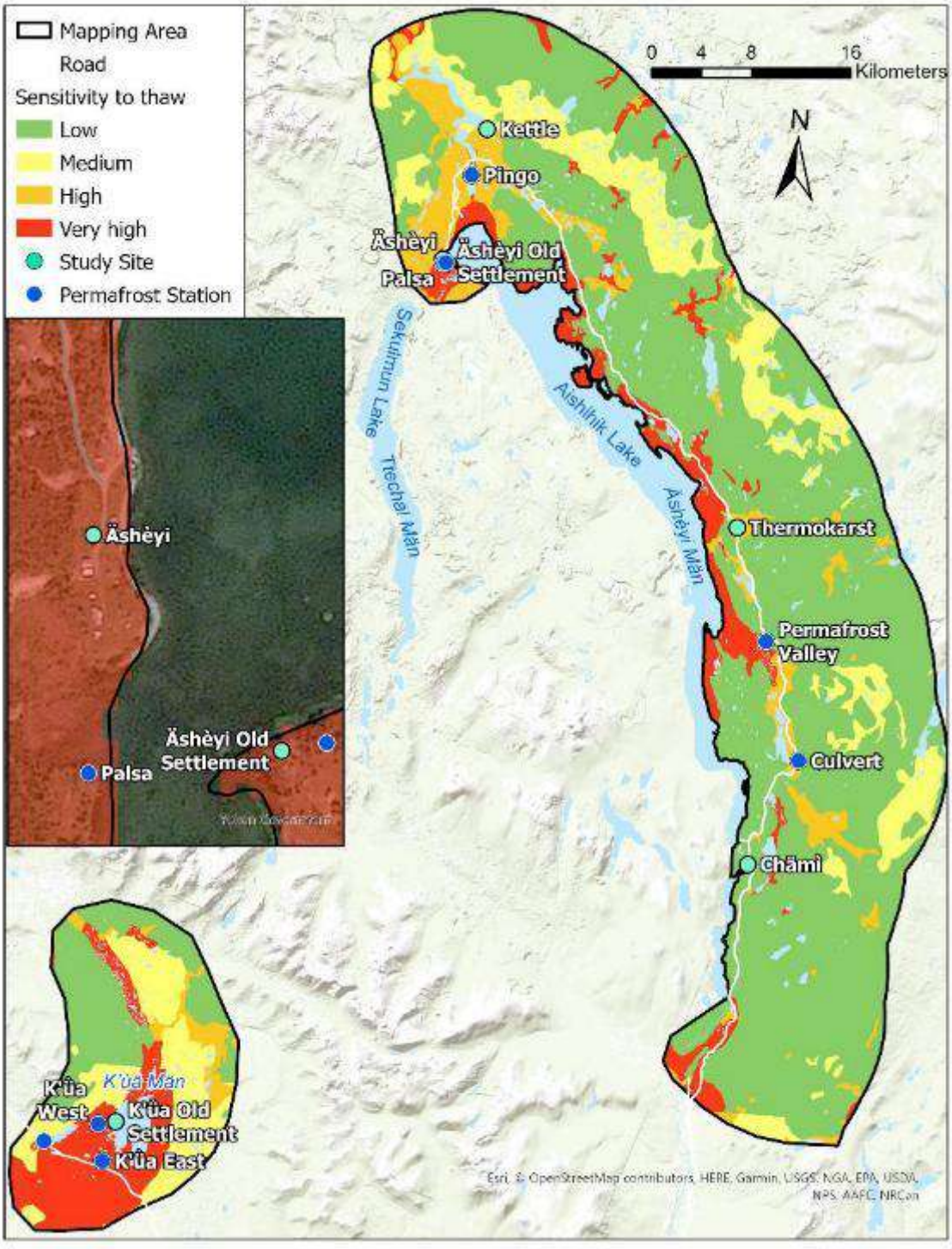

FIGURE 98 CLASSIFICATION OF SURFICIAL DEPOSITS IN 4 CLASSES OF SENSITIVITY TO PERMAFROST THAW.

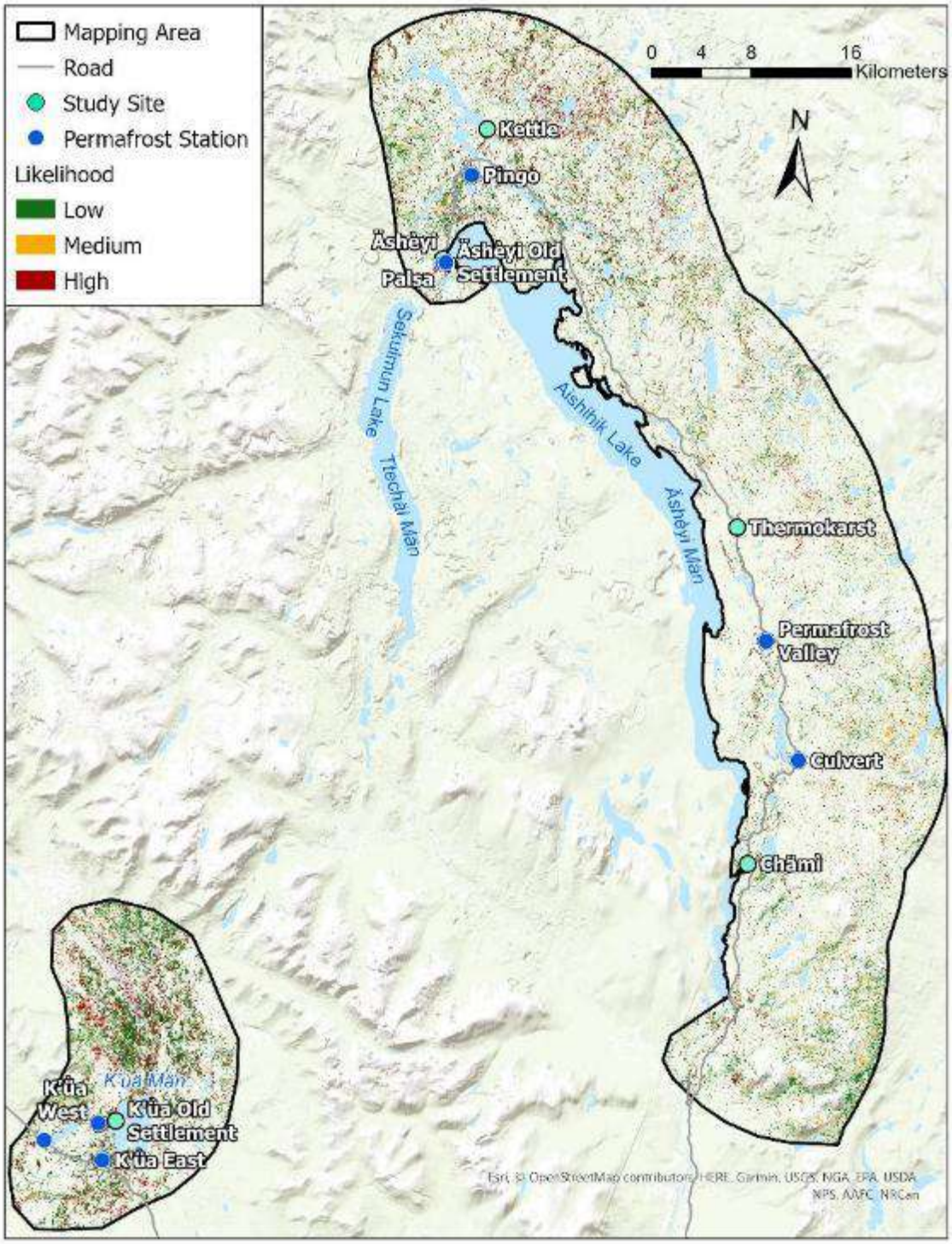

FIGURE 99 LAND COVER CHANGES BETWEEN 1984 AND 2014 CLASSIFIED BY LIKELIHOOD OF BEING CAUSED BY PERMAFROST DEGRADATION.

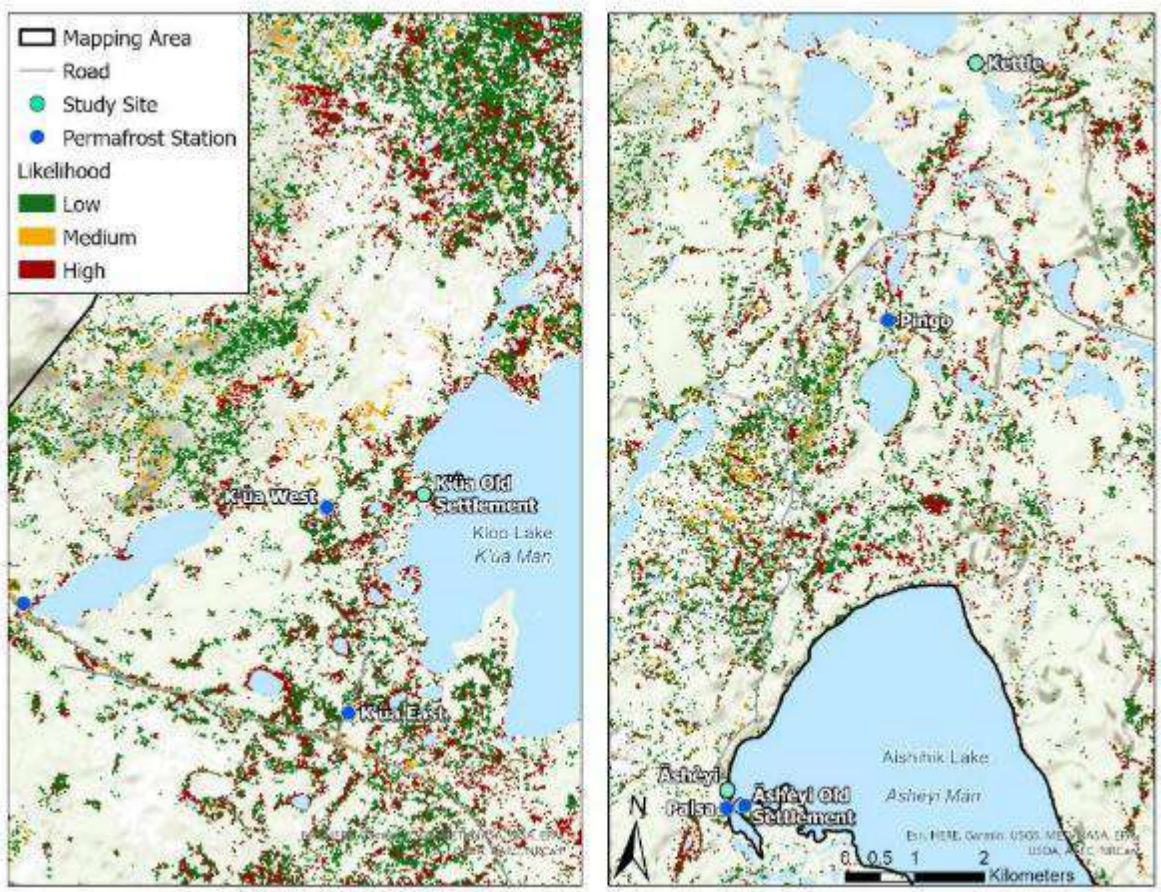

FIGURE 100 LAND COVER CHANGES BETWEEN 1984 AND 2014 CLASSIFIED BY LIKELIHOOD OF BEING CAUSED BY PERMAFROST DEGRADATION FOR THE AREAS OF K'ÙA MĀN (LEFT) AND NORTH OF ÄSHÈYI VILLAGE (RIGHT).

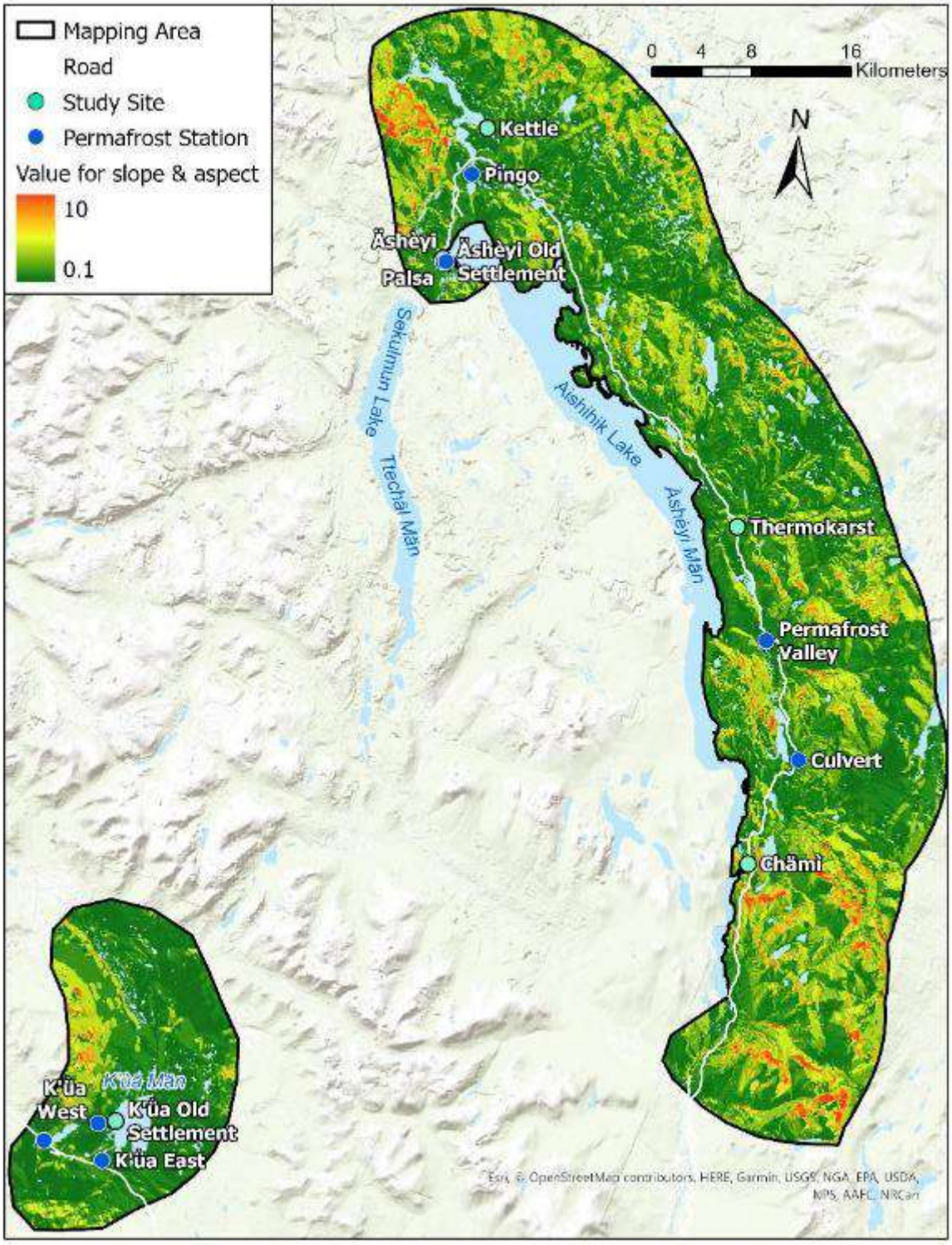

Figure 101 Combination of slope steepness and aspect shown with a colour gradient representing values from 0.1 to 10.

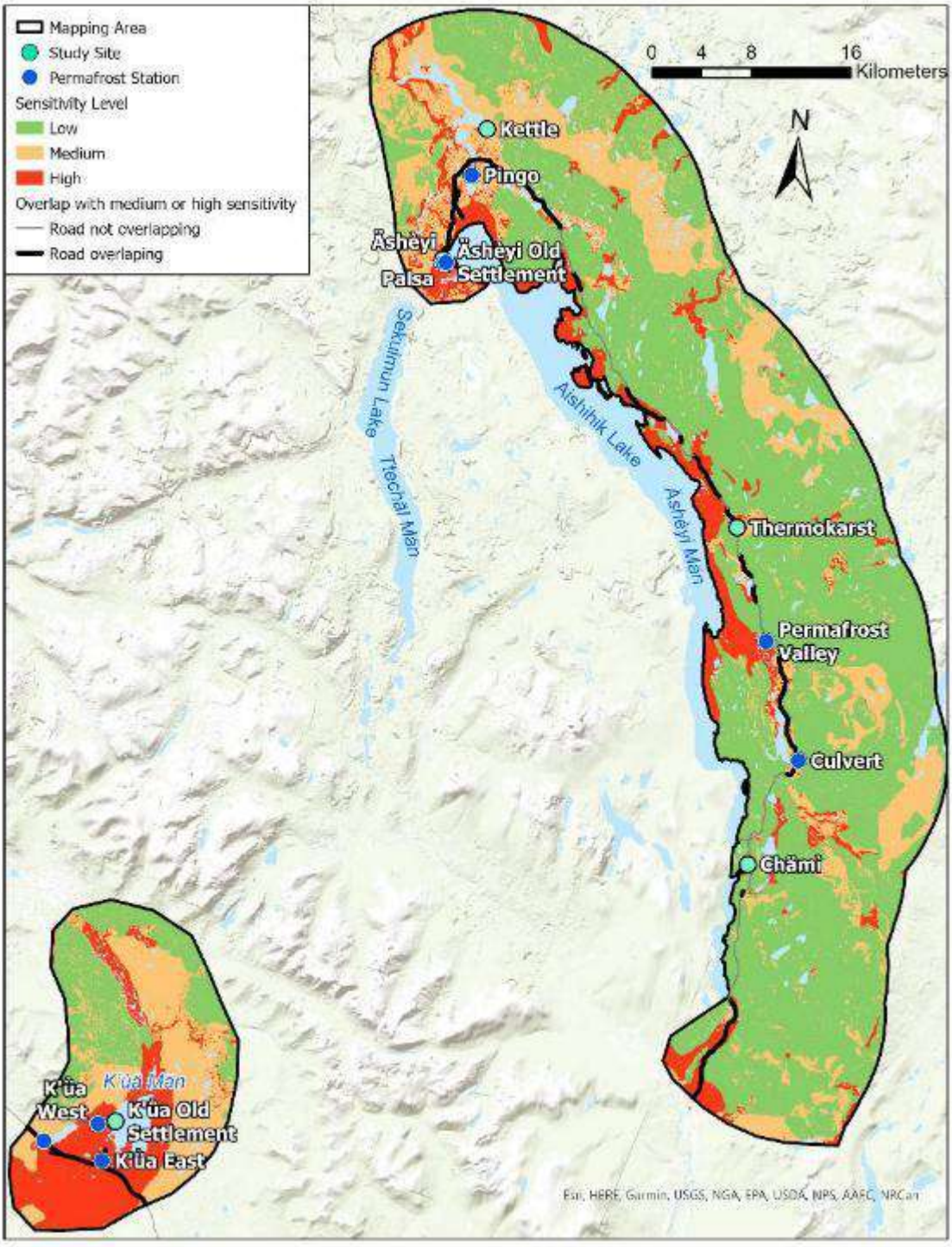

FIGURE 102 FINAL SENSITIVITY MAP SHOWING THREE LEVELS OF SENSITIVITY TO PERMAFROST THAW.

8. Conclusions

The permafrost sensitivity of large areas of the Shadhäla yè Äshèyi Kwädǟn territory, including the Äshèyi village, the Äshèyi Road and the K'ùa Mǟn area, were mapped using field assessments, surficial geology, and topographic observations such as landcover changes, slope orientation, and steepness. The field assessments were based on borehole data, geophysical surveys, drone aerial imagery, and three-dimensional modeling, which were used to guide and validate the mapping process.

The sensitivity of permafrost in the studied areas is determined by the geological context of surficial geology and geological history.

The surficial geology has an impact because the nature of the soil will strongly influence its mechanical properties as well as its ground ice content. This is particularly true for sediment of fluvial and lacustrine origins. These finely textured sediments that contain silt and clay are more likely to contain segregated ice, which requires fine texture, wet conditions, and slow freezing rates to form. These conditions are often met along the shores of, or near lakes. This explains why there are so many areas where permafrost is highly sensitive to thaw along Äshèyi Mǟn and K'ùa Mǟn. The sites assessed in the Äshèyi village, including the old settlement, are good examples of this. While less sensitive to permafrost thaw, fluvial environment can also undergo major changes when permafrost thaws. The sites located along the Äshèyi Road, especially the culvert site, showed that the environment becomes wetter and vegetations is impacted when permafrost degrades. Therefore, they qualify as medium and sometimes highly sensitive areas.

The geological history has an impact because the processes linked to deglaciation may have led to sporadic and discrete, highly sensitive areas. As the ice sheet retreated, some ice may have been buried by outwash in some locations. Most of this buried ice melted before permafrost developed, leaving behind kettle holes or ponds; but in some cases, the ice may have been preserved in permafrost. At present, these buried ice bodies could melt, driven by natural and/or human-driven disturbances. One such site has been identified in the Äshèyi village area, another one is suspected along the Äshèyi Road. Others are suspected in the K'ùa Mǟn area and the Äshèyi old settlement area. These discrete massive ice bodies are expected to occur where fluvial deposits adjoin or overlay morainal deposits.

Morainal deposits may have permafrost, but they are the most thaw stable because their coarser texture does not favor the formation of significant amounts of segregated ice, and glacier ice was unlikely to be preserved in this type of sediment due to their morphology and the post-glacial climatic conditions.

The final sensitivity map reflects the geological conditions, as well as the changes that are already occurring in the landscape, likely driven by permafrost thaw. As such, the map is considered dynamic and can be updated as time goes on. At present, most of the studied area is considered to have low sensitivity (58% of the land surface), and therefore permafrost is expected to have little impact on much of the land. However, 15% is considered to have high sensitivity to permafrost thaw, and that these areas include the Äshèyi village and around Äshèyi Mǟn and K'ùa Mǟn. In fact, most of these sensitive

lands are located on or near lake shores. Permafrost thaw could have impacts on the lake ecosystems by releasing sediment and possibly mercury or other toxins frozen within the permafrost.

The climate records show that mean annual air temperatures in the traditional territories of the Shadhäla yè Äshèyi Kwädān warmed by 1.9°C since the 1945-1975 period. Climate projections suggest that such warming will continue or even increase in the future. Consequently, the warming temperatures in the traditional territories of the Shadhäla yè Äshèyi Kwädān will impact the most sensitive areas mapped during this project, with consequences for the landscape and its ecosystem.

As a follow-up to this study, other areas of interest identified by the community should be assessed and added to the existing sensitivity map. In addition, since most high-sensitivity areas are lake shores, chemical analyses focusing on harmful contaminants should be performed on soil samples to detect possible detrimental effects on health.

9. References

Calmels, F., Allard, M., and Delisle G. 2008. Development and decay of a lithalsa (Northern Québec): A geomorphological history. Geomorphology, 97: 287–299.

CAFN, unpublished 2016. Climate Change Adaptation Plan – Community Infrastructure. Compilation of work from Shadhäla and Äshèyi First Nations funded by IRNAC for the Climate Change Adaptation program – Citizen Engagement (CCAP-CI).

CAFN, 2017. Community-based fish and wildlife management plan for the Shadhäla and Äshèyi Traditional Territory. Shadhäla and Äshèyi Traditional Territory Fish and Wildlife Planning Team, 2017. Environment Yukon, Whitehorse, Yukon. 50 pages.

Environment and Climate Change Canada (2021) Canadian Environmental Sustainability Indicators: Temperature change in Canada. Consulted on 3/2/2022. Available at: www.canada.ca/en/environment-climate-change/services/environmental-indicators/temperature-change.html.

Geurts, M.A., Dewez, V.1985. Le pingo d'Äshèyi, sud-ouest du Yukon : caractères morphogénétiques et cadre temporel. Géographie physique et Quaternaire, vol. 39, n° 3, 1985, p. 291-298.

Ladanyi, B., & Andersland, O. B. (2004). *Frozen ground engineering*. Wiley.

Martinez Cortizas, A., Biester, H., Mighall, T., and Bindler, R., 2007. Climate-driven enrichment of pollutants in peatlands. Biogeosciences, 4, 905-911.

Rydberg, J., Klaminder, J., Rosén, P., and Bindler, R. 2010. Climate driven release of carbon and mercury from permafrost mires increases mercury loading to sub-arctic lakes. Science of the Total Environment, 408. pp4778-4783. doi:10.1016/j.scitotenv.2010.06.056

Slater, A. G., & Lawrence, D. M. (2013). Diagnosing present and future permafrost from climate models. *Journal of Climate*, *26*(15), 5608-5623.

Smieja-Król, B., Fiałkiewicz-Kozieł, B., Sikorski, J., Palowski, B. 2010. Heavy metal behaviour in peat – A mineralogical perspective. Science of the Total Environment, 408, 5924–5931.

Vogt, N., 2021. Influence of permafrost characteristics on the severity of vegetation change in Yukon and Northwest Territories, Canada (Master's Thesis). University of Alberta.

Walvoord, M. A., & Kurylyk, B. L. (2016). Hydrologic impacts of thawing permafrost—A review. *Vadose Zone Journal*, *15*(6).

Wang, J.A., D. Sulla-Menashe, C.E. Woodcock, O. Sonnentag, R.F. Keeling, and M.A. Friedl. 2019. ABoVE: Landsat-derived Annual Dominant Land Cover Across ABoVE Core Domain, 1984-2014. ORNL DAAC, Oak Ridge, Tennessee, USA. https://doi.org/10.3334/ORNLDAAC/1691

World Meteorological Organization. (2017). WMO guidelines on the calculation of climate normals.

10. Glossary

Climate Terms

Mean Annual Air Temperature (MAAT): Mean annual air temperature is the average air temperature for a whole year.

Mean Daily Air Temperature (MDAT): Mean daily air temperature is the average temperature for each day.

Reference period: It is standard in climate analysis to use 30-year periods to

Thaw degree day (TDD): Thaw degree-days are the total sum of temperatures above 0° C, usually for the summer or "thaw season". This indicator helps to identify the intensity of summer.

Growing Degree Day (GDD): Growing degree-days are the total sum of temperatures above 5° C, usually for the summer or "growing season". This indicator helps to identify the intensity of the growing season. 5° C is chosen because it is generally the temperature at which plant growth begins.

FDD (FDD): Freezing degree-days is the total sum of temperatures below 0° C, usually for the winter or "freezing season". This indicator helps to identify the intensity of winter.

Site Assessment Methodology Terms

Orthomosaic: An orthomosaic is a mosaic of orthorectified images. In this case, drone images are tiled together and the resulting mosaic is orthorectified, meaning it is geometrically corrected to remove distortions.

Digital Elevation Model (DEM): A DEM is a computer-generated grid where each pixel represents the elevation at that location. The DEMs are generated from drone imagery, using a process called photogrammetry.

Electrical Resistivity Tomography (ERT): ERT is a geophysical method to image sub-surface structures using electrical resistivity measurements made at the surface. This is done using a resistivity meter that generates and receives a current connected to an array of electrodes. The configuration of the electrodes can be changed, which will in turn change the measurements. The two configurations used in this study are the dipole-dipole and Wenner configurations.

Volumetric excess ice content: Volumetric excess ice content is the volume of ice in the ground which exceeds the total pore volume that the ground would have under natural unfrozen conditions. In standard soil engineering terminology, a soil is considered normally consolidated when its total pore volume or its total water content is in equilibrium with the acting gravity stresses. Due to the presence of ground ice, the total water content of a frozen soil may exceed that corresponding to its normally

consolidated state when unfrozen. As a result, upon thawing, a soil containing excess ice will settle under its own weight until it attains its consolidated state.

Permafrost Landform Terms

Active layer: The top layer of ground that is subject to annual thawing and freezing in areas underlain by permafrost. The thickness of the active layer varies from year to year, depending on the ambient air temperature, vegetation, drainage, soil or rock type, snow cover, and slope degree and orientation.

Aggradational ice: A term for ground ice formed by the incorporation of ice lenses and layers into the permafrost during upward movement of the permafrost table. It is generally associated with syngenetic ice growth.

Cryostructures: The structural characteristics of frozen, fine-grained earth materials. The cryostructure is determined by the amount and distribution of pore ice and lenses of segregated ice. The type and arrangement of ice in the frozen material will depend on the initial water content of the material and the extent of the moisture movement during subsequent freezing.

Frost heave: The upward or outward movement of the ground surface (or objects on, or in, the ground) caused by the formation of ice in the soil.

Frost-stable ground: Ground (soil or rock) in which little or no segregated ice forms during seasonal freezing.

Frost-susceptible ground: Ground (soil or rock) in which segregated ice will form (causing frost heave) under the required conditions of moisture supply and temperature. Frost-susceptible ground will eventually become ice-rich regardless of its initial water content if the appropriate moisture supply and temperature conditions persist. By implication, frost susceptible ground may also be subject to thaw weakening effects when it thaws.

Kettle: A kettle is a depression in an outwash plain caused by the melting of an isolated block of remnant ice that was buried in the outwash sediment. Kettle holes are often filled with water forming ponds or lakes.

Lenticular ice: Lenticular (or microlenticular) ice is an ice body in the shape of a lense.

Permafrost: Ground (soil or rock) that remains at or below 0° C.

Pingo: A pingo is a perennial frost mound consisting of a core of massive ice that is produced primarily by the injection of water and is covered by soil and vegetation.

Palsa: A palsa is a peaty permafrost mound that contains a core of alternating layers of segregated ice and peat or mineral soils. Palsas are typically between 1 and 7m in height and less than 100 m in diameter.

Segregated ice: Ice formed by the migration of pore water to the frozen fringe where it forms into discrete layers or lenses. Segregated ice ranges in thickness from hairline to more than 10 m. It commonly occurs in alternating layers of ice and soil.

Talik: A layer or body of unfrozen ground in a permafrost area. Taliks may have temperatures above 0° C or below 0° C.

Thermokarst: The process by which characteristic landforms result from the thawing of ice-rich permafrost.

Thaw front: The advancing boundary between frozen and unfrozen ground, that will extend through the active layer.

Thaw-stable permafrost: Perennially frozen ground which, upon thawing, will not experience either significant thaw settlement or loss of strength.

Thaw-sensitive permafrost: Perennially frozen ground which, upon thawing, will experience important thaw settlement and suffer loss of strength to a value significantly lower than that for similar material in an unfrozen condition. For example, ice-rich permafrost is thaw-sensitive.

With definitions from the Glossary of permafrost and related ground-ice terms from the Permafrost Subcommittee from the Associate Committee on Geotechnical Research of the National Research Council of Canada (1988).